AD-A261 209

ENTATION PAGE

1. AGENCY USE ONLY (Leave blank)	2. REPORT DATE 10/14/92	3. REPORT TYPE AND DATES COVERED Reprint

4. TITLE AND SUBTITLE
Liquid crystals for laser applications

5. FUNDING NUMBERS
DAAL03-92-G-0147

6. AUTHOR(S)
S.D. Jacobs, K.L. Marshall, and A. Schmid

7. PERFORMING ORGANIZATION NAME(S) AND ADDRESS(ES)

The Institute of Optics
University of Rochester
Rochester, NY 14627

DTIC
ELECTE
FEB 18 1993
S   B   D

8. PERFORMING ORGANIZATION REPORT NUMBER

9. SPONSORING/MONITORING AGENCY NAME(S) AND ADDRESS(ES)

U. S. Army Research Office
P. O. Box 12211
Research Triangle Park, NC 27709-2211

10. SPONSORING/MONITORING AGENCY REPORT NUMBER

ARO 30367.2-PH-UIR

11. SUPPLEMENTARY NOTES

12a. DISTRIBUTION/AVAILABILITY STATEMENT

Approved for public release; distribution unlimited.

12b. DISTRIBUTION CODE

13. ABSTRACT (Maximum 200 words)

This article highlights some of the advances made in the use of liquid crystals for laser applications from 1982 through 1992. New materials and new effects were discovered, many new devices were developed, and novel applications for well-understood phenomena were conceived.

This was quite an eventful time period. Several new books were published on the broad subject of LC's,[1-20] and the international scientific community organized a society devoted to encouraging further scientific and educational advancement in the field.[21] Attention was focused on LC's in October of 1991 when the Nobel Prize in Physics was awarded to Pierre-Gilles de Gennes for his pioneering work toward understanding order phenomena in LC's and polymers.[22]

This article is divided into four sections. The first section discusses new materials, specifically ferroelectric LC's and LC polymers. The former have opened up the realm of submicrosecond response for LC devices, and the latter have significantly reduced the sensitivity of LC optics to temperature. Some new insights into the optical properties of materials are also mentioned. The second section reviews new developments in passive applications for cholesterics and nematics. Included here are the fabrication of cholesteric laser mirrors and apodizers, the use of LC polymers for notch filters and as optical storage media, and some novel nematic retarder concepts such as the distributed polarization rotator. Electro-optic devices extending from high-speed modulators to the variable focus LC lens are covered in the third section of this article, along with a discussion of LC/polymer composite films. Ferroelectric modulators, shutters and variable filters are also covered. The article concludes with a survey of nonlinear optical effects and devices.

14. SUBJECT TERMS
Liquid Crystals, Optical Applications, Laser, Electrooptics, Nonlinear Optics

15. NUMBER OF PAGES

16. PRICE CODE

17. SECURITY CLASSIFICATION OF REPORT	18. SECURITY CLASSIFICATION OF THIS PAGE	19. SECURITY CLASSIFICATION OF ABSTRACT	20. LIMITATION OF ABSTRACT
UNCLASSIFIED	UNCLASSIFIED	UNCLASSIFIED	UL

UR
LLE

Liquid Crystals for Laser Applications

by
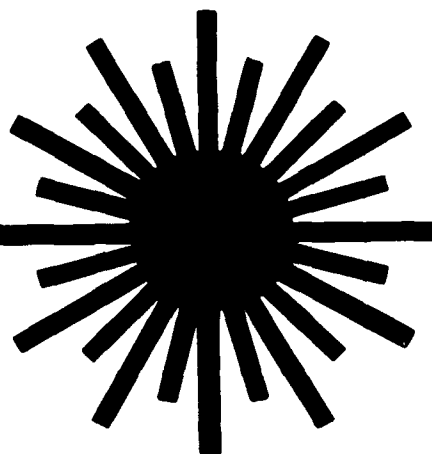
S. D. Jacobs, K. L. Marshall, and A. Schmid

to be published in the

Handbook of Laser Science and Technology

Supplement 2: Optical Materials; Section 14

by CRC Press, Boca Raton, FL

93-03104

July 1992   Laboratory Report No. 233

Laboratory for Laser Energetics

College of Engineering and Applied Science
University of Rochester

93   2   72   716

HANDBOOK OF LASER SCIENCE AND TECHNOLOGY

Supplement 2: Optical Materials

Section 14

Liquid Crystals for Laser Applications

by

S. D. Jacobs, K. L. Marshall, and A. Schmid

DTIC QUALITY INSPECTED 3   MS Date: 1 July 1992

TABLE OF CONTENTS

INTRODUCTION

This article highlights some of the advances made in the use of liquid crystals for laser applications from 1982 through 1992. New materials and new effects were discovered, many new devices were developed, and novel applications for well-understood phenomena were conceived.

This was quite an eventful time period. Several new books were published on the broad subject of LC's,[1–20] and the international scientific community organized a society devoted to encouraging further scientific and educational advancement in the field.[21] Attention was focused on LC's in October of 1991 when the Nobel Prize in Physics was awarded to Pierre-Gilles de Gennes for his pioneering work toward understanding order phenomena in LC's and polymers.[22]

This article is divided into four sections. The first section discusses new materials, specifically ferroelectric LC's and LC polymers. The former have opened up the realm of submicrosecond response for LC devices, and the latter have significantly reduced the sensitivity of LC optics to temperature. Some new insights into the optical properties of materials are also mentioned. The second section reviews new developments in passive applications for cholesterics and nematics. Included here are the fabrication of cholesteric laser mirrors and apodizers, the use of LC polymers for notch filters and as optical storage media, and some novel nematic retarder concepts such as the distributed polarization rotator. Electro-optic devices extending from high-speed modulators to the variable focus LC lens are covered in the third section of this article, along with a discussion of LC/polymer composite films. Ferroelectric modulators, shutters and variable filters are also covered. The article concludes with a survey of nonlinear optical effects and devices.

ADVANCES IN MATERIALS

Ferroelectric LC's

Ferroelectricity in liquid crystals was first suggested in 1974 by R. B. Meyer[23] who, by means of an elegant symmetry argument, postulated that spontaneous dipolar ordering should be possible in liquid crystal systems composed of a layered structure of chiral molecules in which the long molecular axis is tilted with respect to the normal to the layers. The experimental determination of a finite spontaneous polarization in the chiral smectic C compound DOBAMBC was reported in the same paper[23] by Meyer's co-workers, Liebert, Strzelecki, and Keller. This work spawned one of the most active and widely-pursued areas of liquid crystal research of the past decade. The vast majority of these efforts have been focused on ferroelectric liquid crystals belonging to the chiral smectic C (or smectic C*) class; however, the recent discovery of ferroelectricity in other chiral smectic phases has begun to arouse interest in the potential of these new materials systems for applications in optical devices as well.

Eight ferroelectric smectic liquid crystal phases have been identified and characterized to date: the C*,F*,G*,H*,I*,J*, K* and, most recently,[24] the M* phase. These tilted chiral smectic phases are classified according to the nature of the intermolecular

packing within individual layers and the extent of long-range molecular correlations between adjacent layers. Several examples of smectic phases are portrayed in Figure 1. The helical structure of chiral smectic mesophases draws its origins from the same source as in cholesteric liquid crystals, namely steric interactions between bulky side groups attached to the chiral centers of neighboring molecules. Extended terminal alkyl chains and off-axis dipole moments cause the chiral smectic molecules to adopt a tilted orientation with respect to the layer planes. This results in an overall reduction in symmetry for the chiral smectic phases (C_2) as compared to the cholesteric (D_∞) and nematic ($D_{\infty h}$) cases.[25] Although the existence of a spontaneous polarization is possible only in tilted chiral phases, *orthogonal* smectic phases made up of chiral molecules, e.g., smectic A*, can also show ferroelectric properties in the presence of an electric field applied parallel to the layer planes. Under these conditions, a field-induced tilt of the molecules within the layers (the "electroclinic" or "soft-mode" effect) is produced, due to a molecular rotational bias that occurs as the lateral dipoles align with the applied field. A reduction in overall symmetry of the orthogonal chiral smectic phase from D_∞ (non-ferroelectric) to C_2 (ferroelectric) occurs, and a macroscopic polarization appears along the electric field direction.[25] A more detailed discussion of symmetry considerations in liquid crystal systems is beyond the scope of this work and will not be undertaken here; instead, the interested reader is referred to a number of excellent review articles on the subject.[25–31]

The discovery of ferroelectric properties in the Schiff base DOBAMBC led to the eventual synthesis over the next several years of an extensive series of smectic C* compounds belonging to this particular chemical class. Several examples of these materials are shown in Figure 2. The initial popularity of the Schiff base class of materials stemmed primarily from two factors: (1) the synthesis methods for this class of compounds were uncomplicated and well-documented, having been used extensively in the preparation of nematic compounds for twisted nematic and other E-O device applications research; and (2) the starting materials used in the syntheses (both chiral and nonchiral) were inexpensive and readily available. The combination of these two factors made it possible to generate a large number of new compounds with minimal effort over a relatively short period of time. The advantage of synthetic expediency in this first generation of ferroelectric materials, however, was unfortunately offset by several serious drawbacks in their physical properties. In addition to being both chemically and thermally unstable, the majority of these compounds possessed ferroelectric phases only at elevated temperature, which made the fabrication, characterization, and testing of devices extremely difficult. Because of these limitations, ferroelectric LC device technology advanced at a relatively lethargic pace throughout the remainder of the late 1970's.

Following a trend that was previously established in nematic liquid crystal materials research, chemists in the early 1980's turned to the more stable phenyl benzoate class of materials in their efforts to develop smectic C* compounds that would be useful both for studies of basic structure/properties relationships and in the formulation of broad range, multicomponent eutectic mixtures for ferroelectric LC device research. The earliest examples of this class of compounds employed (S)-2-methylbutanol almost exclusively as the chiral component, largely due to its ready availability in high optical purity and low cost.[27] Figure 3 shows the composition and physical properties of one of the first stable,

Smectic A
(A)

Smectic C
(B)

short-range
hexagonal order

no long-range
correlations
between layers

Smectics I and F

Chiral Smectic C

(C)

(D)
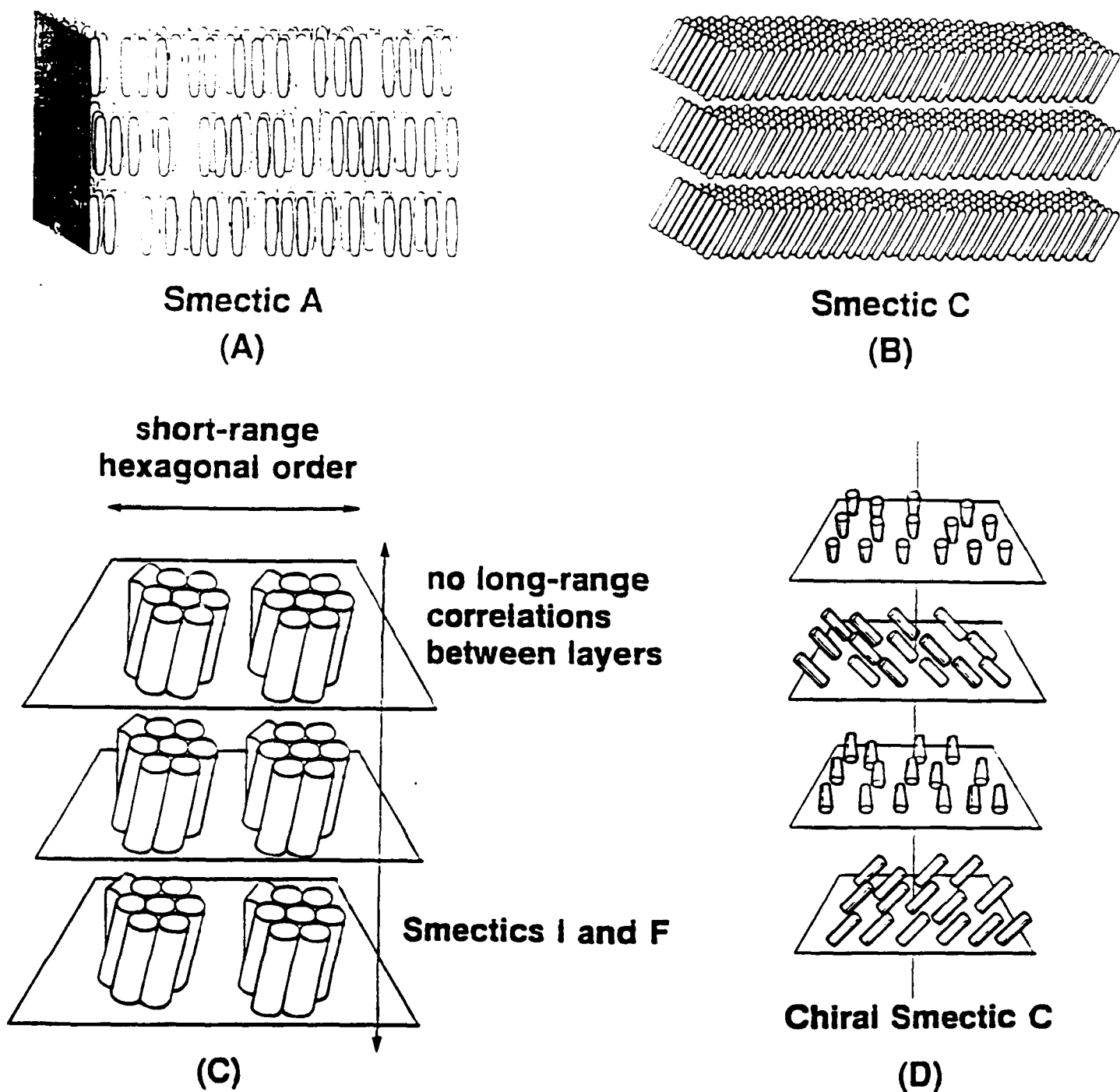
G1931

FIGURE 1   Examples of the molecular packing in various smectic liquid crystal phases. (a) The smectic A (and A*) phase; (b) the smectic C phase; (c) the smectic I and F phases; (d) the smectic C* phase.

3

Structure	S_C^* range
$C_{10}H_{21}O$—⬡—CH=N—⬡—CH=CH—C(=O)—O—CH$_2$—HC*(C_2H_5)(CH$_3$) **DOBAMBC**	85–90°C
$C_6H_{13}O$—⬡—CH=N—⬡—CH=CH—C(=O)—O—CH$_2$—HC*(Cl)(CH$_3$) **HOBACPC**	62–74°C
C_2H_5CH(CH$_3$)(CH$_2$)$_5$O—⬡(O–H)—CH=N—⬡—C_8H_{17} **MORA 8**	12–97°C
C_2H_5CH(CH$_3$)CH$_2$O—⬡(O–H)—CH=N—⬡—C_8H_{17} **MBRA 8**	57–64°C

G3290

FIGURE 2   Several examples of early Schiff base smectic C* mesogens.

4

room temperature ferroelectric liquid crystal eutectic mixtures prepared using phenyl benzoates.[32] The weak spontaneous polarization afforded by the nonpolar 2-methylbutyl group, combined with the relatively short pitch length and high intrinsic viscosity of these mat .ials, generally made it necessary to fabricate extremely thin (1 μm or less) cells or use drive voltages in excess of 50–80 V in order to achieve submillisecond switching speeds.[33] Materials synthesis efforts were therefore directed toward the development of smectic C* mesogens with chiral groups that were capable of enhancing the spontaneous polarization. This goal was realized with the synthesis of a series of smectic C* phenyl benzoates containing polar chiral groups derived from amino acid precursors (Higuchi *et al.*[34]) and lactic acid derivatives (Walba *et al.*[35] and Bone *et al.*[36]), several of which are shown in Figure 4. These compounds have special significance in that they were the basis for several of the first commercially available ferroelectric liquid crystal mixtures introduced in 1986 by Displaytech, Inc. of Boulder, CO, and Merck Ltd. of Poole, England (formerly BDH Chemicals).

Development of useful ferroelectric liquid crystal mixtures depends heavily on the ability to independently control several important physical parameters, such as spontaneous polarization, helical pitch length, intrinsic viscosity, and phase transition temperatures. One approach relies on the use of compounds that all possess the same type of liquid crystal 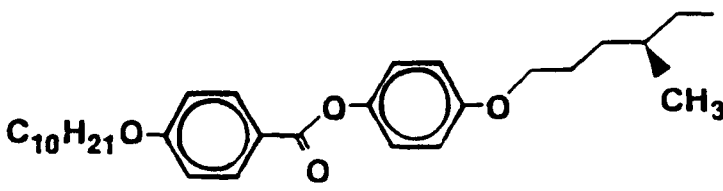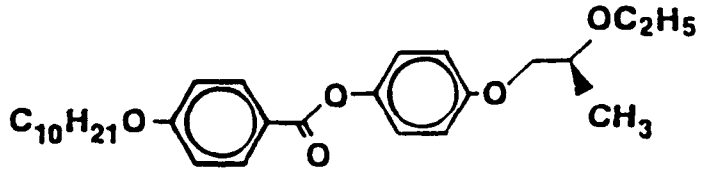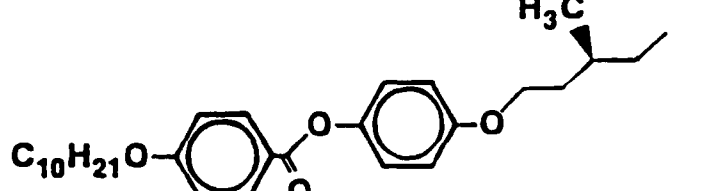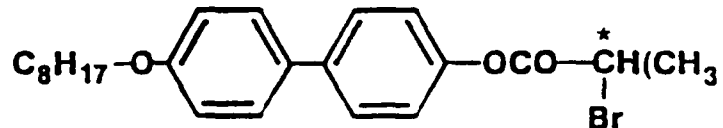phase, in this case smectic C*, as components of the mixture. This approach is analogous to that previously employed in the formulation of broad-range nematic liquid crystal mixtures, and was used in the development of early ferroelectric liquid crystal mixtures such as that shown in Figure 3. One disadvantage of this approach is that the branched alkyl chains of the chiral substituents result in mixtures that have a higher intrinsic viscosity than mixtures composed of straight-chain analogs. To control the helical pitch length without compromising the spontaneous polarization of the mixture, chiral mesogens of the opposite twist sense and the same polarization sense (positive or negative) are required, which can severely limit the number of useful compounds for mixture formulation. A more recent approach relies on the use of a low-viscosity, nonchiral smectic C mixture as a host material that is doped with a suitable quantity of a smectic C* compound or mixture that has a very large spontaneous polarization. A particular advantage of this approach is that both the magnitude of the spontaneous polarization and the helical pitch length can be independently controlled as a function of chiral dopant concentration. The technique is analogous to the well-known method for controlling the selective reflection wavelength in chiral nematic mixtures (see later portions of this article). Reduced cost of the resultant mixtures is an added benefit, since smaller amounts of the more costly chiral components are required per unit volume of the mixture. Using this latter approach, a wide variety of ferroelectric liquid crystal mixtures have been developed over the past three to four years by the major liquid crystal vendors. Tables 1 and 2 list the range of ferroelectric and electroclinic LC mixtures, and their physical and electro-optical properties, that are currently available from the Merck group (E. Merck, Darmstadt, and Merck Ltd., Poole). The development of new ferroelectric liquid crystal compounds and mixtures for device applications continues to be a subject of intense investigation in both the academic community and the private sector. Table 3 lists the molecular structures of several new compounds recently reported by several different research groups that show potential for use in device applications.

(XIV) $C_8H_{17}O$—⟨benzene⟩—COO—⟨benzene⟩—$COOCH_2\overset{*}{C}HC_2H_5$ 17%
                                                                      CH_3

(XV) $C_{10}H_{21}O$—⟨benzene⟩—$CH=CHCOO$—⟨benzene⟩—$COOCH_2\overset{*}{C}HC_2H_5$ 55%
                                                                              CH_3

(XVI) $C_{10}H_{21}O$—⟨benzene⟩—⟨benzene⟩—OCO—⟨benzene⟩—$CH_2\overset{*}{C}HC_2H_5$ 28%
                                                                              CH_3

$$Iso \xleftrightarrow{\ 97\ } S_A \xleftrightarrow{\ 50\ } S_C$$

m.p.   calc.
 10   14
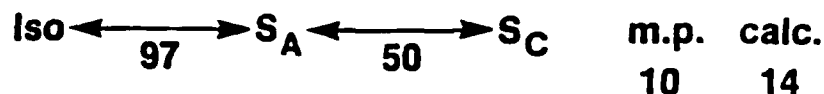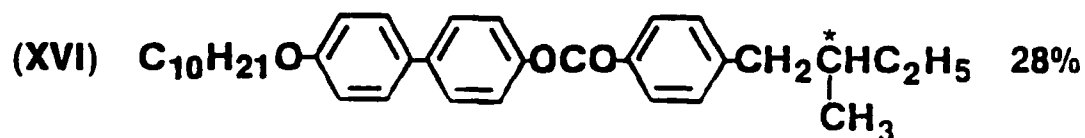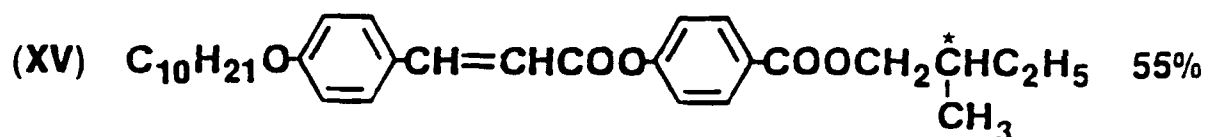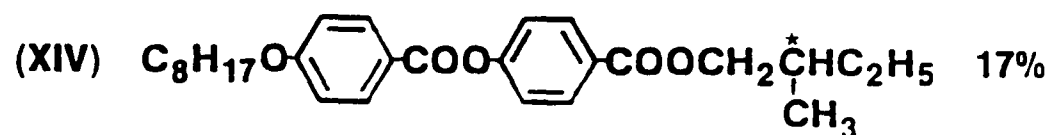
G1949

FIGURE 3   The composition of a stable, room temperature ferroelectric LC eutectic mixture containing phenyl benzoate derivatives with 2-methylbutyl groups. [From Goodby, J. W., and Leslie, T. M., *Mol. Cryst. Liq. Cryst.*, 110, 190, 1984. With permission.]

6

Structure S^*_c Range

$C_{10}H_{21}O$—[benzene]—C(=O)—O—[benzene]—O—CH$_2$CH$_2$CH$_2$—CH(CH$_3$)—CH$_2$CH$_3$ 30.5–70.5°C

$C_{10}H_{21}O$—[benzene]—C(=O)—O—[benzene]—O—CH$_2$—CH(OC$_2$H$_5$)(CH$_3$)   9.0–27.8°C

$C_{10}H_{21}O$—[benzene]—C(=O)—O—[benzene]—O—CH$_2$—CH(H$_3$C)—CH$_2$CH$_3$ 15.0–56.5°C

C_8H_{17}—O—[biphenyl]—O—CO—$\overset{*}{C}H(CH_3)_2$ with Br   35.0–48.0°C

G1950

FIGURE 4   The molecular structures of several ferroelectric liquid crystal compounds with enhanced spontaneous polarization.
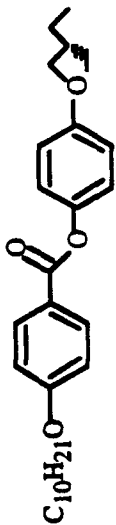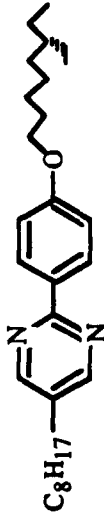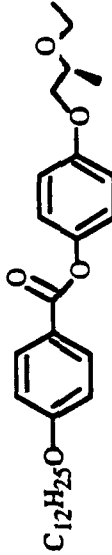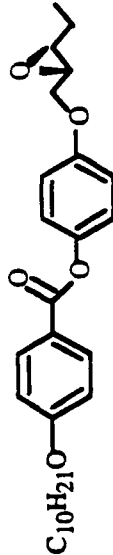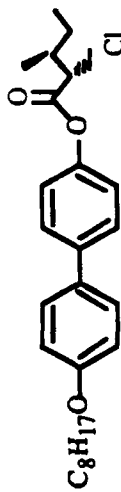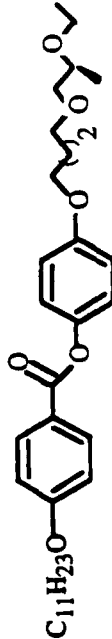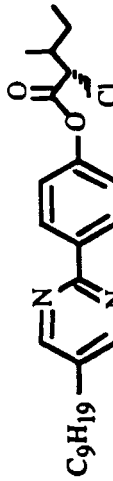
TABLE 1
Ferroelectric and electroclinic smectic liquid crystal mixtures — Merck, Ltd. (Poole)
[From 1991 catalog, with permission.]

Ferroelectric Mixtures:		SCE 8	SCE 13	SCE 13R
$S_I \to S_C^*$	[°C]	<−20	<−20	<−20
$S_C^* \to S_A^*$	[°C]	+59	+60.8	+60.8
$S_A^* \to Ch$	[°C]	+79	+86.3	+86.3
$Ch \to I$	[°C]	+100	+100.8	+100.8
Spon. Polar. [nC cm^{-2}] [20°C]		+6.3	+27.8	~0
Tilt Angle (°) (20°C)		19.5	22.0	—
Pitch (µm) Ch Phase near S*$_A$-Ch Transition		>80	>80	>80
Swiching Time (µs) (20 V/µm, 20°C)		98	11	—
Δε (100 kHz, 20°C)		−2.0	−0.5	—
Δn (589 nm, 20°C)		0.16	0.18	—
Rot. Visc. γ [mPa·s] (20°C)		160	—	—

Electroclinic Mixtures:		764 E	854 E	868 E	869 E	870 E
$S_C^* \to S_A^*$	[°C]	+28	+41.6	+20.8	+14.6	+17.2
$S_A^* \to Ch$	[°C]	+73	+95.7	+74.3	+69.2	+71.2
$Ch \to I$	[°C]	+89 to +92	+109.3	+83.5	+81.6	+82.4
Electroclinic Tilt Angle (°)†						
10 V/µm		10.5	7.5	7.5	7.5	7.5
15 V/µm		12	9.0	9.0	9.0	9.0
20 V/µm		14	10.5	10.5	10.5	10.5
23 V/µm		—	11.5	11.5	11.5	11.5
25 V/µm		13	—	—	—	—

†Value for 764 E at 29°C, all others at 22°C

TABLE 2
Ferroelectric smectic liquid crystal mixtures —E. Merck Darmstadt
[From 1991 catalog, with permission.]

Mixture: ZLI-		4237-000	4237-100	4654-000	4654-100	4655-000	4655-100	4851-000	4851-100	5014-000	5014-100
Date of Development		5/88	4/88	8/89	9/89	9/89	9/89	9/90	9/90	8/90	1/91
$K \to S_C^*$	[°C]	<−20	<−20	<−10	<−10	<−10	<10	<−10	<−20	<−10	<−10
$S_C^* \to S_A^*$	[°C]	63	61	65	61	60	61	64	67	64	65
$S_A^* \to Ch$	[°C]	72	73	69	65	69	72	70	71	68	70
$Ch \to I$	[°C]	79	83	76	74	72	76	74	76	70	72
Spon. Polar. [nC cm^{-2}]	[20°C]	−7.0	−20	+7.2	+13.8	+7.0	+22.6	−4	−22	−2.8	−20
Tilt Angle (°)	(20°C)	25.0	24.5	23.5	25.5	23.0	25.0	24.0	30.5	24.5	28.5
Pitch (µm)	(Chol.)	−29	−11	+60	>+55	>+40	+28	>+40	+12	—	+11
Pitch (µm)	(20°C)	ca.40	10	—	—	—	14	—	—	—	—
Switching Time (µs) (15 V/µm, 20°C)		90	40	100	67	81	42	138	38	150	45
Δn	(589 nm, 20°C)	0.13	0.14	—	—	—	—	—	—	—	—
Δε	(20 kHz, 20°C)	−0.5	−1.2	−1.3	−1.4	−0.8	−1.7	−0.7	−1.1	−0.9	−1.3
Rot. Visc. γ [mPa·s]	(20°C)	154	185	170	170	120	160	—	—	150	—
Spec. Resistivity [Ω·cm]	(20°C)	>1E10	>1E10	>1E10	>1E10	>1E10	>1E10	>1E10	>1E10	>1E10	>1E10

9

Molecular structures of several new compounds that show potential for future use in device applications. The values of P indicated are for a doped chiral smectic C system with this compound as the chiral dopant. [Adapted from Skarp, K. and Handschy, M., "Ferroelectric liquid crystals. Material properties and applications," *Mol. Cryst. Liq. Cryst.*, 165, 439–509, 1988. No permission required.]

Structure	Phase transitions (°C)	Spontaneous Polarization P (nC/cm²)	[Ref.]
$C_{10}H_{21}$ …	X 44 C* 53.8 A 67 L	3	[37]
C_8H_{17} …	X 3 S_X 14.2 C* 48.6 A 56.3 L	0.5	[28]
$C_{12}H_{25}O$ …	X 44 (34.8 C*) A 46 L	10	[38]
$C_{10}H_{21}$ …	X 75 (57 S_3) C* 80 A 81 N* 97 L	30	[39]
$C_8H_{17}O$ …	X 30 C* 53A 66 L	220	[40]
$C_{11}H_{23}$ …	X 32 (B 31.2) C* 45.3 A 50.9 L	4	[41]
C_9H_{19} …	C* 71 A 77 N* 94 L	14.3	[42]

Another area of ferroelectric liquid crystal materials research that has received increasing attention of late is the relationship of various aspects of molecular structure to materials properties. Several authors have previously treated this subject from a mathematical and statistical point of view,[43-47] as well as from a more generalized and pictorial approach.[26,47-49] More elaborate models that describe the origins of the ferroelectric polarization in terms of molecular structure have recently been proposed and experimentally verified by both Goodby et al.[50,51] and Walba et al.[38,39] Due in part to the improved understanding of structure-properties relationships afforded by these models, the scope of ferroelectric liquid crystal materials research has recently expanded to include such topics as ferroelectric phases in polymeric mesogens and nonlinear optical applications and devices. Recent examples of this trend include the reported evidence of efficient second harmonic generation in a ferroelectric liquid crystal compound designed and synthesized especially for this purpose,[52] as well as several reports of polymeric smectic C* materials that have been shown to be potentially useful for both electro-optical[53,54] and nonlinear optical[55] devices.

LC Polymers

In the early 80's, Tsutsui and Tanaka[56,57] published work showing that the temperature sensitivity of low molecular weight LC fluids could be avoided by constructing thermotropic cholesteric LC polymers. With a poly(γ-butyl-L-glutamate)-butyl acrylate system, they demonstrated selective reflection effects for optical applications in free-standing films prepared by homogeneous mixing of two components followed by photo-irradiation. Other thermotropic acrylate and methacrylate systems[58,59] and one lyotropic system, hydroxypropyl cellulose,[60,61] have been studied with some success. Both the synthesis and characterization of LC polymers have been reviewed by Koide.[62]

Thermotropic liquid crystal polymers exhibit several types of structures, as shown schematically in Figure 5. Arrangement D, wherein mesogenic units are linked via flexible spacers to the side of the polymeric backbone, was shown by Finkelmann's work with polysiloxanes[63-65] to be the most successful for optical applications. A comparison of phase behavior for low molar mass and side-chain polymeric LC's (see Figure 6) illustrates that there is no crystallization for the latter. The glass transition, defined by the second-order transition in the volume/temperature curve, may occur anywhere from 10°C to 120°C.[65] Special molecular ordering, which creates optical properties such as selective reflection in the LC phase, may be frozen into the bulk polymer by high viscosity near the glass transition. The result is reduced sensitivity of optical effects to broad temperature variations.

Because of the flexible spacer between the pendant LC moiety and the polymer main chain, LC polymers can respond to external fields. Electric field threshold voltages are comparable to those of conventional LC's,[66-70] provided the pendant spacer length is short.[62] For fast response, polymers are designed to incorporate long, flexible spacers and a large dielectric anisotropy of the pendant group.[62] High viscosity impedes the motion of molecules, but Finkelmann was able to achieve electric field response times below 200 ms in polysiloxane polymers at temperatures well above the glass transition.[69] Newly
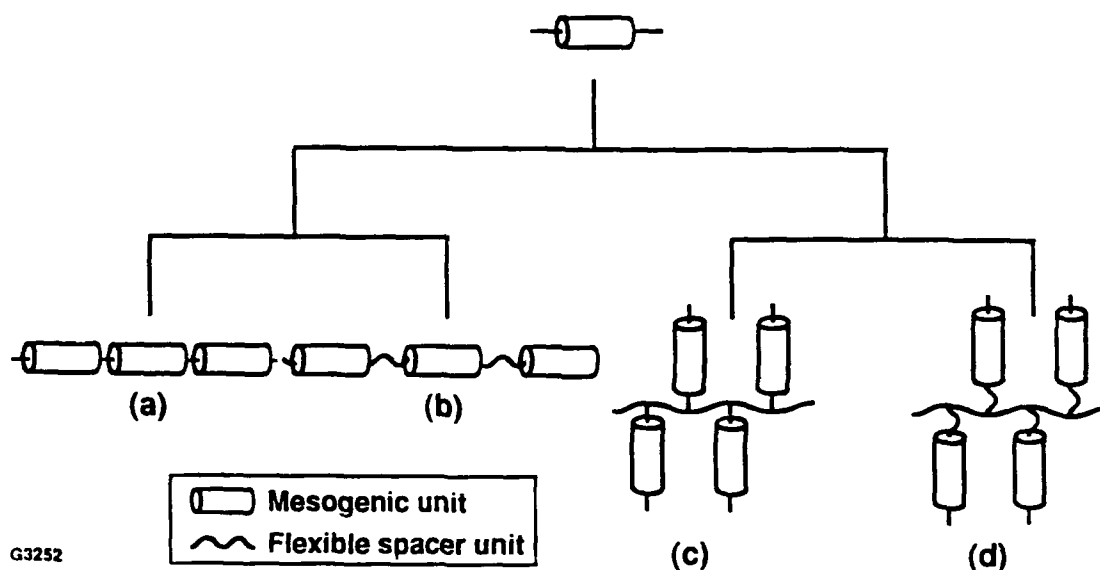
FIGURE 5   Schemes of main-chain type and side-chain type liquid crystalline polymers: (A) rigid, (B) semi-rigid. Mesogenic group is attached to the polymeric backbone without a flexible spacer (C) and with a flexible spacer (D). [From Koide, N., *Mol. Cryst. Liq. Cryst.*, 139, 49, 1986. With permission.]
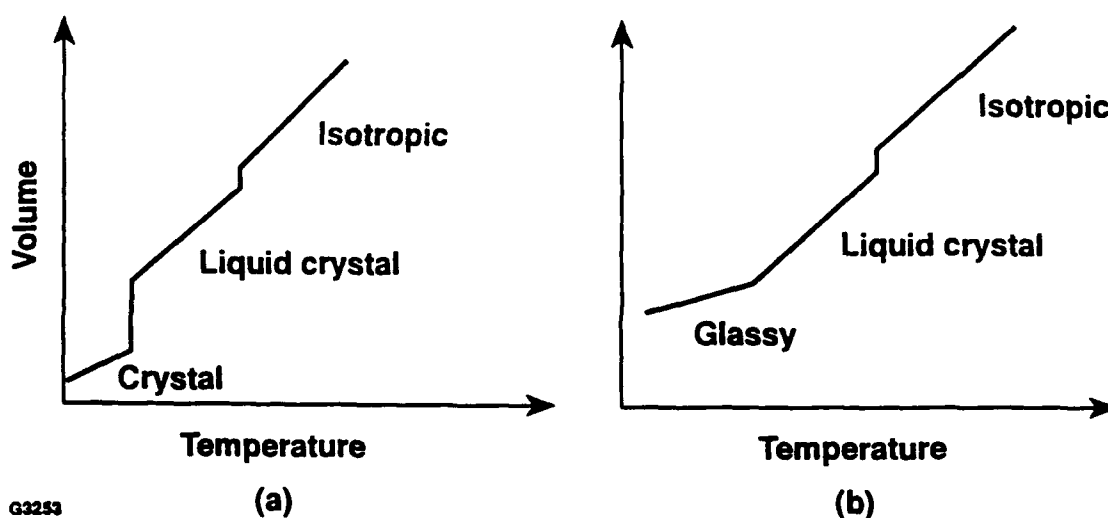
FIGURE 6   Schematic volume-temperature behavior of (a) low molar mass liquid crystals, and (b) LC side-chain polymer. [From Finkelmann, H. and Kock, H. J., *Disp. Technol.*, 1, 85, 1985. With permission.]

12

discovered ferroelectric polymers have demonstrated submillisecond effects. Response versus temperature is shown in Figure 7 for a dye-doped ferroelectric smectic side-chain polymer.[71] Electroclinic (field linear) and field independent behaviors were observed in regions of differing smectic order.

Structure and Basic Optical Properties

Improved understanding of the relationship between liquid crystal optical properties and chemical structure has occurred as a result of work by several groups. Scatter, absorption and birefringence were studied by S. T. Wu et al. for many commercially available nematics.[72-76] Figure 8 shows the scatter coefficient for E7 as a function of temperature. Its value drops by two orders of magnitude between the low temperature, unaligned nematic and high temperature isotropic phases at a wavelength of 633 nm.

With a thermostatically controlled, variable path length cell, Wu et al.[73] confirmed that the electronic absorption tails of E7 and MBBA decrease as λ^{-2} (see Figure 9). Table 4 gives polarized absorption data and associated physical properties for 13 nematic compounds doped into a nematic host. These results were obtained in the UV with special techniques, which included the use of a dichroic LC polarizer. Among the structure-property relations observed was a correlation between conjugation and absorption strength. The series 5PCH, 5CB, 5CT shows a UV absorption peak shift and increase in absorption as structure changes from one to two to three phenyl rings.[74] Conjugation length was also shown to be important for constructing a model to relate three UV resonance absorption bands to birefringence dispersion in nematics.[75] IR absorption and birefringence were also studied.[72,76] Two examples are given in Figure 10.

Improved photostability against the near-UV radiation generated by high-intensity projectors motivated A. M. Lackner et al.[77] to study alternatives to E7 for LC light valves. Eight commercial nematics were tested in acetonitrile or hexane solutions for resistance to change (variations in surface tilt, reductions in cell resistivity) during exposure to filtered light from a cw xenon lamp. After moderate-to-small amounts (less than 1 wt.%) of polar impurities were removed from some of the commercial products, Lackner et al. found that systems with a high degree of saturation (Merck 1800, 1132) were more stable than mostly unsaturated systems (BDH E7; RO-TN619, 2025, and 653; Merck 1738). S. Papernov et al.[78] have made a similar observation with regard to pulsed-laser damage resistance in the UV (described later).

The SED-SOL rules for predicting helical twist sense (or handedness) in low molecular weight cholesterics, as proposed by Gray and McDonnell,[79] have not been successfully applied to the new thermotropic LC polymers. In a series of papers, S. H. Chen and co-workers[80-82] have shown that, for side chain systems where spacers decouple the thermodynamic features of mesogenic side groups from the polymer backbone, configurational characteristics around the asymmetric carbon center determine handedness. Figure 11 shows the rudiments of their model for predicting helical twist sense. For the three chiral moieties shown, a favorable face-to-face arrangement of chiral and nematic components gives rise to a left-handed helical configuration.
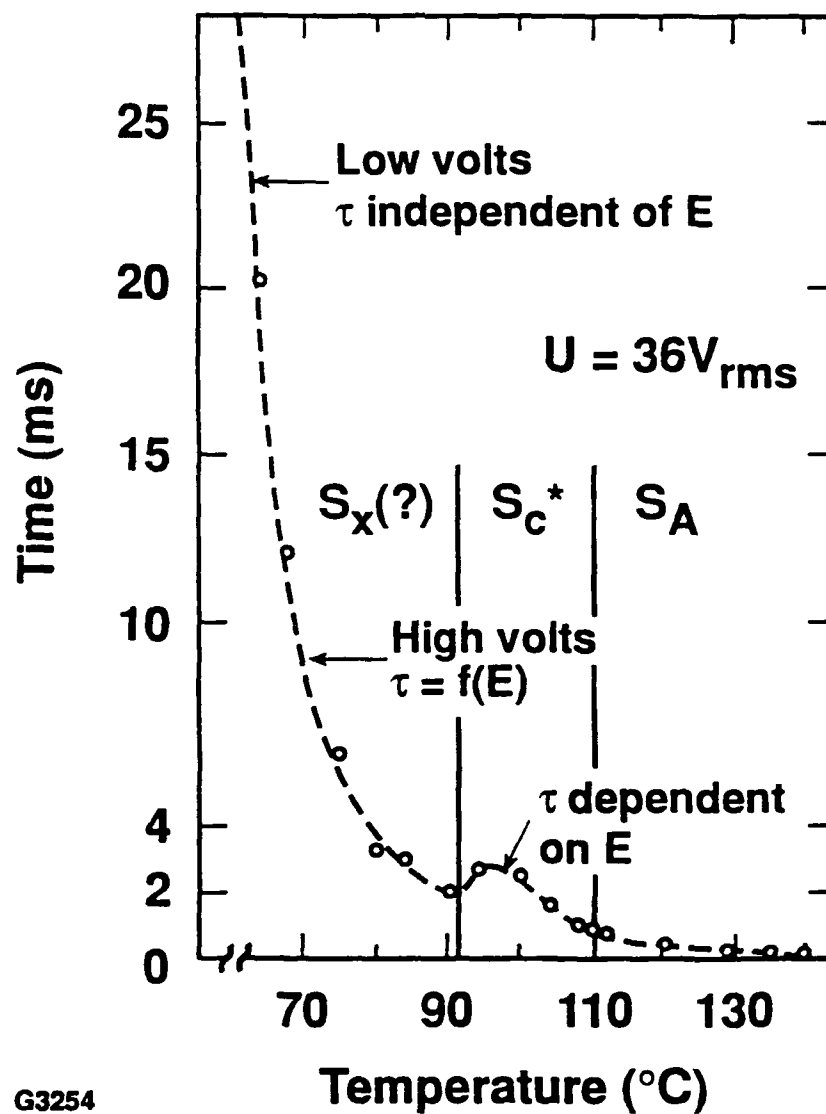
FIGURE 7   LC copolymer response time τ versus temperature for a 4-μm sample thickness [From Scherowsky, G., Beer, A., and Coles, H. J., *Liq. Cryst.*, 10, 815, 1991. With permission.]
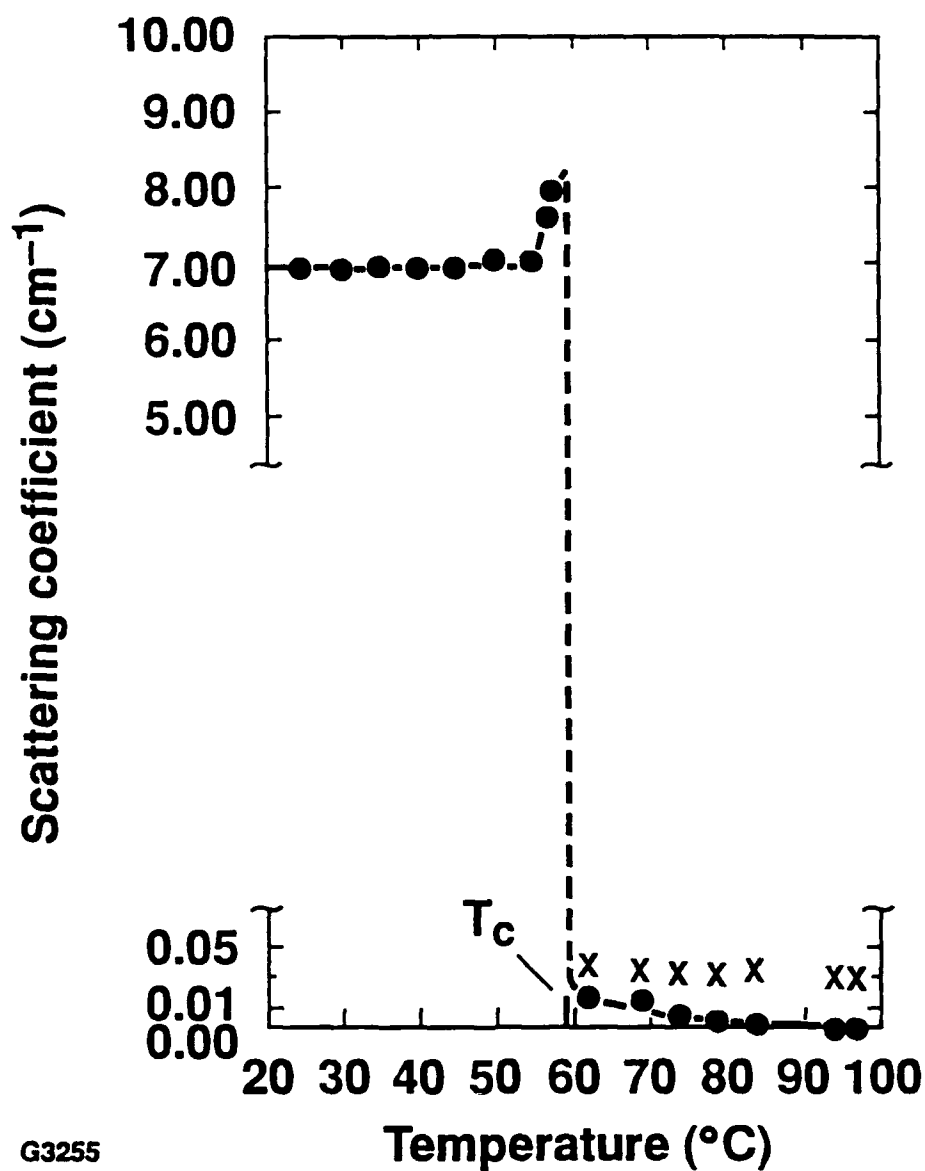
FIGURE 8   Temperature-dependent scattering coefficient for unaligned E7. The clearing point is ~59.5°C. The cross data points represent the corresponding absorption coefficients. The measurement wavelength is λ = 633 nm. [From Wu, S.-T. and Lim, K. C., *Appl. Opt.*, 26, 1726, 1987. With permission.]

15
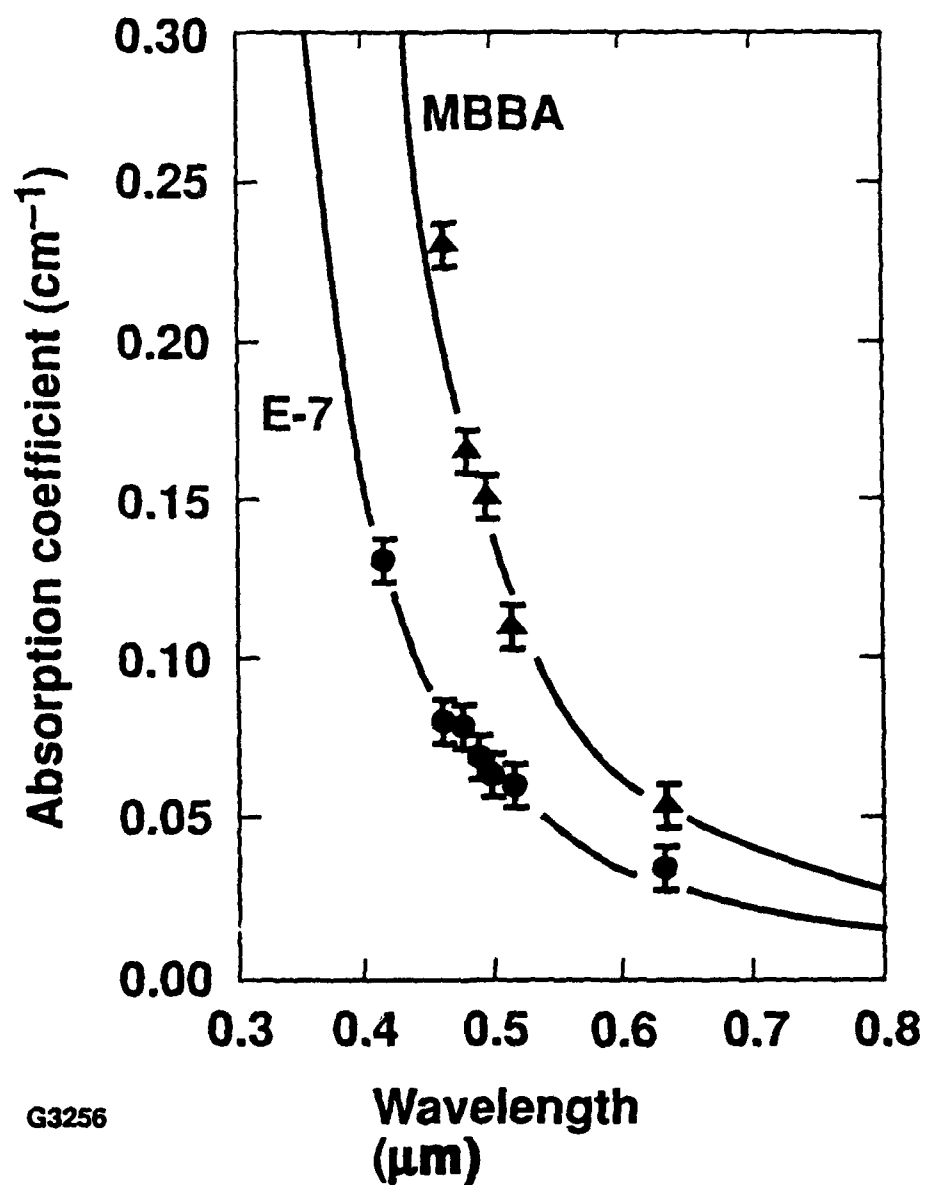
FIGURE 9   Wavelength-dependent absorption coefficients for E7 and MBBA at T = 90°C and T = 60°C, respectively. [From Wu, S.-T. and Lim, K. C., *Appl. Opt.*, 26, 1726, 1987. With permission.]

16

TABLE 4

Chemical, physical, and optical properties of 13 LC compounds used for absorption measurements. Δn–birefringence at $T = 20°C$ and $\lambda = 589$ nm, $\Delta\varepsilon$–dielectric anistropy, ν–flow viscosity, ΔH–melting enthalpy, λ_2–peak(s) of one UV absorption band, $\alpha_{\parallel}$ and $\alpha_{\perp}$–absorption coefficient measured at $T = 22°C$ for 1 wt% of each nematic in LC host ZLI-2359. [Wu, S. T., Ramos, E., and Finkenzeller, U., *J. Appl. Phys.*, 68, 79 and 84, 1990. With permission.]

LC	Structure	Nematic Range (°C)	Δn	$\Delta\varepsilon$	$\nu 20°C$ (mm^2/S)	ΔH (KCal/Mole)	λ_2 (nm)	$\alpha_{\parallel}$ (μm^{-1})	$\alpha_{\perp}$ (μm^{-1})
1. 5PCH	C_5H_{11}–(H)–(O)–CN	30–55	0.12	13	22	5.1	235	26.6	4.8
2. 3NCS	C_3H_7–(H)–(O)–NCS	39–41	0.20	13	8	3.6	272 284	27.2 28.8	4.2 4.4
3. 5CB	C_5H_{11}–(O)–(O)–CN	22–35	0.20	17	24	4.1	282	52.6	9.5
4. 5OCB	$C_5H_{11}O$–(O)–(O)–CN	52–68	0.23	17	37	6.9	298	51.8	8.3
5. 5CDP	C_5H_{11}–(O)–C≡C–(O)–CN	77–(71)	0.30	10	40	6.9	304 323	56.0 55.2	9.0 9.2
6. 3OCDP	C_3H_7O–(O)–C≡C–(O)–CN	98–103	0.32	12	40	5.0	318 334	58.5 56.7	8.7 8.6
7. PTP-502	C_5H_{11}–(O)–C≡C–(O)–OC_2H_5	61–89	0.27	0.2	20	5.6	294 313	47.9 42.4	7.1 6.0
8. PTP-502FF	C_5H_{11}–(O)–C≡C–(O,FF)–OC_2H_5	57–61	0.25	–4.4	17	6.2	292 311	72.1 67.5	10.9 10.0
9. T-33FF	C_3H_7–(O)–(O)–(O,FF)–C_3H_7	132–149	0.24	–1.9	33	6.8	287	53.9	7.8
10. T-3FF3	C_3H_7–(O)–(O,FF)–(O)–C_3H_7	95–131	0.24	–1.7	31	5.8	283	55.4	7.5
11. 5CT	C_5H_{11}–(O)–(O)–(O)–CN	131–240	0.30	16	86	6.1	306	54.3	6.2
12. PTPT-35	C_3H_7–(O)–C≡C–(O)–C≡C–C_5H_{11}	72–(40)	0.30	0.5	26	7.5	304 324	73.6 69.0	11.5 11.5
13. PTTP-55	C_5H_{11}–(O)–C≡C–C≡C–(O)–(O)–C_5H_{11}	86–111	0.36	0.8	32	4.6	296 315 336	46.3 60.9 49.3	5.8 7.8 6.9

17
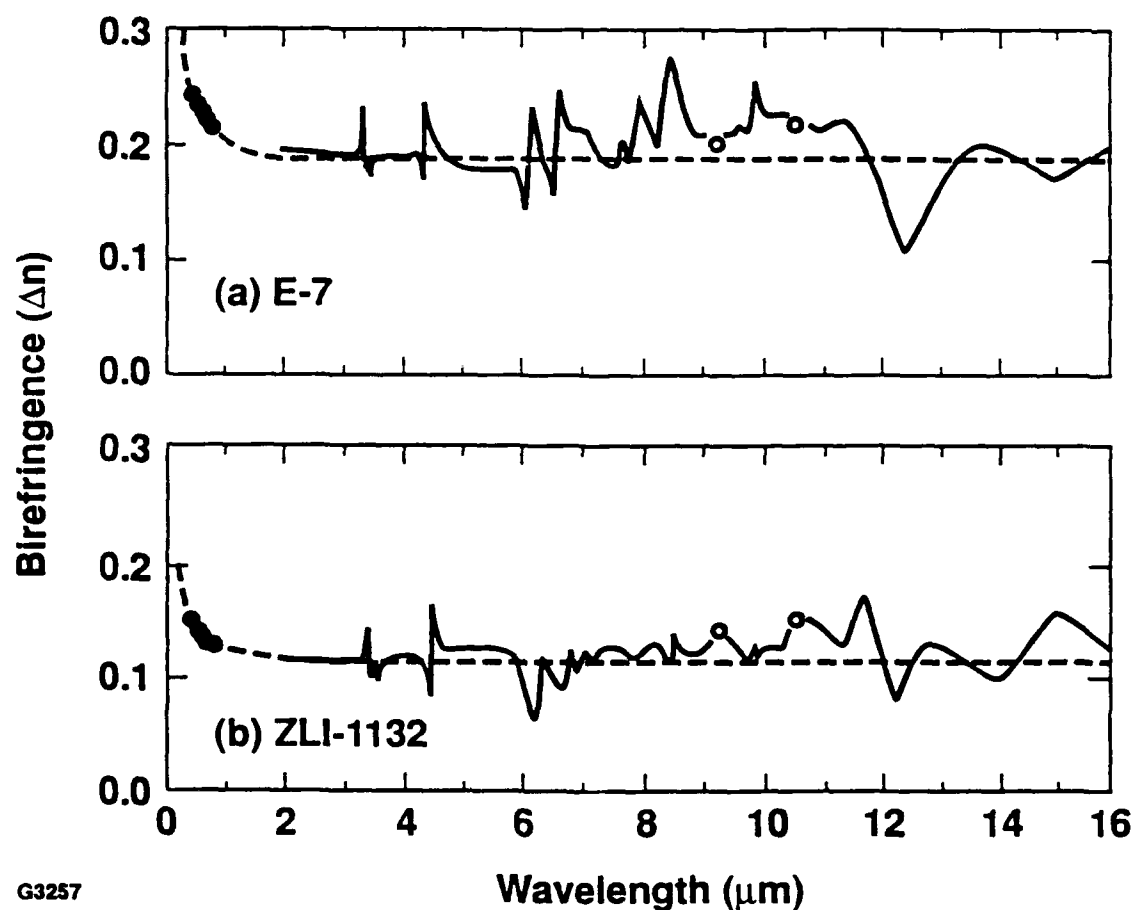
FIGURE 10   Wavelength-dependent birefringence for two LC compounds: (a) E7, (b) ZLI-1132. Closed circles represent data obtained at discrete Ar+ and He-Ne laser wavelengths. Solid lines represent the IR birefringence measured at 9.27 and 10.59 μm CO_2 laser wavelengths. The dashed lines represent a theoretical calculation. [From Wu, S.-T., *Opt. Eng.*, 26, 122, 1987. With permission.]

18
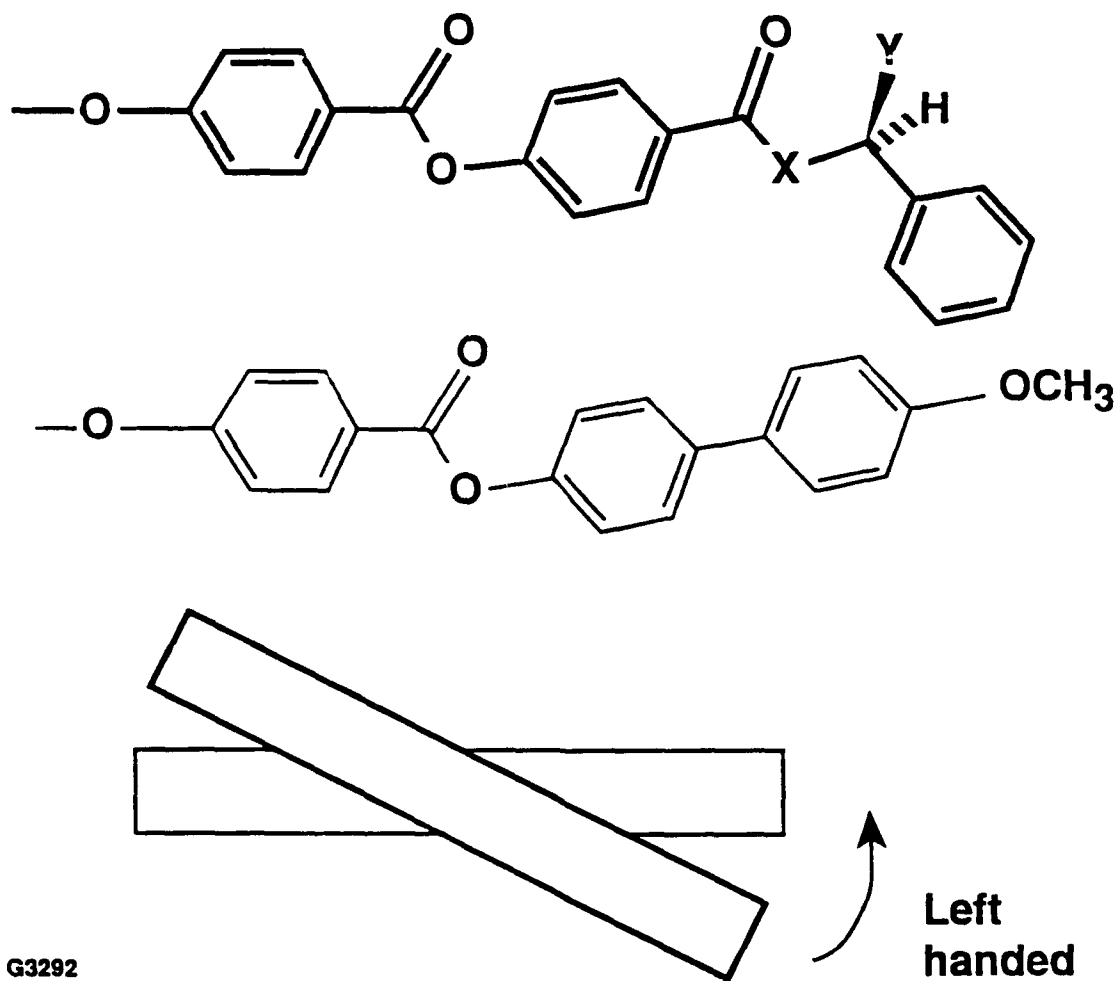
FIGURE 11 Chiral/nematic molecular interaction model for the interpretation of left-
handedness of copolymer 1, X = O and Y = CH$_3$, copolymer 2, X = NH
and Y = CH$_3$, and copolymer 3, X = O and Y = COOCH$_3$ [From
Krishnamurthy, S. and Chen, S. H., *Macromolecules*, 24, 3483, 1991.
With permission.]

19

PASSIVE ELEMENTS AND APPLICATIONS

Selective Reflection

Passive liquid crystal elements like polarizers, filters or mirrors consist of a chiral nematic medium confined between two flat glass substrates as shown in Figure 12. The helical structure depicted in this figure leads to the important optical properties of selective (wavelength) reflection and circular polarization (circular dichroism). The optical field reflected by a chiral-nematic liquid crystal (CLC) preserves its sense of polarization, whereas the field reflected by a dielectric mirror changes its polarization from right to left circular or vice versa.[83]

To understand both the exact and approximate expressions for reflection and reflection-bandwidth, Lee and Jacobs[84] considered a right-handed CLC cell with thickness L in Figure 12 whose helical axis is oriented along the z-axis. When right circularly polarized light with wavelength λ propagates along the z-axis at normal incidence, the reflectivity is given by[85]

$$R = \frac{\sinh^2\left(\kappa L\sqrt{1 - (\delta/\kappa)^2}\right)}{\cosh^2\left(\kappa L\sqrt{1 - (\delta/\kappa)^2}\right) - (\delta/\kappa)^2} ,$$

(1)

where $\delta = 2\pi(1/\lambda - 1/\lambda_0)\sqrt{\varepsilon_{av}}$ is the detuning parameter; $\kappa = \frac{2\pi}{\lambda}\frac{\varepsilon_a}{4\sqrt{\varepsilon}}$ is the coupling coefficient; $\lambda_0 = \sqrt{\varepsilon_{av}}\,P_0$ is the peak wavelength of the selective reflection band, where P_0 is the pitch length of CLC; $\varepsilon_a = \varepsilon_{\parallel} - \varepsilon_{\perp}$ is the optical dielectric anisotropy; $\varepsilon_{av} = (\varepsilon_{\parallel} + \varepsilon_{\perp})/2$ is the average optical dielectric constant; and L is the CLC fluid thickness. Here $\varepsilon_{\parallel}$ and $\varepsilon_{\perp}$ are the optical dielectric constant parallel and perpendicular, respectively, to the director. Since $\sqrt{\varepsilon_{av}} \approx n_{av}$, the parameters described above can be approximated as follows:

$$\kappa = \frac{\pi}{\lambda}\Delta n$$

(2)

$$\frac{\delta}{\kappa} = \frac{2}{\gamma}\left(1 - \frac{\lambda}{\lambda_0}\right)$$

(3)

$$\gamma = \frac{\varepsilon_{\parallel} - \varepsilon_{\perp}}{\varepsilon_{\parallel} + \varepsilon_{\perp}} \approx \frac{\Delta n}{n_{av}} ,$$

(4)

where $\Delta n = n_e - n_0$ is the optical birefringence and $n_{av} = (n_e + n_0)/2$ is the average refractive index. Here n_e and n_0 represent the extraordinary and ordinary refractive indices, respectively, of the nematic substructure shown in Figure 12.
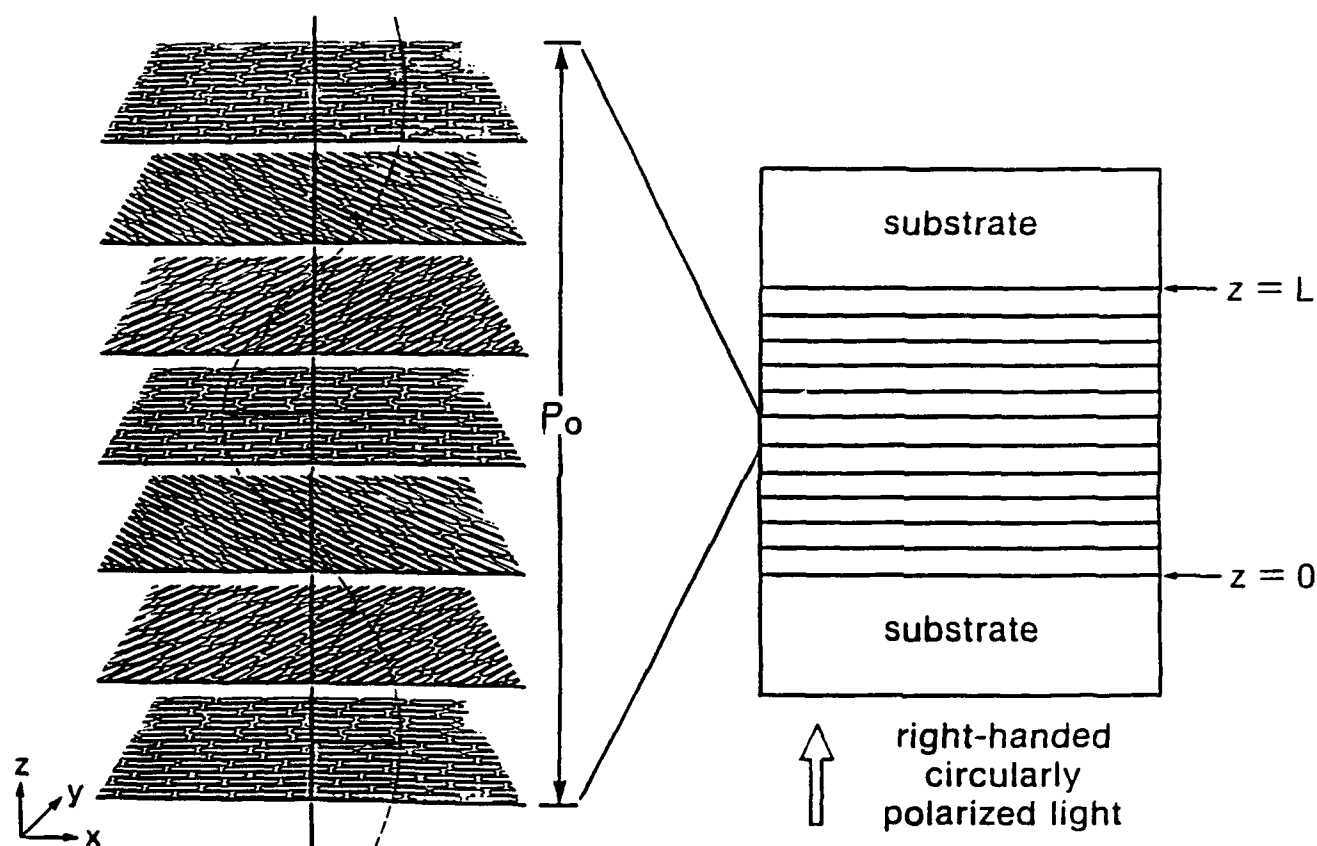
FIGURE 12   Schematic diagram of a chiral-nematic liquid crystal cell. The left-handed
side of the figure shows one pitch length of the helical structure in the CLC.
Arrows within each plane indicate director orientation [From Lee, J.-C. and
Jacobs, S. D., *J. Appl. Phys.*, 68, 6523, 1990. With permission.]

21

When $\lambda = \lambda_0$, the CLC structure is well phase-matched to the input wavelength, and the reflectivity in Equation 1 reduces to

$$R = \tanh^2(\kappa_0 L) .\qquad(5)$$

where $\kappa_0 = \dfrac{\pi}{\lambda_0} \Delta n$. To maximize selective reflection with R = 0.999, the $\kappa_0 L$ required is equal to 4.147. To act as a partial reflector with R = 0.90, the $\kappa_0 L$ required is equal to 1.818. Since the coupling coefficient is proportional to birefringence, materials with lower birefringence require more CLC fluid thickness than those with higher birefringence. These trends are illustrated in Figure 13 for wavelengths in the visible and near-infrared.

A plot of reflectivity, R, as a function of λ/λ_0 for $\kappa_0 L = 4.59$ (which corresponds to R = 0.9991) is shown in Figure 14. It can be seen that when $\lambda/\lambda_0 = 1.076$, the reflectivity of the CLC goes to zero. The ripples in this figure are due to phase mismatching. The selective reflection bandwidth may be defined as the wavelength difference between the first zeros. From Equation 1, the exact selective reflection bandwidth $\Delta\lambda$ is given by

$$\Delta\lambda = 2 \frac{\sqrt{1 - \left(1 - \gamma^2/4\right)\left[1 - \left(P_0/2L\right)^2\right]}}{1 - \left(P_0/2L\right)^2} \lambda_0 .\qquad(6)$$

Note that the selective reflection bandwidth depends on the thickness in this exact expression. When $P_0/L \ll 1$, the selective reflection bandwidth reduces to[83]

$$\Delta\lambda = \gamma \lambda_0 \approx \frac{\Delta n}{n_{av}} \lambda_0 .\qquad(7)$$

This equation shows that the bandwidth of a CLC element tuned to a visible wavelength ($\lambda_0 = 532$ nm) is narrower than that for an element tuned to a near-infrared wavelength ($\lambda_0 = 1064$ nm) by a factor of 2. Bandwidth is also proportional to the birefringence of the material. The birefringence dispersion in the near-infrared is negligible, as shown in Figure 10, so that the birefringence measured at λ_0 can be used. Fluid thickness no longer enters into the equation.

To experimentally verify the relationships in Equation 5 and Equation 6, the refractive indices of two different CLC blends were first measured to calculate the coupling coefficient κ_0. The procedure for measuring the refractive index of a CLC is straightforward. CLC's have a birefringence which is related to that of the nematic substructure (see Figure 12) perpendicular to the helical axis by the following equations:[86]

$$n_{e,ch} = n_{o,n}, \qquad n_{o,ch} = \left[0.5\left(n_{e,n}^2 + n_{o,n}^2\right)\right]^{\frac{1}{2}} ,\qquad(8)$$

22

$$R = \tanh^2 (\kappa L), \text{ where } \kappa = \frac{\pi}{\lambda} \Delta n$$

At $\lambda_o = 500$ nm

At $\lambda_o = 1000$ nm
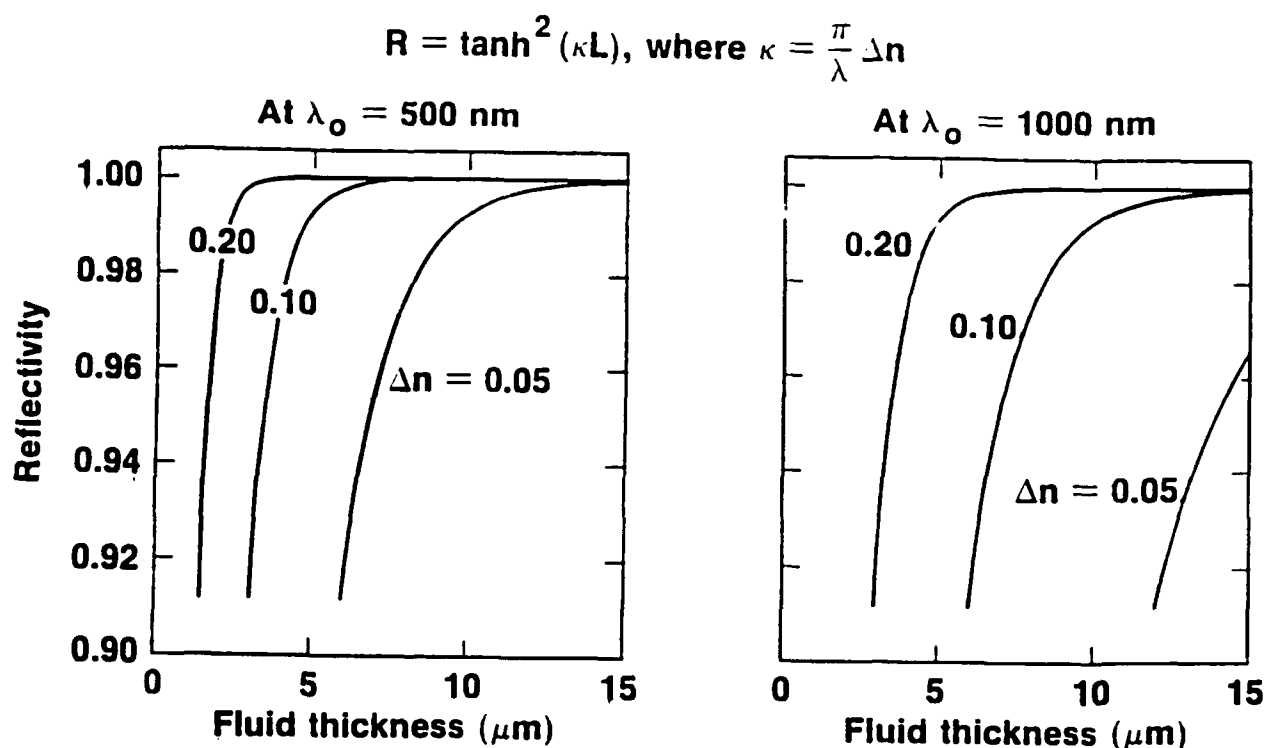
G3069

FIGURE 13   Calculated cholesteric liquid crystal element reflectivity at λ_o, the wavelength for selective reflection, as a function of medium layer thickness, L. Materials with high birefringence give high values of reflectivity in thin layer thickness.

23
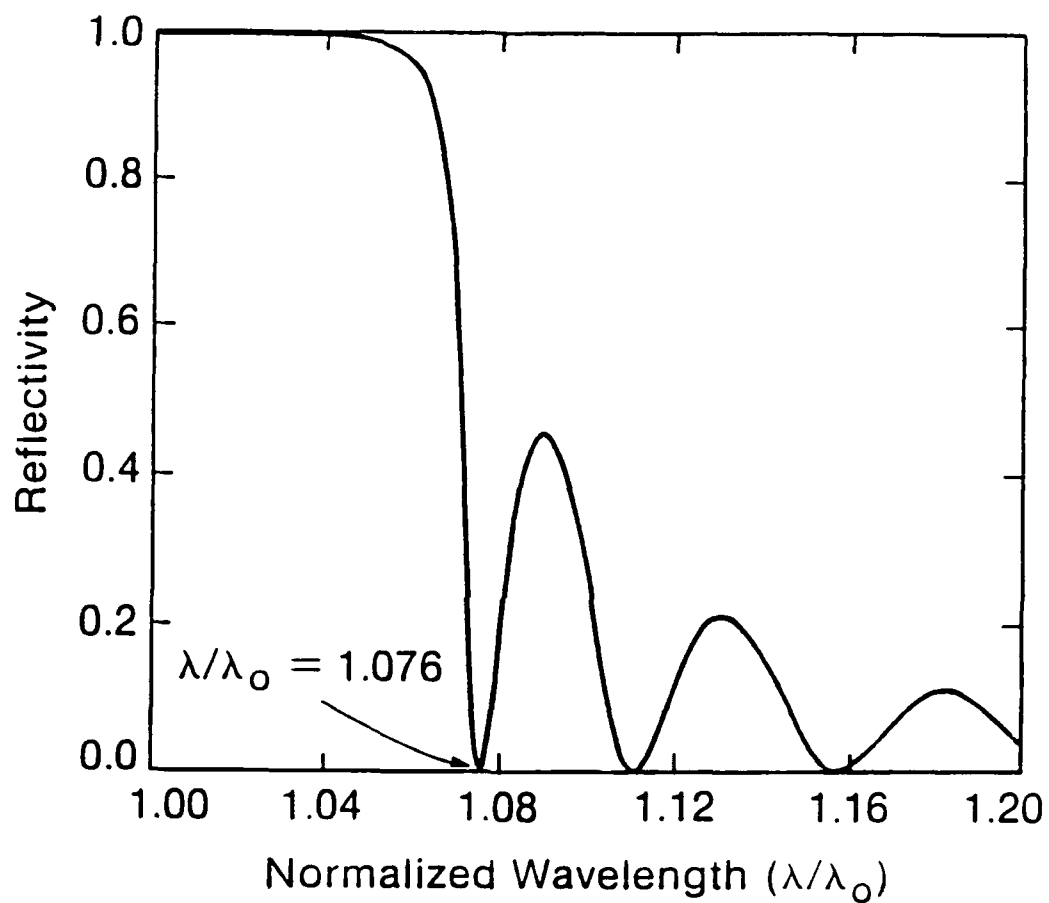
G2704

FIGURE 14 Reflectivity R as a function of normalized wavelength λ/λ_0 for $\kappa_0 L = 4.59$. [From Lee, J.-C. and Jacobs, S. D., *J. Appl. Phys.*, 68, 6525, 1990. With permission.]

24

where $n_{e.ch}$, $n_{o.ch}$ represent the refractive indices for the chiral structure and $n_{e.n}$, $n_{o.n}$ for the nematic substructure. When an Abbé refractometer is used to measure the refractive indices of the CLC, $n_{e.ch}$ and $n_{o.ch}$ are obtained. The refractive indices $n_{e.n}$, $n_{o.n}$ are calculated from Equation 8 as well as the average refractive index, the birefringence, and the coupling coefficient κ_0. The measurements and calculations are summarized in Table 5 for the two CLC blends identified as mixtures II and III.

TABLE 5 Measurements and calculations of refractive index and coupling coefficient at 22°C for two CLC mixtures. [Lee, J. C. and Jacobs, S. D., *J. Appl. Phys.*, 68, 6524, 1990. With permission.]					
Blends with λ_O = 1064 nm	$n_{e,n}$	$n_{o,n}$	n_{av}	Δn	κ_0
Mixture I: 21.4 wt% CB15 + 78.6 wt% E7	1.6860	1.5121	1.5991	0.1739	0.5182
Mixture II: 19.29 wt% CB15 + 80.71 wt% ZLI1167	1.5495	1.4703	1.5099	0.0792	0.2238

In order to confirm Equation 5, a wedged cell with weak anchoring[87] on both inner substrate surfaces was fabricated. The reflectivity as a function of thickness is sho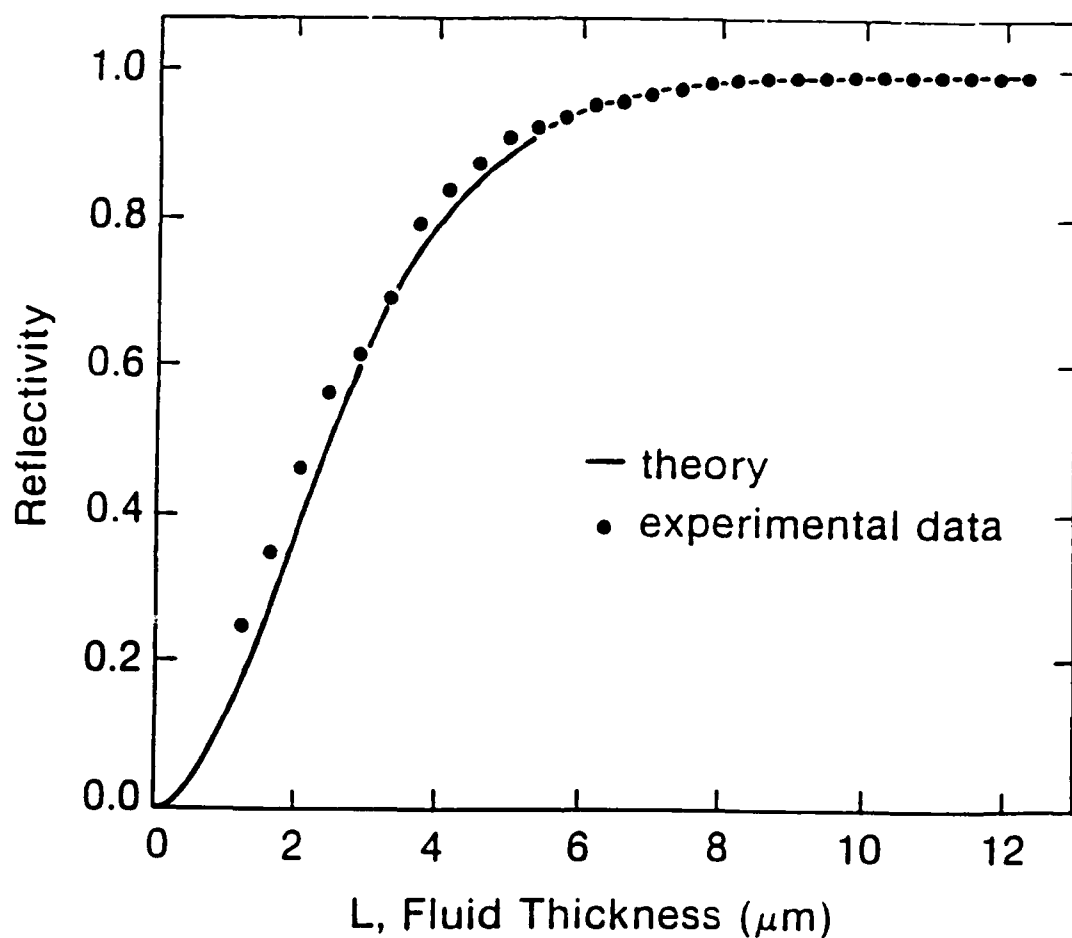wn in Figure 15. The close match of theoretical and experimental data supports the validity of Equation 5. From Equation 5, the thicknesses required for R = 0.999 are calculated to be 8.0 μm and 18.5 μm, respectively, for mixtures I and II.

In order to confirm Equation 6, two 38-mm-diam CLC elements were assembled using BK-7 glass substrates, separated by Mylar® spacers. Each gap was filled by capillary action with one of the right-handed CLC mixtures I and II described in Table 5. Spectral transmission scans are shown in Figure 16. From this figure, the wavelength separation between the first maxima was used as a measure of the bandwidth. The bandwidths for mixture I with a 9-μm fluid thickness, and for mixture II with a 12-μm fluid thickness are summarized in Table 6 with theoretical calculations from Equation 6 and Equation 7. The experimental results for both mixtures agree well with theoretical calculations from Equation 6. The use of the approximate Equation 7 gives close to a 30 nm difference in bandwidth for both mixtures.

TABLE 6 Theoretical calculations of selective reflection bandwidth and the measured results. [Lee, J. C. and Jacobs, S. D., *J. Appl. Phys.*, 68, 6525, 1990. With permission.]				
	L [μm]	**$\Delta\lambda$[nm] measured**	**$\Delta\lambda$[nm] from Equation 6**	**$\Delta\lambda$[nm] from Equation 7**
Mixture I:	9	150	146	115
Mixture II:	12	84	82	56

G2703

FIGURE 15   Reflectivity R measured at $\lambda = 1064$ nm, as a function of thickness L, for mixture I: E7 and CB15 tuned to exhibit a selective reflection band peak at $\lambda_0 = 1064$ nm. The solid line represents the result of theoretical calculation, and the circles represent experimental data. [From Lee, J.-C. and Jacobs, S. D., *J. Appl. Phys.*, 68, 6525, 1990. With permission.]
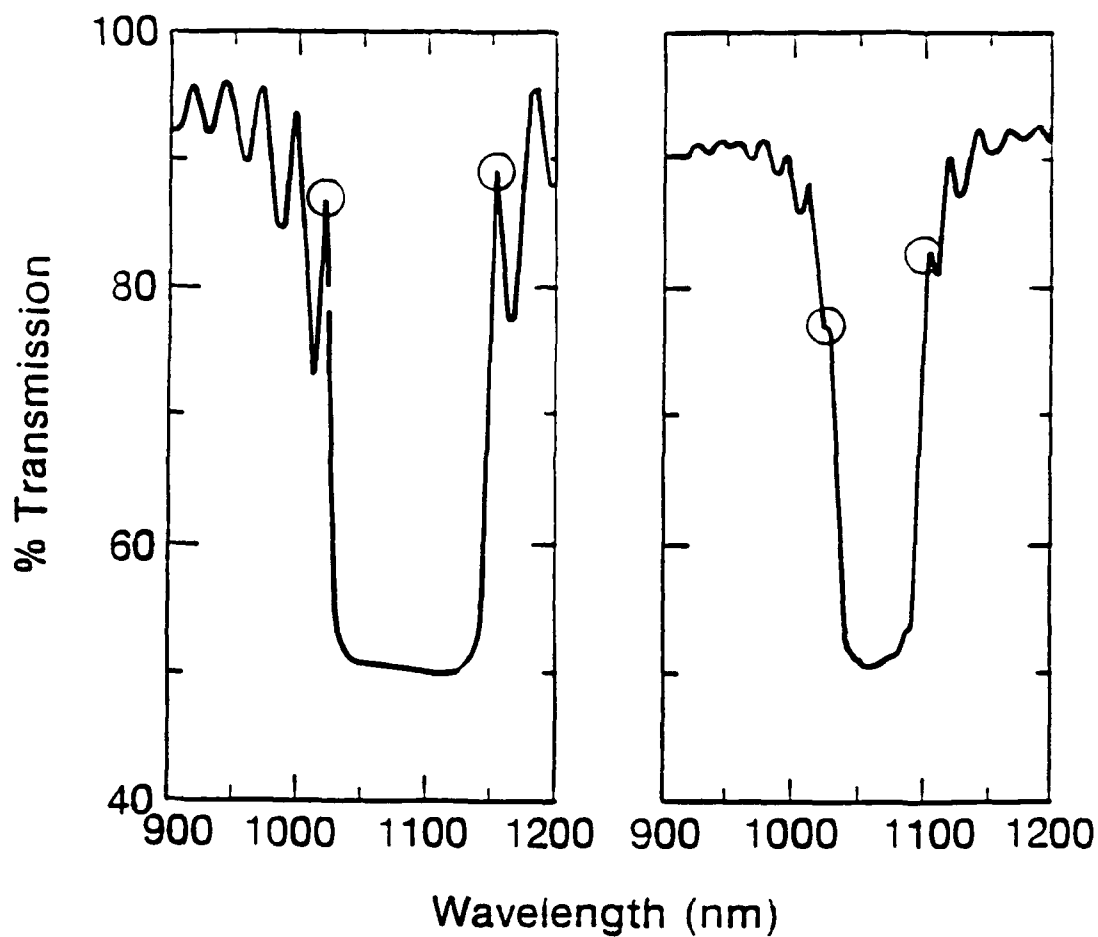
FIGURE 16 Spectral transmittance scans for two CLC mirrors: (a) mixture I: E7 and CB15; (b) mixture II: ZLI 1167 and CB15. Maxima used to calculate bandwidth are circled. [From Lee, J.-C. and Jacobs, S. D., *J. Appl. Phys.*, 68, 6525, 1990. With permission.]

The selective reflection effect in CLC's for light propagating obliquely to the helical axis has been studied by H. Takezoe and co-workers.[88-90] The evolution of a region exhibiting total reflection within the selective reflection band was documented with measurements taken in reflection at angles of incidence varying from 38° to 62°. A series of spectra taken on a very high quality monodomain CLC with nearly LH or RH circular polarization is shown in Figure 17. The major features of these spectra are shown to be consistent with theories previously proposed.[91,92] The total reflection band is centered within the selective reflection band. It becomes distinct at angles beyond 40° and for cell thicknesses above 18 μm. Takezoe *et al.* have proposed a tunable optical rotator based upon this total reflection effect.[93]

Devices and Applications

Passive CLC elements have been incorporated into a number of electro-optic systems. Although not laser-based, an all-liquid crystal color projection system proposed by M. Schadt and J. Fünfschilling[94] contains many unique features. The nonreciprocal, nonabsorbing nature of the selective reflection effect and its wavelength selectivity permit the device in Figure 18 to be envisioned. Here, nine passive CLC elements, tuned individually to the red, green or blue with left or right handedness, convert unpolarized white light to a polarized state with nearly 100% efficiency. The low molecular weight CLC mixtures are temperature-compensated blends that possess a low-temperature coefficient for selective reflection peak position of $d\lambda_o/dT < 0.1$ nm/°C between 0°C and 50°C. The total reflection bandwidth is minimized for these oblique incidence CLC polarizing beam splitters by using 8-μm-thick fluid layers.

An all-liquid crystal 2×2 switch for multimode fiber-optic systems has been constructed and tested by N. K. Shankar and colleagues.[95] The nonreciprocal nature of the 19-μm-thick, right-handed CLC polarizer/beam splitter permits this passive element in Figure 19 to discriminate between orthogonal circular polarization states generated by electro-optic liquid crystal wave plates. The result is a nonmechanical switch operating at $\lambda = 1318$ nm with 1.4 dB insertion loss to a connected port and crosstalk of -28 dB to an unconnected port. Soref[96] suggested several ways to extend the Shankar concept to 4×4, 1×4, and 1×16 arrays.

High-optical quality CLC polarizer/isolators have been incorporated into the design and operation of high-peak power solid-state laser systems used to investigate inertial confinement fusion. Researchers at the University of Rochester improved the beam-to-beam energy balance of OMEGA, their 24-beam Nd:glass laser system, by installing sixty 100-mm-diameter CLC polarizer/isolators at various stages between beamline amplifiers during 1986.[83]

Each element consisted of a right-handed fluid layer, 18 μm thick, sandwiched between two AR-coated borosilicate glass substrates. Single-pass transmitted wavefront quality of ≤0.1 wave at $\lambda = 1054$ nm was demonstrated. This was found to be limited by epoxy sealants that distorted assembled cells. Easily installed and used at near-normal incidence, a typical RH element exhibited a transmittance, T > 98% for LH circularly polarized, forward propagating laser radiation at $\lambda = 1054$ nm, and an extinction for back-reflected laser radiation of >2000:1.

18-μm-thick cell
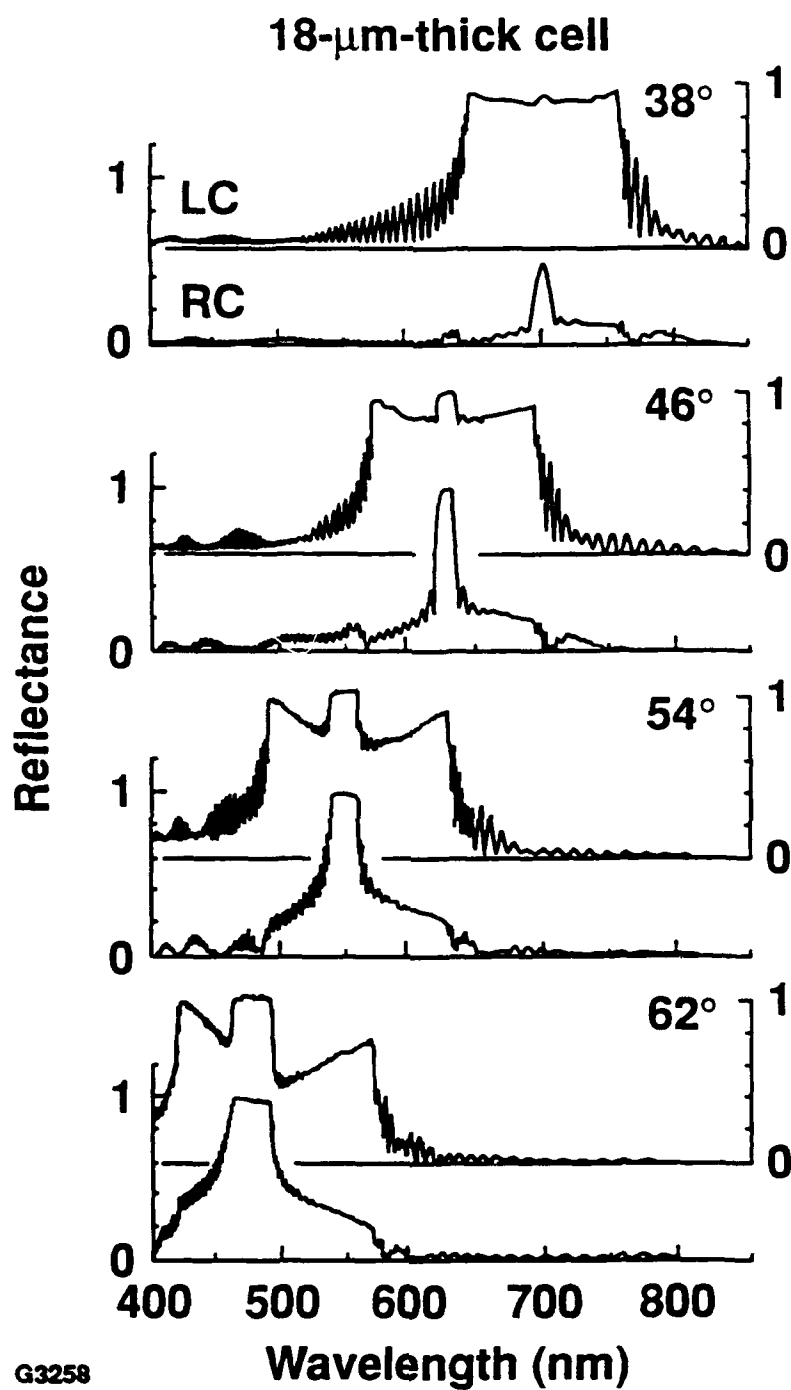
G3258

FIGURE 17   Reflection spectra in a monodomain cholesteric liquid crystal cell of 18 μm thickness at various angles of incidence. The incident polarizations used are (nearly) left and right circular polarization. An analyzer is not used. [From Takezoe, H., Ouchi, Y., Hara, M., Fukuda, A., and Kuze, E., *Jpn. J. Appl. Phys.*, 22, 1083, 1983. With permission.]

29
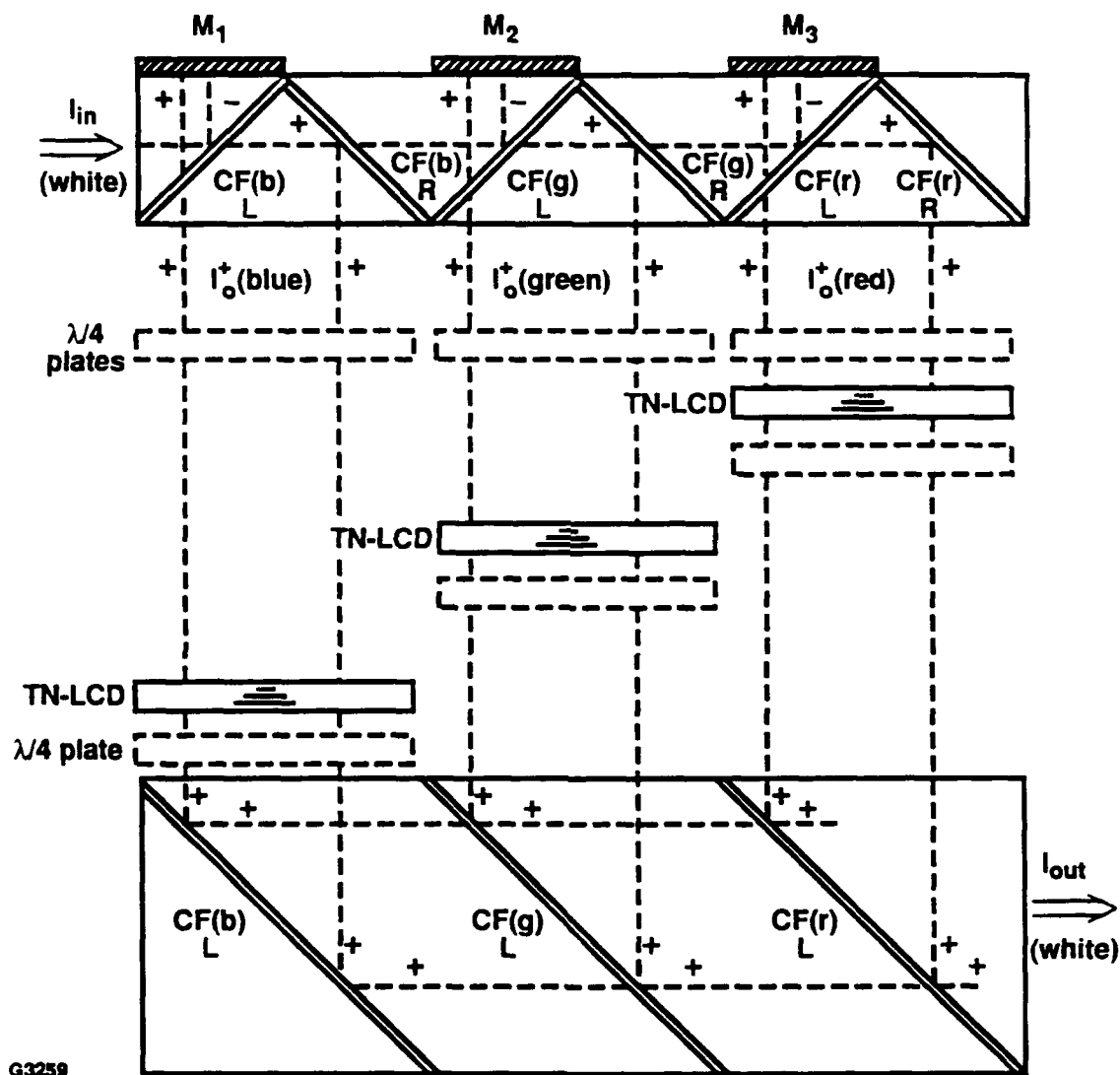
FIGURE 18   Schematic diagram of the liquid crystal polarized color projection (LC-PCP)
optics. M_i = mirrors; CF_L, CF_R = left- and right-handed cholesterics filters;
TN-LCD = twisted nematic LC devices. [Schadt, M., and Fünfschilling,
Jpn. J. Appl. Phys., 29, 1980, 1990. With permission.]
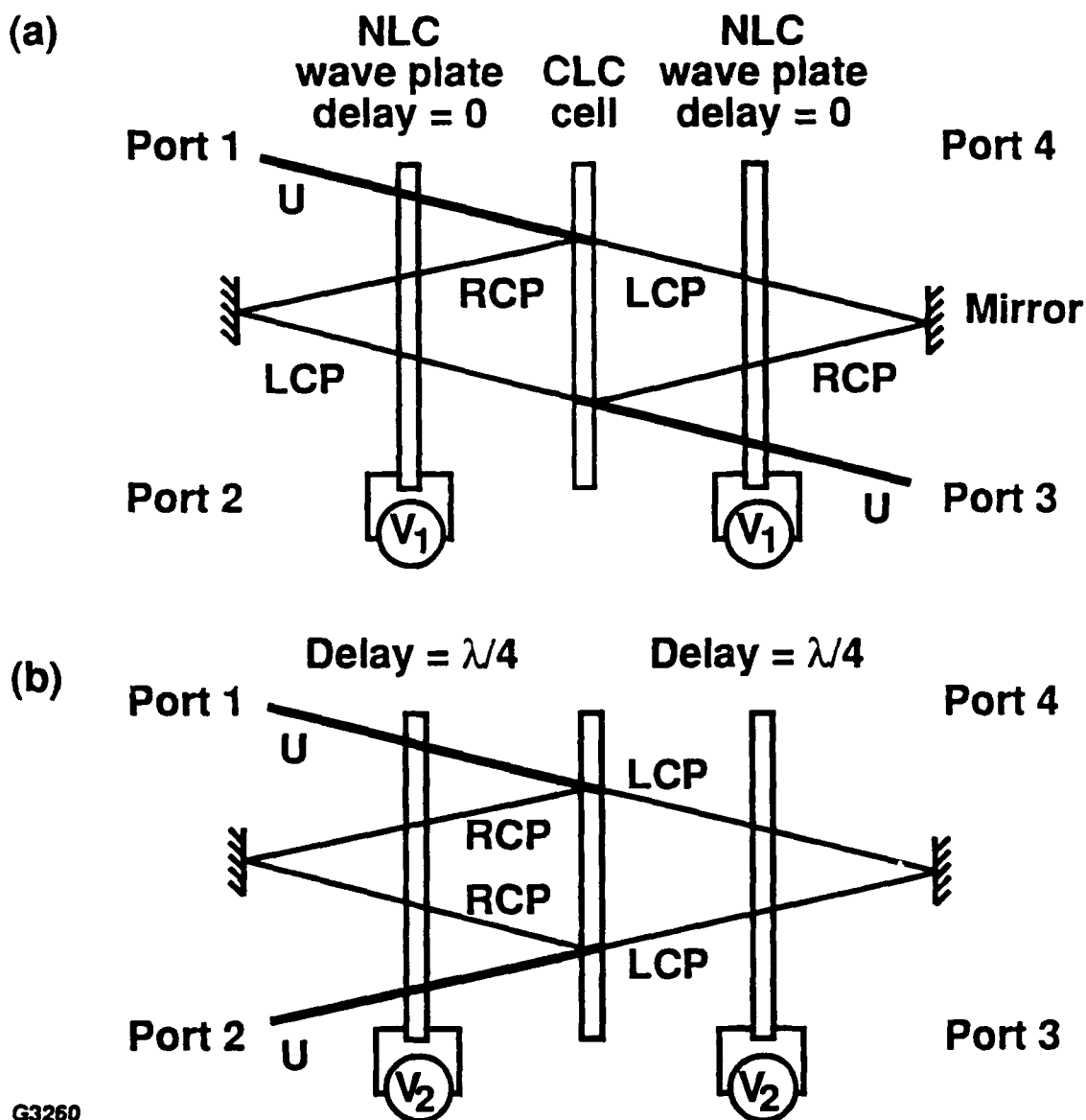
30

FIGURE 19 Schematic operation of the 2 × 2 CLC switch. "U," "RCP," and "LCP" refer to unpolarized, right circular polarized, and left circular polarized light, respectively. With the wave plates at zero-delay (a), port 1 connects to port 3. With the wave plates at quarter-wave delay (b), port 1 connects to port 2. The beam paths from port 4 have been omitted for clarity. [Shankar, N. K., Morris, J. A., Yakymyshyn, C. P., and Pollock, C. R., *IEEE Photon. Tech. Lett.*, 2, 148, 1990. With permission.]

Issues of laser damage originally limited the useful life of CLC elements to less than a few hundred shots. The removal of extrinsic impurities (e.g. dust) during device assembly, and the use of saturated nematics as discussed later in this article, eliminated long-term degradation at fluences of several joules per cm^2.

The polarization/isolation features of CLC elements and the simplicity of their construction have made them attractive in systems similar to OMEGA, where propagation of circularly polarized laser radiation is preferred.[97] Low cost and scalability prompted the Rochester group to demonstrate CLC polarizer/isolator elements in diameters of 135 mm and 200 mm during 1991. Fabrication of over 200 such elements has begun in anticipation of their installation in the OMEGA Upgrade[98] laser in 1994.

Extensive development has occurred in tailoring the properties of CLC's for laser filter applications. Charlet and Gray[99] studied aqueous phases of (hydroxypropyl) cellulose. Although it is lyotropic and requires sealing to prevent loss of moisture, HPC is interesting because of its right-handed structure and low birefringence. This last feature leads to elements with bandwidths less than 10 nm. Fluid layer thicknesses greater than 200 μm were required to observe intense polarization effects.

Following Tsutsui et al.,[56,57] Ishihara and co-workers[100] characterized free-standing optical filters from lyotropic polypeptide compounds stabilized against mechanical distortion and temperature variations by photoinitiated polymerization. Films were prepared by polymerizing triethylene glycol dimethacrylate (TGDM) in poly[γ-butyl-L-glutamate] (PBuLG-right handed) and poly[γ-butyl-D-glutamate] (PBuDG-left handed). Using the definitions given in Figure 20, Ishihara's group determined the changes in CLC filter absorbance and bandwidth as film thickness was varied from 50 μm to 300 μm (see Figure 21). Film pairs were successfully laminated together to form notch filters without supporting substrates.

Another form of environmentally stable notch filter, composed of poly[γ-benzyl-L-glutamate] (RH) and CLC silicones (LH), was constructed by Tsai et al.[101] with an alignment quality good enough to permit a blocking extinction of 100:1 to be achieved at λ = 545 nm. Vastly improved temperature stability for CLC silicones has recently been achieved (see Figure 22) by crosslinking the structure with methacrylated mesogenic monomers.[102]

Laser-beam apodization has been a goal of solid-state laser researchers since the early 1970's. Apodizers based upon CLC's are fundamentally different from all other technologies. Since the selective reflection effect is nonabsorptive, it can be used to attenuate laser radiation without such loss. This decoupling of the rejection mechanism from the optical refractive index permits the construction of devices that exhibit a level of optical quality that remains high over the device clear aperture and well into the region of apodization.

Early CLC apodizers studied by Jacobs et al.[83] were constructed from a notch filter configuration with the flat central spacer element replaced by a biconvex lens (see the discussion and figure in Sec. 4: Filter Materials, by Lee M. Cook). Refractive index

32
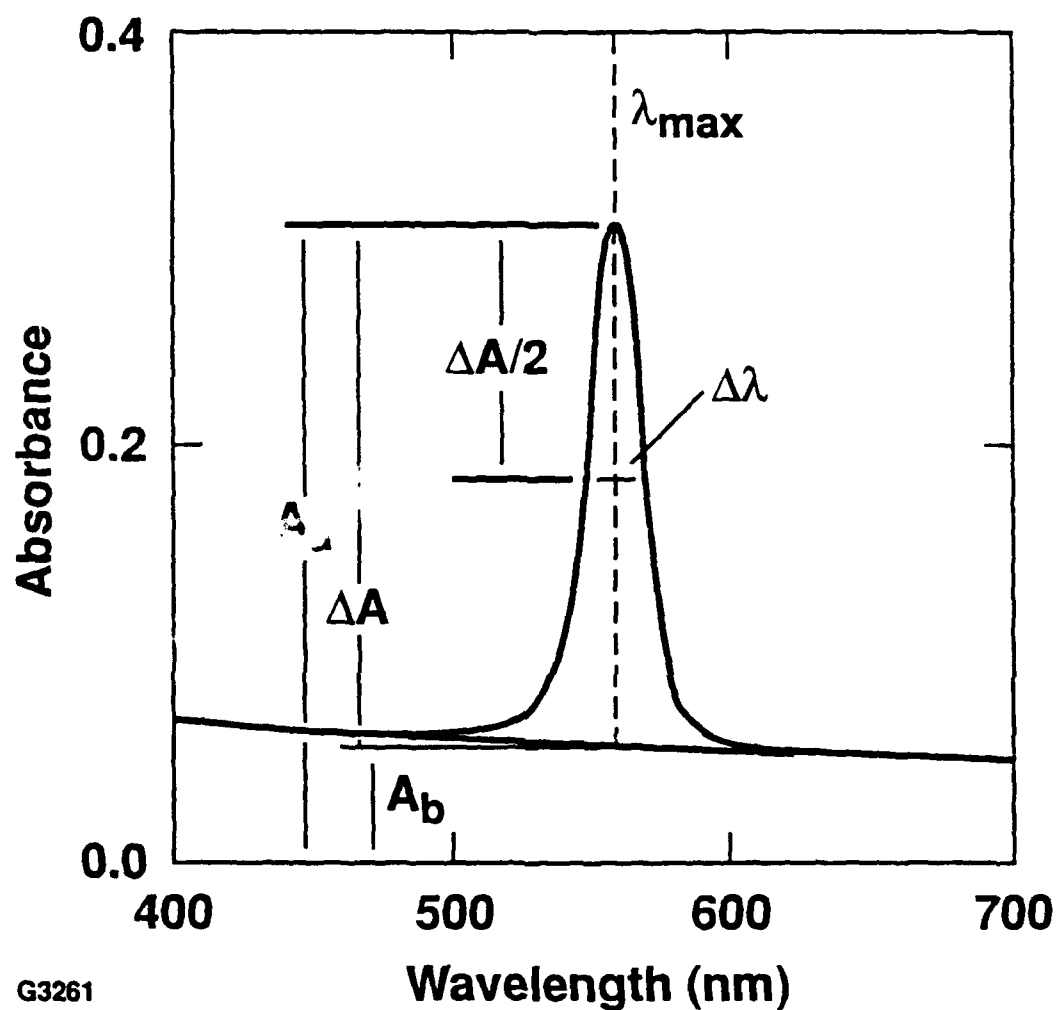
FIGURE 20   Transmission spectrum of a PBuDG/TGDM (56/44) solution at 25.9°C. Definitions of terms are as follows: λ_{max}, peak wavelength of selective reflection; A_a, absorbance at λ_{max}; A_b, apparent absorbance of CLC film; $\Delta A(=A_a - A_b)$, degree of selective reflection; and $\Delta\lambda$, half-width of the selective reflection spectrum. [From Ishihara, S., Yokotani, F., Matsuo, Y., and Morimoto, K., *Polymer*, 29, 2142, 1988. With permission.]

33
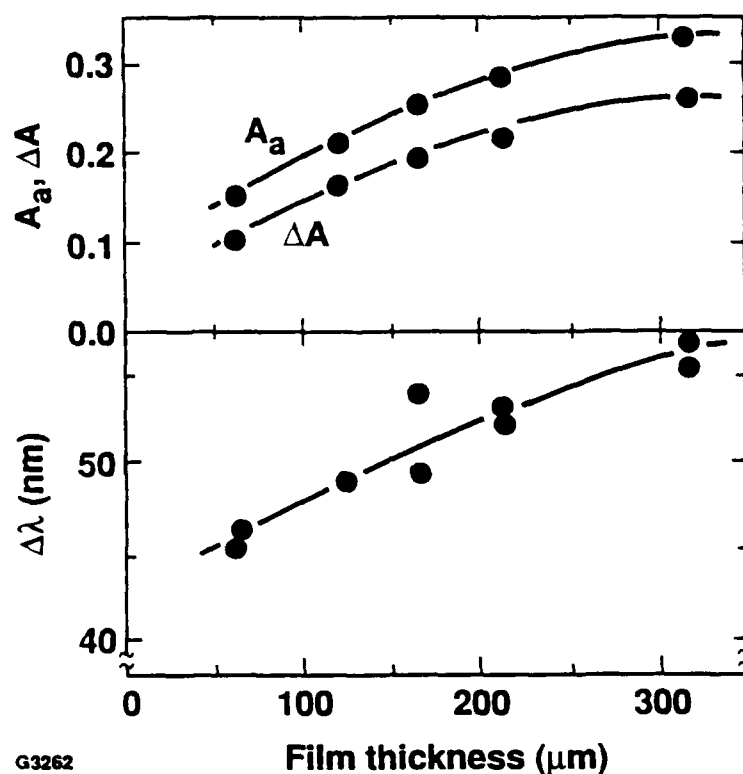
G3262

FIGURE 21   Influence of the film thickness of A_a, A, and $\Delta\lambda$ for PBuLG/TGDM (50/50) solid films. [From Ishihara, S., Yokotani, F., Matsuo, Y., and Morimoto, K., *Polymer*, 29, 2143, 1988. With permission.]
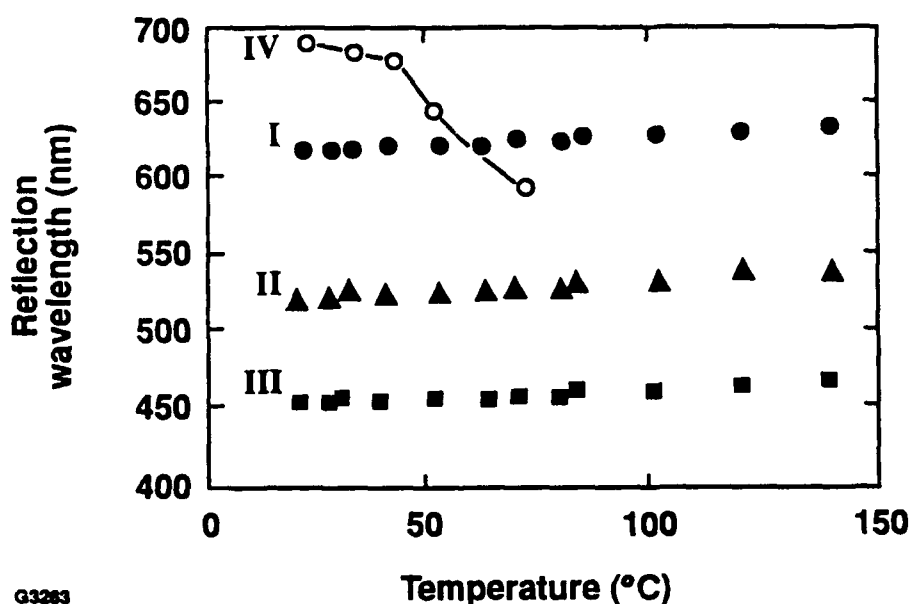
G3263

FIGURE 22   Temperature dependence of the reflection wavelength for crosslinked layers of CLC-silicone: I-III crosslinked; IV before crosslinking. [Haberle, N., Leigeber, H., Maurer, R., Miller, A., Stohrer, J., Buchecker, R., Fünfschilling, J., and Schadt, M., International Display Research Conference Record, p. 58, SID, San Diego, CA, 1991. With permission.]

34

matching of the CLC fluid to the confining glass substrates allowed these early devices to preserve optical wavefront quality of $\lambda/4$ at the 10% transmission point in the soft edge, but a limited number of edge profile shapes were available. J.-C. Lee[103] made several improvements to the concept which opened up a broader range of devices.

V. V. Danilov et al.[104] constructed an intracavity LC apodizer for a compact TEA CO_2 laser operating at $\lambda = 10.6$ μm. Based upon the cholesteric-nematic phase transition, the device clear aperture could be varied from 2 to 15 mm with the application of 20–60 V to the LC.

The properties of CLC's as replacements for multilayer dielectric thin-film reflectors in cw Nd:YAG lasers were studied by J.-C. Lee and co-workers.[105] By varying the fluid layer thickness and the anchoring conditions of the molecules adjacent to inner cell surfaces,[106] they discovered that highly reflecting cavity end mirrors and output couplers with high efficiency (i.e., low scattering losses) could be constructed. A key to the performance of these elements is the optically induced pitch dilation of the bulk CLC fluid, caused by the Gaussian optical intensity profile of the laser beam internal to the cavity. The resulting effects, which these researchers called *retro-self focusing* and *pinholing*, were shown to automatically force their laser into TEM_{oo} mode and single longitudinal mode operation.[107] (See the discussion of resonator control devices later in this article.)

An application for CLC polysiloxanes in the field of optical storage has been proposed. Pinsl, Brauchle and Kreuzer[108] were able to write spots in 30-μm-thick polysiloxane films using a variety of cw and pulsed laser sources. Disruption of the helical structure was made permanent and irreversible by incorporating benzophenone (BP) or carbon black (CB) dopants into the films. A photoreaction between the additive and the cholesteryl groups of the liquid crystalline polymer could be initiated above a threshold intensity of 7×10^{-9} W/μm^2 (350 nm, cw, BP) or a threshold energy of 2.54×10^{-9} J/μm^2 (1064-nm,10-ns single pulse, CB). The authors suggest that writing rates of 100 MHz using semiconductor lasers would make these CLC polymers competitive with other optical write-once storage media.

Birefringence in Nematics

Fluorination and hydrogenation of LC materials has broadened the range of refractive index values available for device applications. Lower refractive index values[109] have made it possible to use nematic LC's in waveguiding applications.[110] With materials whose ordinary refractive indices fall below that of fused silica, researchers have replaced fiber cladding with LC fluid layers that act as polarizers[111] and intensity modulators.[112] Others have studied the problem of confining nematic LC's within fiber cores.[113] Green and Madden found that scatter is greatly diminished when nematic LC's are confined to fiber cores of 10-μm diameter or less.[114]

Refractive index data for three nematic mixtures, Merck Ltd. 14616, 14627, and 18523,[115] whose ordinary refractive indices fall below that of fused silica, are given in Table 7. [Note: In early 1992, the mixture 14616 was slightly altered and given a new designation, 18523. Most physical properties were not significantly affected.] The Δn

values for these materials are exceedingly low as well. This fact and their high laser-damage resistance[78,83] have had an impact on the design of passive wave plates for laser applications.

TABLE 7 Refractive indices and birefringence values for low Δn mixtures 14616, 14627, and 18523 at 20°C. [Merck, Ltd. product literature. With permission.]									
	14616*			14627			18523		
λ,nm	n_0	n_e	Δn	n_0	n_e	Δn	n_0	n_e	Δn
435	1.4630	1.5131	0.0501	1.4650	1.5000	0.0350	1.4696	1.5202	0.0506
509	1.4587	1.5071	0.0486	1.4586	1.4929	0.0343	1.4632	1.5132	0.0500
577	1.4554	1.5037	0.0483	1.4554	1.4897	0.0343	1.4604	1.5091	0.0487
589	1.4553	1.5033	0.0480	1.4551	1.4893	0.0343	1.4596	1.5085	0.0489
636	1.4533	1.5012	0.0479	1.4531	1.4874	0.0343	1.4574	1.5063	0.0490
644	1.4529	1.5008	0.0479	1.4531	1.4872	0.0341	1.4565	1.5062	0.0498
* No longer available									

The concept of optical retarders constructed from nematic LC's is very attractive. Aperture and cost limitations imposed by crystalline alternatives like quartz, mica, sapphire and magnesium fluoride are circumvented. Optical quality and laser-damage issues associated with commercial stretched polymers are removed.

Using nematic LC's, wave plates can be made that, in principle, have the following advantages:

- fluid blending to create the exact birefringence required
- refractive index matching of the fluid to the substrate
- selection of fluids for high laser-damage resistance
- zero order retarders with reduced angular sensitivity
- high optical wavefront quality in transmission
- scalability to large apertures

Research has been carried out for nearly a decade at the University of Rochester's Laboratory for Laser Energetics to resolve the numerous technical issues impeding the development of high optical quality, large-aperture LC wave plates. Early devices exhibited retardance nonuniformities.[116] Fluid gap waviness was caused by the use of thin substrates that distorted when assembled cells were edge-sealed with epoxies. This and problems with laser damage (from impurities and/or from using inappropriate LC fluids) were mostly resolved[83] for 100-mm-diameter cells intended for use at $\lambda = 1054$ nm. More

recent work has concentrated on improving optical wavefront quality with special epoxies and procedures for tacking and sealing, the use of precision thin film spacer tabs to set gap thickness, *in-situ* cleaning with dry-ice snow[117] to remove buffing fiber residues, and scaling up fabrication procedures to 200-mm clear apertures.

A pair of optical retardance profile maps[118] for a zero order, 100-mm-diameter wave plate made using Merck, Ltd. 14627 Nematic LC is shown in Figure 23. Orientations of the wave plate fast axis parallel and at 45° to the polarization axes indicate the quality of homogeneous alignment and the retardance uniformity, respectively. To be useful in laser applications, large aperture retarders must exhibit a retardance uniformity of ±5% about the target quarter-wave or half-wave value. This is not easily achieved, in light of Wu and Efron's[119] description of director misorientation for thin LC fluid layers.

The recent determination that certain LC nematics and polymer alignment layers are resistant to pulsed UV laser radiation[78] has made it possible to design and fabricate special wedged, high multiple-order wave plates for laser-fusion applications. Called distributed polarization rotators (DPR's), these elements are inserted into the frequency-converted output beams of a Nd:glass laser system.[120] By changing the polarization state/orientation in one dimension across the spatial profiles of the 351-nm beams, these devices are expected to reduce interference effects and subsequent intensity modulation when the beams come together on the surface of a fusion target. Off-line testing of a 100-mm DPR, constructed from BDH14616/14627 with a 75-μm wedge (see Figure 24) reduced modulation in a 351-nm cw test beam by 40%.[120,121]

The design of LC wave plates and polarizers from nematic polymers has been proposed by Finkelmann and Kock.[65] Sandwiched between glass plates and heated above T_g, a nematic polymer LC could be aligned into a positive, uniaxial orientation with an applied external electric or magnetic field. Cooling would lock the polymer into a glassy state with a birefringence of approximately 0.15. Dye-doping of such a nematic polymer could be used to construct dichroic linear polarizers.

ELECTRO-OPTIC DEVICES

This section deals with devices that employ reorientation of liquid crystal molecules to alter the properties of laser radiation. Three divisions are made. Devices whose operating principles are based primarily upon electrically controlled birefringence (ECB) are covered first. Devices employing ferroelectric LC's are then described, and the section ends with a review of LC/polymer composite effects and devices.

Electrically Controlled Birefringence and Related Effects

Optical engineers have long sought a nonmechanical replacement for the Soleil compensator.[122] Gilman *et al.*[123] developed a nematic LC variable retarder to satisfy this need. A 25-mm-diameter device was tunable to zero order retardance levels of λ/4 or λ/2 in the visible with <5 V rms. Retardance uniformities of ±2 nm over the clear aperture were
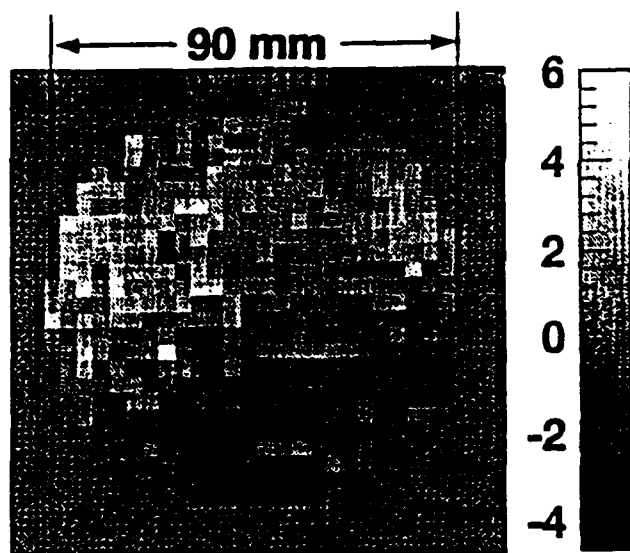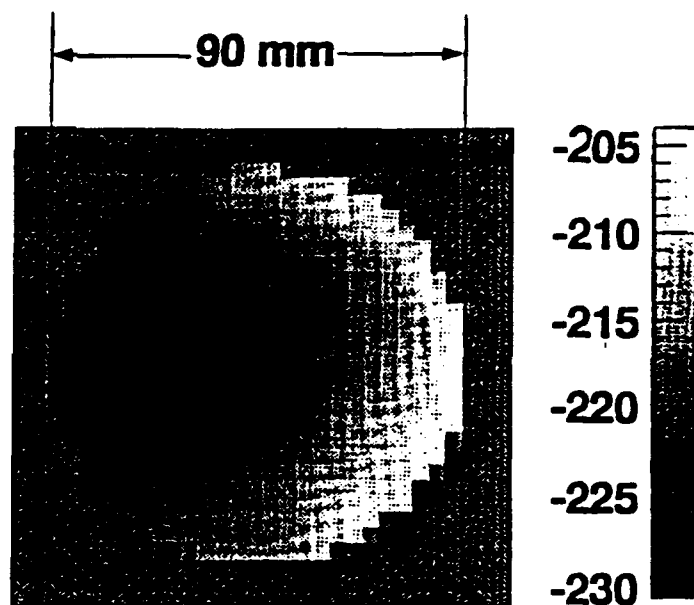
FIGURE 23 Retardance profile maps, taken with a modulated transmission ellipsometer at $\lambda = 633$ nm, show two orientations of the LC wave plate fast axis with respect to the polarization axes. The fluid layer thickness is 6.5 μm and the fluid is Merck, Ltd. 14627. (a) The wave plate fast axis is oriented at 0° to the incident polarization axis. This indicates the quality and uniformity of homogeneous alignment across the cell's clear aperture. The sample's residual average retardance is 0±1.5 nm. There is a 10-nm retardance variation across the part due to localized regions of misalignment. (b) The wave plate fast axis is oriented at 45° to the polarization axes indicating the magnitude of retardance and its uniformity. The average sample retardance is 217±5 nm. There is a 26 nm retardance variation across the part due to wedge between the substrates' inner surfaces.

38

Vertical polarization incident

Vertical wedge

Nematic liquid crystal fluid

Molecules are oriented at 45° (in the plane of the substrate)

t

$t\Delta n$ increases

D = 100 mm

(a) Side (perspective)

(b) Front

E5808
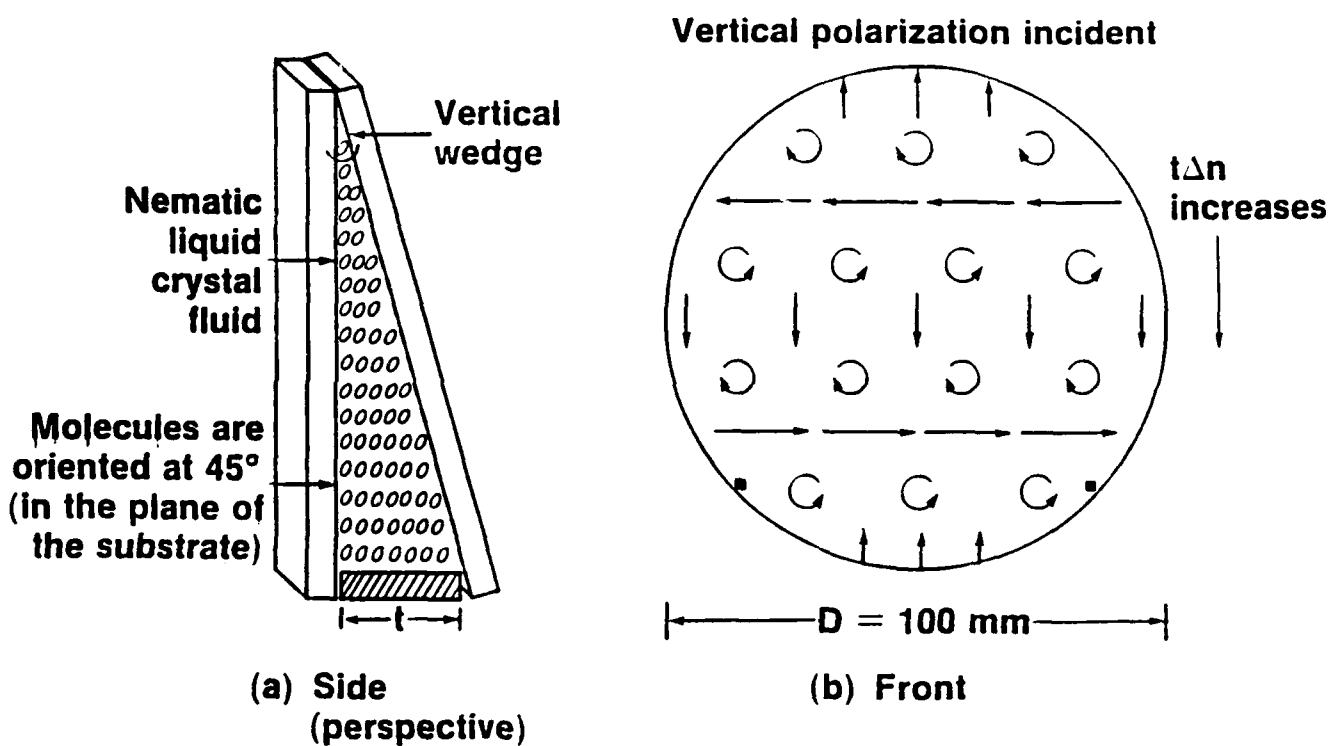
FIGURE 24　The distributed polarization rotator (DPR) is an optical device that converts one polarized beam into two orthogonally polarized beams. The wedged DPR is a continuously varying wave plate that produces two co-propagating, orthogonally polarized, complimentary interference patterns. A nematic liquid crystal fluid fills a wedge formed between two parallel plates, (a), yielding enough retardance to produce several polarization cycles along one dimension of the beam, (b).

39

demonstrated. Sharp et al.[124] extended this concept to $\lambda = 10.6$ μm, where they found that a wave plate made with E7 between germanium substrates could act as an electrically controlled retarder at peak laser intensities from 5 to 900 W/cm^2. Performance was somewhat degraded at the high end due to thermal heating of the fluid.

A number of groups have used ECB LC retarders in electro-optically tunable filters. J. Staromlynska[125] investigated broadband tunable filters. He constructed a variable birefringent filter (VBF) and a Fabry-Perot (FP) etalon from a range of LC materials (K15, E44, and BDH16522) and compared performance in white light and at the krypton ion-laser wavelengths of 647, 531, and 476.2 nm. He achieved contrast ratios in excess of 1000:1 with the VBF geometry, while noting better wavelength selectivity with the FP geometry. Large tuning ranges were achieved at very low voltages ($\leq$10 V).

P. J. Miller[126] measured the performance of a 5-element Lyot type filter designed for astronomical imaging, which was composed of LC tunable retarders. A novel tuning technique with a laser diode at 1300 nm was used to determine the transmittance (11%), bandwidth (30 nm), and leakage (0.7%). Advantages of this filter compared to others were large peak retardance (1500 nm) and drive voltages below 15 V.

J. R. Andrews[127] constructed a two-stage birefringence tuner, composed of ECB LC elements in a cavity external to a diode laser, to select any one of 12 longitudinal output modes between 783 nm and 786 nm. The average scan rate was 27 Å/V. The maximum voltage requirement was 1.7 V.

Two groups have been especially active in the area of ECB LC Fabry-Perot devices for wavelength division multiplexing in optical communications. In a series of papers beginning in 1990, J. S. Patel et al.[128–131] developed and refined the concept of a polarization-insensitive LC FP filter for low-power wavelength tuning in the infrared. The output from a fiber was directed into a pair of calcite prisms separated by the LC element (see Figure 25). Displaced, orthogonally polarized beams traversed regions of the LC cell where appropriate and orthogonal initial alignment conditions were imposed. The application of 0–10 V was sufficient for tuning between 1450 nm and 1550 nm. Fifteen dB intensity fluctuations caused by random polarizations were reduced to <1 dB by the device.

Design refinements to LC FP technology have been done. Hirabayashi et al.[132-135] achieved high finesse (150–410), high transmittance (20%–70%), narrow transmission peaks (FWHM:0.17–0.35 nm), and a voltage-induced wavelength shift >50 nm at a wavelength of 1500 nm. McAdams et al.[136] developed a model and successfully demonstrated an LC FP operating at oblique angles of incidence.

The ECB effect was used in many ways to construct variable focal length (VFL) lenses. The concept of a LC VFL lens is shown in Figure 26. Plano-concave and plano-convex LC lenses, originally devised by S. Sato,[137] scattered light due to fluid path lengths of 500 μm. Sato and co-workers reduced fluid paths to 100 μm with a Fresnel lens LC structure.[138] They demonstrated that variations in focal length from f = 20 cm to f = 70 cm (see Figure 27) could be achieved with improved response and recovery times.

Fiber lens   Fiber lens

Liquid crystal
etalon filter

Calcite
crystal   Calcite
crystal
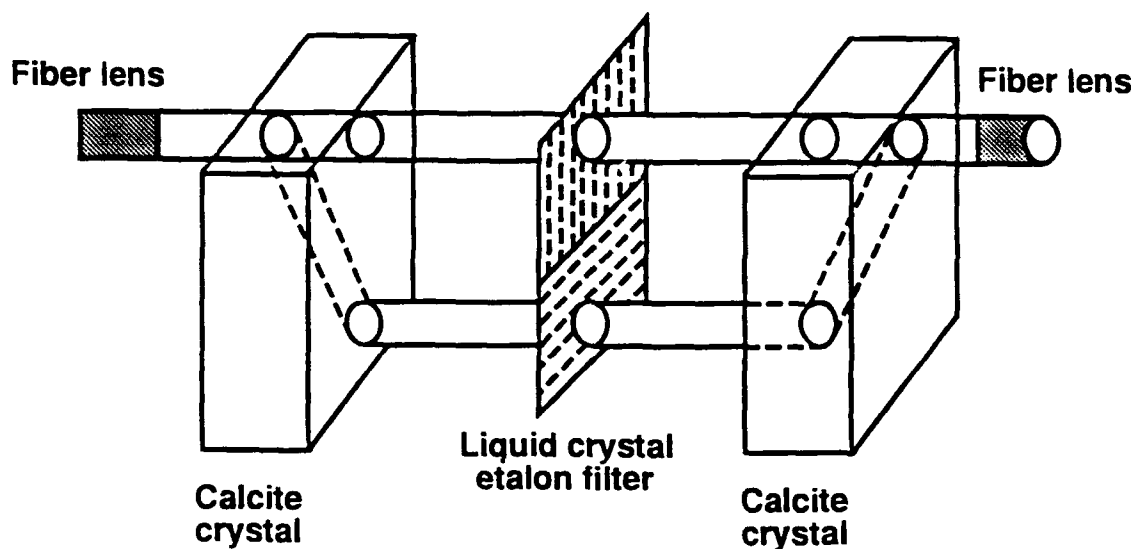
G3264

FIGURE 25   Polarization insensitive liquid crystal electro-optic Fabry-Perot etalon filter. The cell is 10 μm thick. Photolithographic techniques are used to set up conditions of orthogonal LC alignment shown in the figure. [From Patel, J. S. and Maeda, M. W., *IEEE Photon. Tech. Lett.*, 3, 740, 1991. With permission.]

$V = V_{max}$

$V = 0$

$f = \left(\frac{1}{f_o} + \frac{1}{f_o}\right)^{-1}$ $V = V_{max}$

$f = \left(\frac{1}{f_e} + \frac{1}{f_o}\right)^{-1}$

Alignment of nematic liquid crystal molecules between ITO coated substrates

Unpolarized input light

$V = 0$
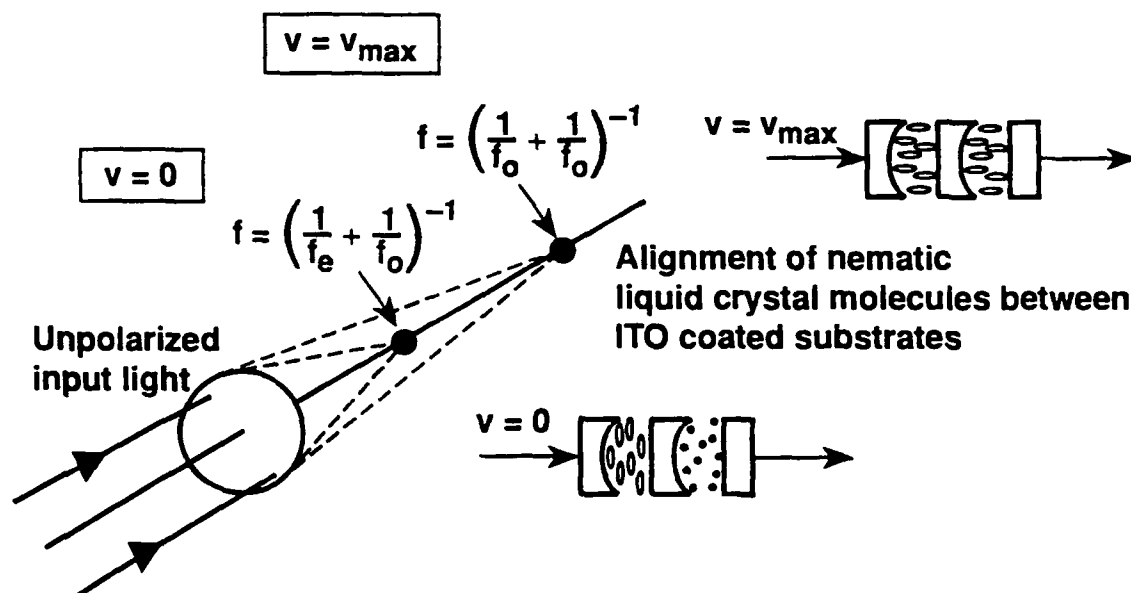
G3291

FIGURE 26   A cascade of curved substrates enclosing two separate, curved nematic LC fluid layers comprises a LC lens. Unpolarized light is brought to a single focus, which shifts as a function of applied voltage. f_o and f_e refer to orthogonal polarization components of the incident light that experience the corresponding ordinary and/or extraordinary refractive indices in the LC fluid layers. This concept comes from the work of S. Sato in Ref. 137.

41
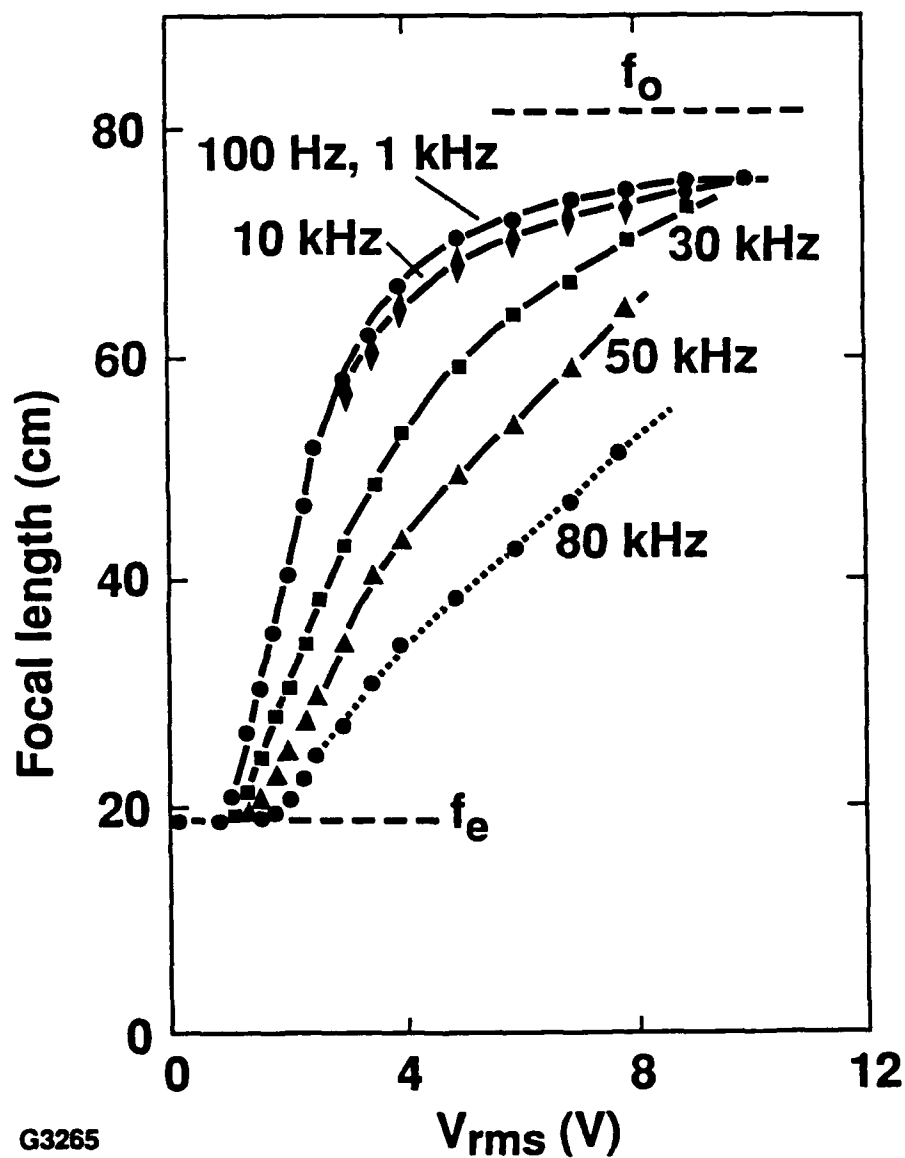
FIGURE 27 Change of focal length for a plano-convex Fresnel-type liquid crystal lens as a function of applied voltage. The groove depth of the lens is 100 μm and the LC fluid is K15. [From Sato, S., Sugiyama, A., and Sato, R., *Jpn. J. Appl. Phys.*, 24, 1626–1628, 1985. With permission.]

Aberrations were a problem which these researchers studied by inducing radial and tangential director orientations in their cells.[139]

Other approaches included Kowel et al.'s liquid crystal adaptive lens,[140–142] which used flat substrates and patterned, linear electrodes in a stack of ECB cells; Nose et al.'s LC microlens,[143,144] which consisted of a hole-patterned electrode opposite to an indium-tin-oxide-coated counter-electrode; and a polarization-independent, 8 × 8 Fresnel lens array of Patel and Rastani.[145]

There have been significant improvements in speed of response for nematic LC ECB devices. Driven mostly by display applications, these advancements reduced response times from hundreds of milliseconds to less than 100 µs. Fergason showed that fast response in an ECB cell could be achieved by preventing the bulk of the LC fluid from participating in the molecular reorientation process.[146,147] Using a small field to hold the bulk fluid in a homeotropic orientation, he manipulated the orientation of thin fluid layers near opposing inner cell surfaces to effect variations in retardance (see Figure 28). Fergason called these cells "surface mode devices." He constructed shutters based upon switching between 0 λ and 0.5 λ conditions, which exhibited response times of a few hundred microseconds.[148]

Bos and coworkers[149] expanded the usefulness of the surface mode concept by orienting the tilt of near surface molecules in ways that broadened field of view for display applications. Figure 29 shows the effect of off-axis self-compensation for their device, termed a "pi cell," in comparison to an un-self-compensated device.

S. T. Wu and coworkers studied the details of low holding voltages applied to thin nematic cells for reducing response time.[150,151] Using IR-41, a eutectic mixture (diphenyldiacetylenes[152] and isothiocyanates[153]) optimized for high birefringence and reduced viscosity, they demonstrated 100 µs response.[154] The dynamics of their "transient nematic effect" concept are shown in Figure 30. In a further refinement they employed an LC compensator in tandem with the ECB cell to cancel out residual birefringence and achieve contrast ratios of about 1000:1 (2-mm diameter beam at 633 nm).[155]

Ferroelectric Devices

Ferroelectric liquid crystals have been classified by several authors[25,26] as improper or pseudo-proper ferroelectric materials, since the spontaneous polarization in these materials is a microscopic quantity confined to each layer and averages to zero in the bulk due to the presence of a helical structure. If the helix is unwound by an external force (e.g., a strong electric or magnetic field), global averaging of the dipole moments no longer occurs, and the medium will now exhibit ferroelectric properties. This "poling" effect is shown schematically in Figure 31. If the sign of the applied dc electric field is reversed, the ferroelectric liquid crystal molecules will reorient to keep the spontaneous polarization direction aligned with the polarity of the applied electric field. Since permanent dipole moments are involved, coupling of the applied field with the spontaneous polarization is much stronger than with the dielectric anisotropy at similar applied field strengths. A direct result of this stronger coupling is a large improvement in electro-optic temporal response,

43
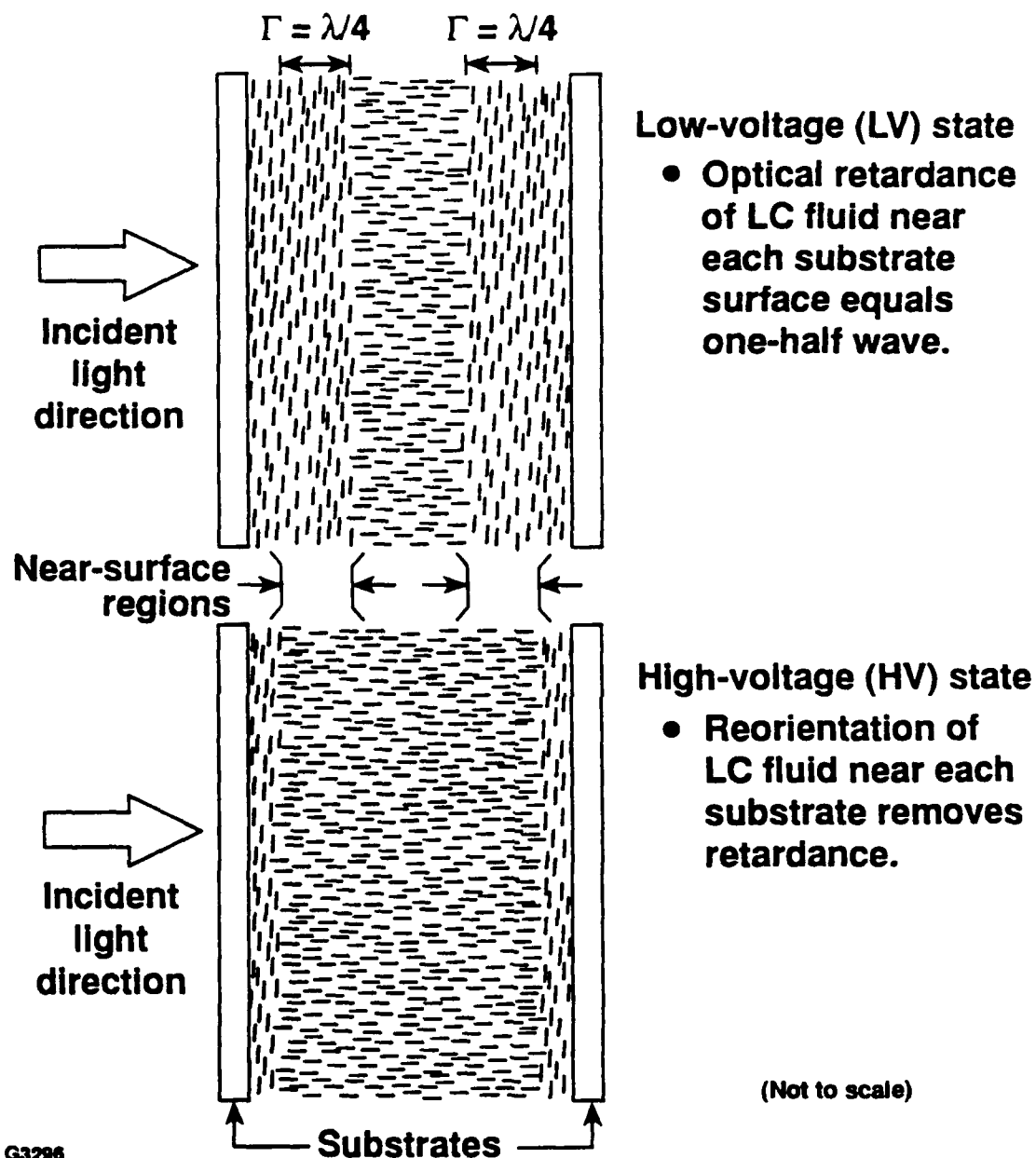
FIGURE 28   Operating states of the surface mode device. In the low voltage (LV)
condition, retardance (Γ) of one-quarter wave per surface layer makes the
cell a half wave retardation plate. In the high voltage (HV) state, enough of
the molecules near the inner surfaces reorient to remove retardance from the
device. Because molecules in the bulk experience a continuous field bias,
they remain oriented parallel to the field direction and do not participate in
the effect.

44
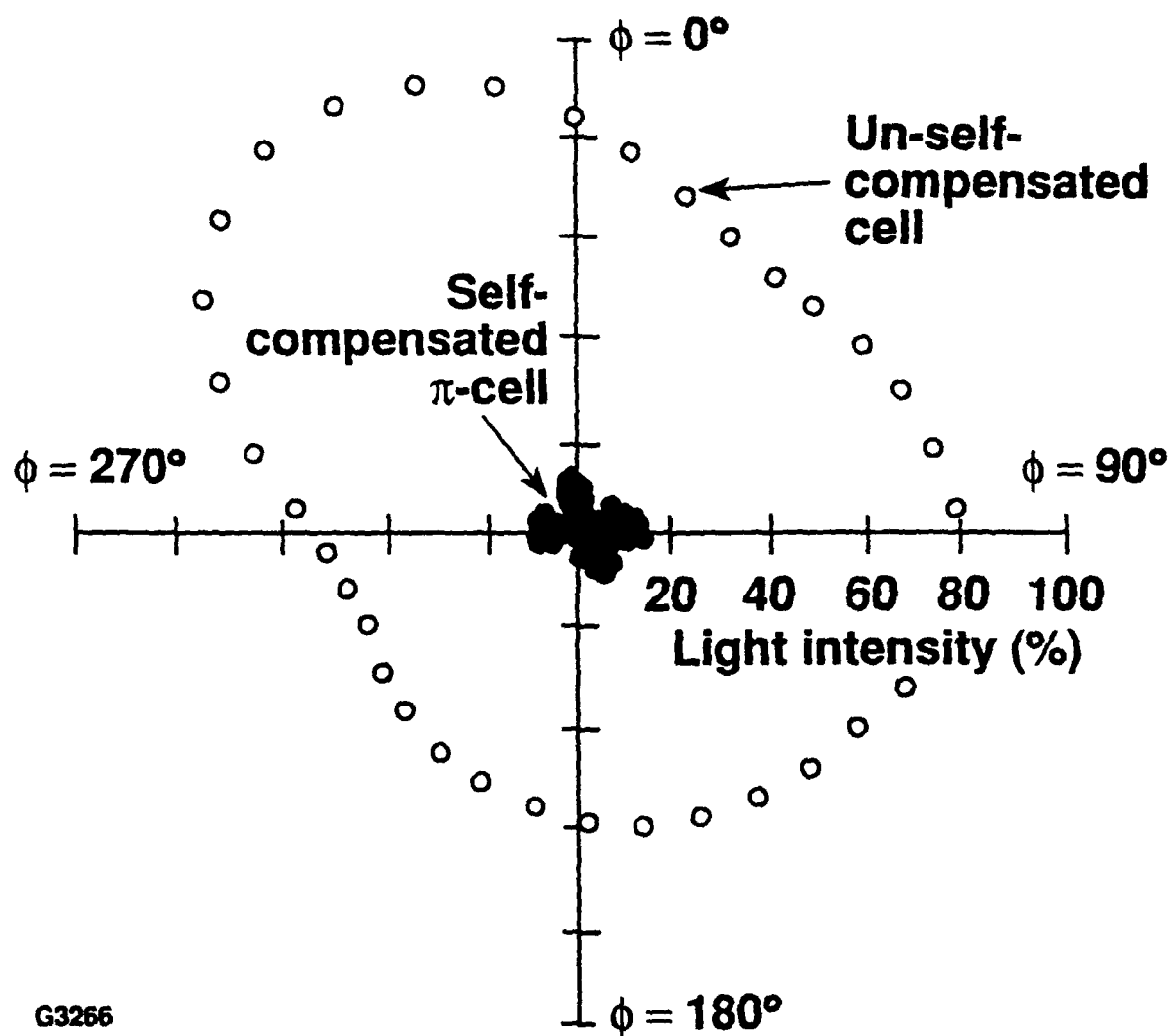
FIGURE 29   Transmitted light intensity through a self-compensated π-cell (solid dots) and an un-self-compensated cell (open circles) placed between parallel polarizers. The light (λ = 545 nm) was incident at 40° to the cell normal. Both cells were in the low voltage state of half wave retardation. [From Bos, P. J., and Koehler/Beran, R., *Mol. Cryst. Liq. Cryst.*, 113, 334, 1984. With permission.]

45
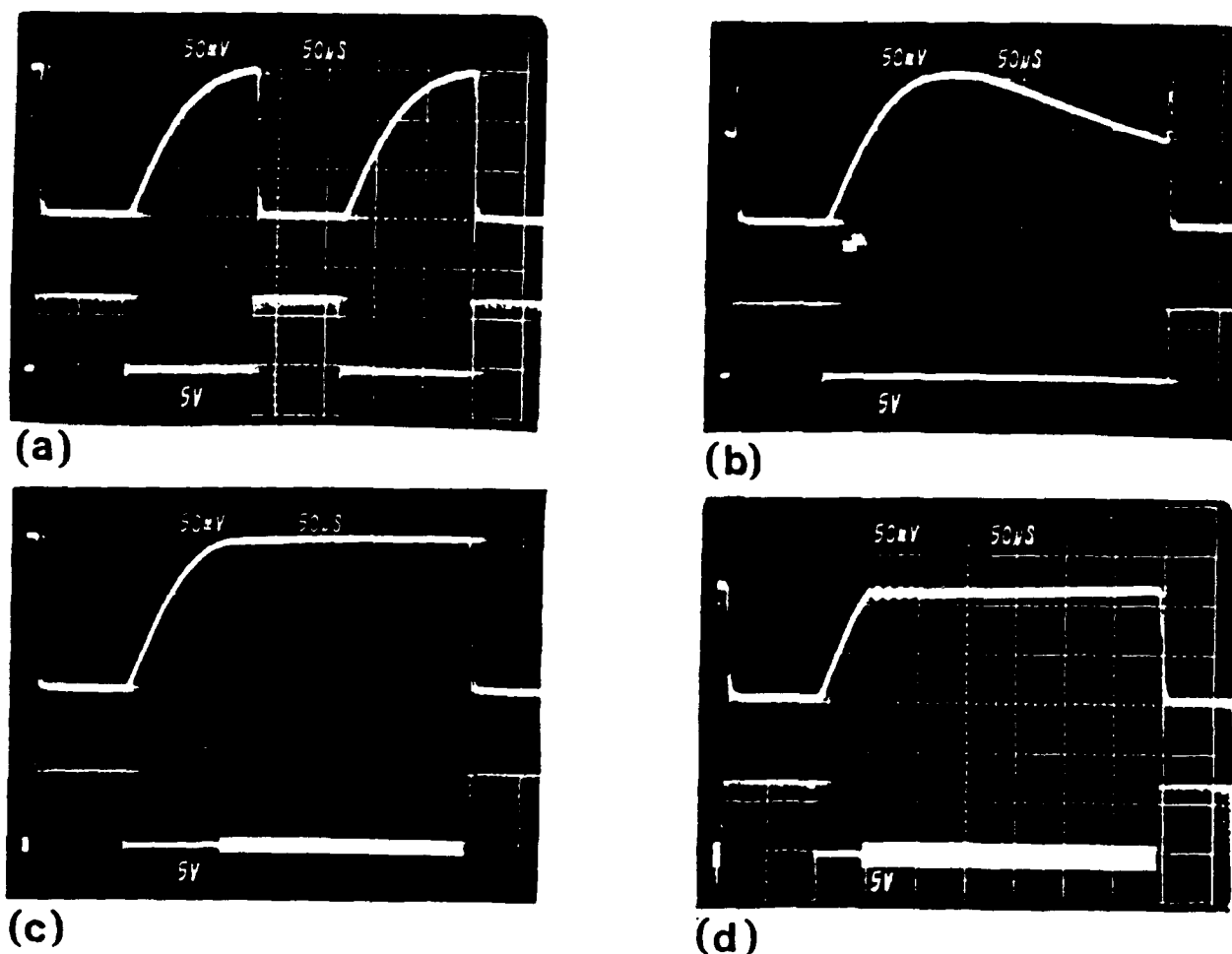
FIGURE 30 Dynamic response of a 4.6 μm thick LC ECB cell filled with the eutectic IR-41. The device is operated double pass in reflection at $\lambda = 514.5$ nm. The lower traces represent applied voltage signals and the upper traces are the corresponding optical response. (a) A regular ON/OFF state of the LC modulator using the transient nematic effect. (b) Lengthening the voltage-off state to see the modulator relax to a condition with more retardance than is required for optimum contrast. (c) A small holding voltage is applied to the cell to hold the bright on state for a period of time. (d) This small holding voltage is applied earlier to get a faster turn-on time with some sacrifice in modulation contrast. Time scale: 50 μs/div and voltage scale: 50 V/div. The ac voltage signals consist of 50 kHz sinusoidal waves. [From Wu, S.-T., *Appl. Phys. Lett.*, 57, 987, 1990. With permission.]

which can be as much as three to four orders of magnitude faster than LC devices employing dielectric E-O effects. A wide variety of electro-optic effects including polarization rotation, field-induced tunable birefringence, diffraction, scattering, TIR switching, and guest-host effects are possible depending on the device configuration, cell path length, molecular alignment conditions, and the characteristics of the particular ferroelectric liquid crystal employed. These electro-optic effects, as well as a number of device concepts employing them, will be explored in detail in the following sections. For the purpose of this discussion, emphasis is placed on applications of smectic C* and A* materials, since these two ferroelectric LC classes have received the greatest attention to date.

Helical Ferroelectrics

The absence of a bulk spontaneous polarization in helical ferroelectric liquid crystal phases requires that a method of unwinding or destabilizing the helix be employed before ferroelectric properties can be observed and exploited for device applications. A strong electric (or magnetic) field can be used to unwind the helical structure, but this method is inconvenient and somewhat impractical for device applications due to the requirement for specialized, high-voltage drive electronics and the risk of rapid electrochemical degradation of the LC material at the required high dc field strengths. Bulk cancellation of the helical structure can also be achieved by combining two chiral smectic compounds with the opposite twist sense but the same spontaneous polarization direction. The limitations of this technique for device applications were cited earlier in this article. Another method of helix suppression is to confine the ferroelectric LC material between a pair of substrates so that the liquid crystal material path length is considerably shorter than its helical pitch. In this geometry, the molecules are constrained by both surface anchoring forces and the thin (1–2 μm) cell spacing to align parallel to the substrate surfaces, while the layer planes are oriented approximately normal to the substrates. This "bookshelf" geometry, shown in Figure 32, is the basis of an important electro-optic device concept first introduced by Clark and Lagerwall[156] in 1980 and known as the surface-stabilized ferroelectric liquid crystal (SSFLC) device. This device geometry has several attractive features: (a) large changes in field-induced birefringence (>0.2) for short material path lengths (2–4 μm); (b) electro-optic response times ranging from ten to several hundreds of microseconds at room temperature and at near T₁L voltage levels; (c) the ability to rapidly switch between two bistable states using dc voltage pulses of the opposite polarity, i.e., an erasable optical memory that can be used in either direction;[29] and (d) the ability to produce multiple combinations of bistable and nonbistable switching effects in one device by using different surface anchoring conditions on each substrate.[29,30,157] Figure 33 shows a schematic representation of the SSFLC device in its simplest form. Application of a dc electric field causes the ferroelectric LC molecules to rotate through an angle equal to approximately twice the molecular tilt angle (θ) from the layer normal. The magnitude of θ is highly dependent on the molecular structure and composition of the particular liquid crystal compounds or mixtures used in the device. Compounds and mixtures with values of θ near 22.5° are designated *low-tilt* materials; while those whose molecular tilt angles range from 42°–45° are termed *high-tilt* materials.

47

E (H)
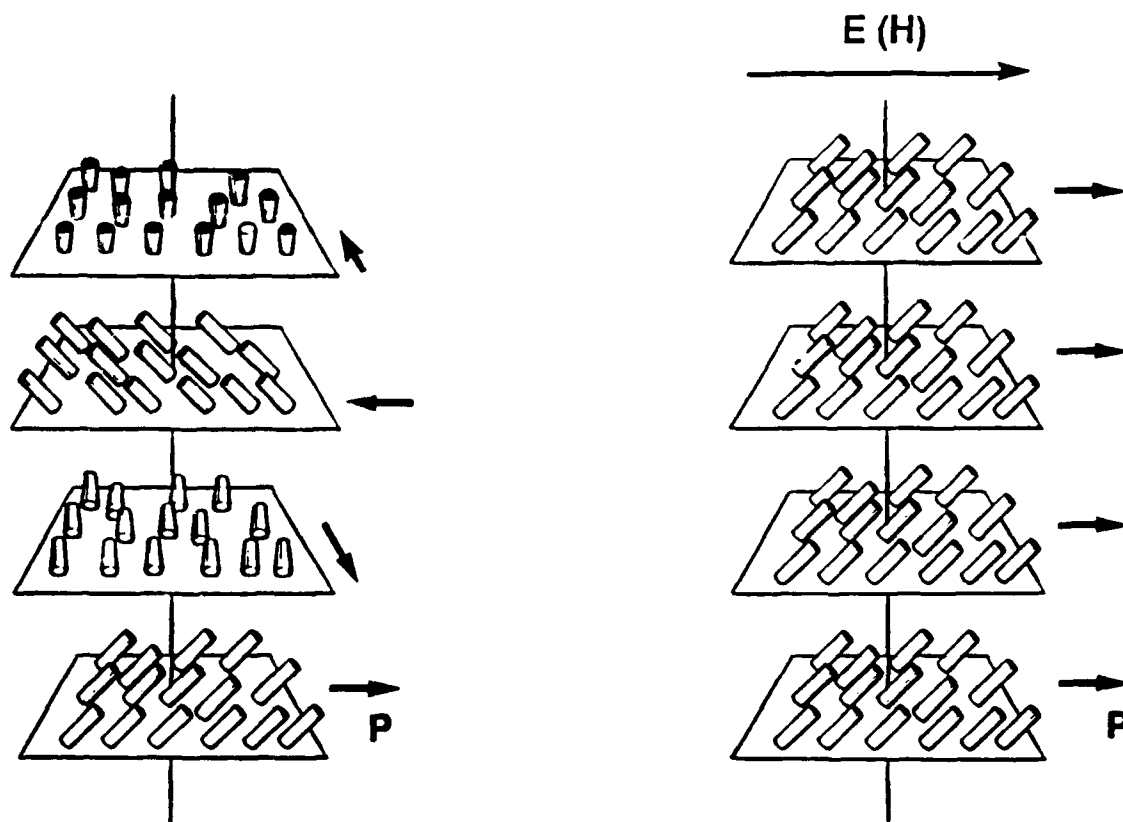
(a) **twisted structure**
net average dipole moment = 0
no bulk ferroelectric properties.

(b) **untwisted structure**
nonzero average dipole
ferroelectric properties exhibited.

G1932

FIGURE 31   Generation of bulk spontaneous polarization in chiral smectic C materials by
helix unwinding. (a) The rotation of the molecular dipole moment about the
helix axis causes bulk cancellation of the spontaneous polarization (P) in the
twisted chiral smectic C structure. (b) Unwinding of the helical structure by
an electric (E) or magnetic (H) field applied parallel to the layer planes aligns
the dipole moments in a common direction and renders the medium
ferroelectric.

48
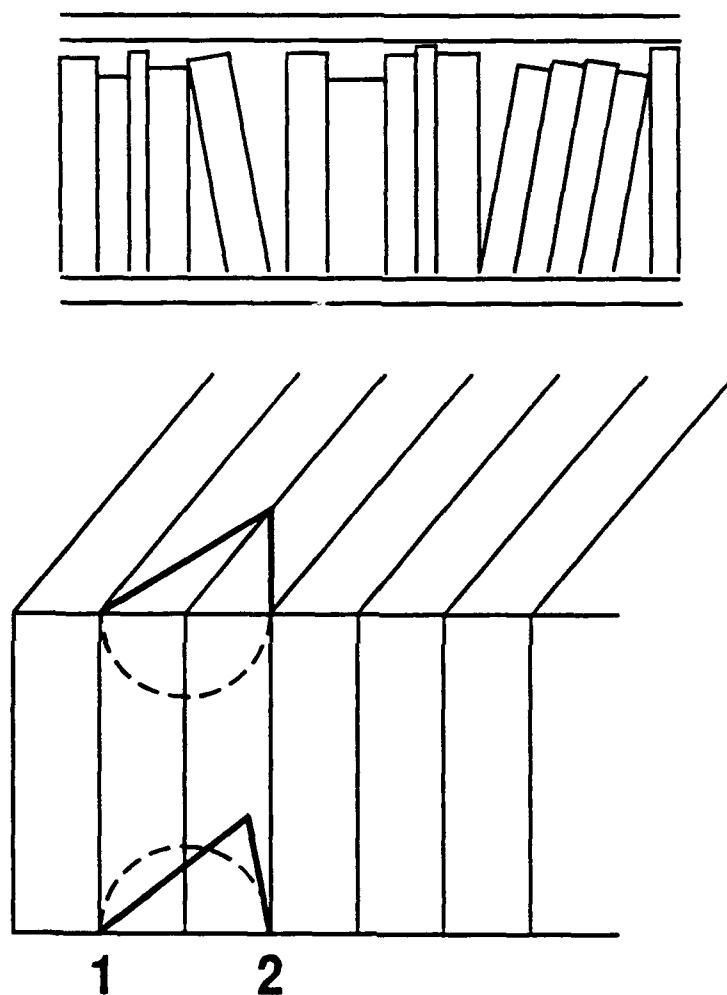
FIGURE 32 The "bookshelf" geometry of the SSFLC device. (a) The smectic layers are perpendicular or at a slight incline to the glass plates, resembling books in a bookshelf. (b) The sample thickness is chosen so that the helical structure is suppressed and the director orientation is parallel to the substrates. The optic axis can switch between two bistable states (positions 1 and 2) as a consequence of the device geometry. [From Clark, N. A. and Lagerwall, S. T., *Appl. Phys. Lett.*, 36, 899–901, 1980. With permission.]

When low-tilt materials are employed in the SSFLC device geometry, a device is produced that acts like a switchable uniaxial half-wave plate when operated between crossed polarizers; this is the form of the example shown in Figure 33. One of the earliest implementations of this device configuration was as a simple, high-speed, nonbistable light valve for the visible spectral region. First introduced in the marketplace by Displaytech, Inc. in 1986, this half-inch clear aperture device operated over a frequency range of 0–30 KHz driven by ±15 V at a contrast ratio of 100:1.[29] Although not capable of bistable operation, this device aroused considerable interest as an alternative to nematic liquid crystal devices in applications where a fast electro-optic response time is crucial, such as spatial light modulators for incoherent-to-coherent image conversion, spatial filtering, and single-element optical logic gates. The feasibility of using a SSFLC cell for spatial light modulation has been demonstrated by Armitage et al.;[158] the single-crystal bismuth silicon oxide photoconductive photosensor used in this device, however, limited its response time to the millisecond regime. Considerable improvements in performance were achieved by Takahashi et al.[159] (400-μs response time) and Moddel et al.[160] (155-μs response time with bistable operation) using a-Si:H photodiode photosensors and thin (1.8–3 μm) ferroelectric LC layers. The bistability of the SSFLC device is a distinct advantage for this application, in that the write beam need be applied only long enough to effect the initial switching; the written image is then retained by the cell's intrinsic memory.

Another area in which the inherent bistability and fast response characteristics of the SSFLC device plays an important role is in multiple-element matrix devices. The simplest form of these is a one-dimensional matrix or linear array; this device was initially proposed[157] as an optical element for use in high-speed copier and printer applications, and has recently been introduced as a commercial product.[29] The next level of SSFLC device complexity, the two-dimensional matrix-addressed device, has been the subject of recent intense investigations for several reasons. Multiplexed operation in SSFLC matrix devices is considerably simplified as compared to nematic LC matrix devices, which require individual thin-film transistor (TFT) elements for each pixel in order to overcome the lack of an intrinsic memory function. This intrinsic memory of the SSFLC device would, in principle, allow the possibility of producing devices with an almost unlimited number of addressable lines—an attractive feature for high information content devices, such as large-area video display terminals and television screens. Examples of some of the first efforts in this area were demonstrated by Seiko Instruments and Electronics in 1985, and the British Joers/Alvey project in late 1986. The Seiko device, a 12-in. display containing 640 × 400 elements each of 0.4 μm × 0.4 μm size, operated at approximately 20 V with a ±5 V ac bias and a duty ratio of 1/400 (stationary image) and a contrast ratio of 5:1.[29] The British Joers/Alvey device, although modest in size (64 × 64 elements), showed flawless performance in displaying moving images at video rates.[27] The current state of the art is represented by the Canon, Inc. engineering prototype SSFLC monochrome computer terminal, first demonstrated in 1988.[29] The 14-in. diagonal flat-panel screen containing 1280 × 1120 lines with a resolution of 5 lines/mm produced completely flicker-free scrolling images at drive voltages of ±20 V and a 50-μs line access time, which corresponds to a frame refresh frequency of 6 Hz. Although the contrast ratio ranged from 5:1 to 10:1, the small viewing angle dependence of the device allowed good rendition of newspaper-quality text that was easily readable from nearly any viewing
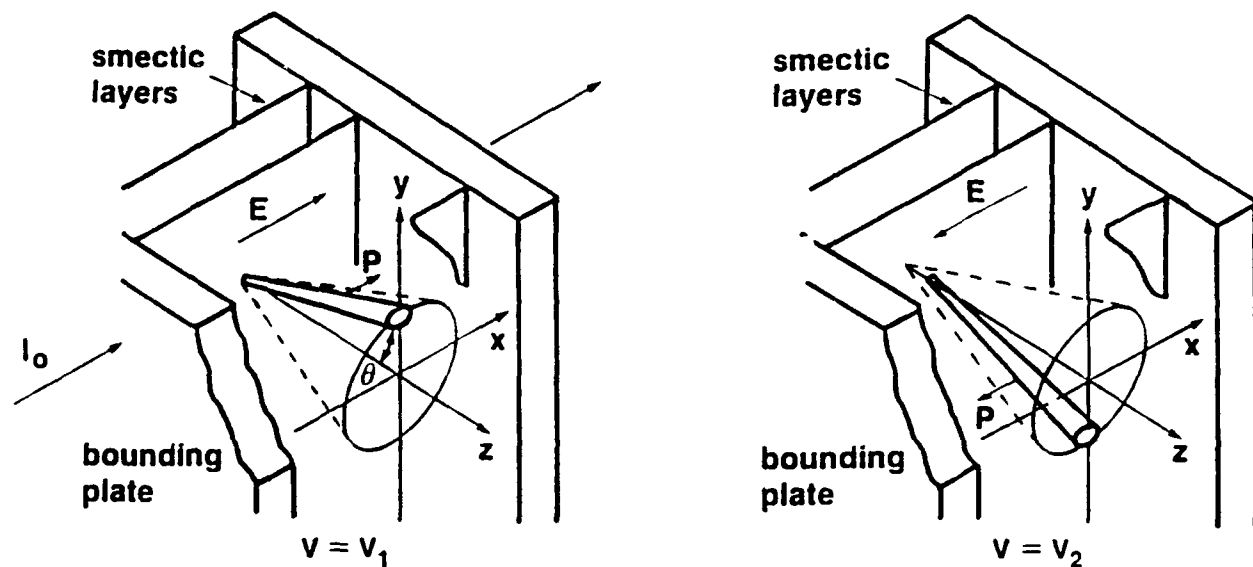
- **Angle of deflection = 2θ (θ = molecular tilt angle within smectic layer)**

- **Typical values for θ are between 22.5° and 45° (material dependent)**

G1941

FIGURE 33   Director reorientation in the SSFLC device. Upon application of a dc field (E), the director rotates about the surface of a cone, allowing the molecular spontaneous polarization (P) to align with the applied electric field. The angle of rotation is equal to twice the molecular tilt angle θ, where θ generally ranges between 22.5 and 45°. The propagation direction of the incident light is indicated by I_0.

51

direction. Work to extend SSFLC technology to produce full-color displays is currently underway, with prototype devices having been demonstrated by Toshiba in Japan[29] and Thorn EMI in Great Britain.[161]

Ferroelectric LC devices are also finding applications in areas outside of the realm of information display. Johnson et al.[162] have used 32 × 32 and 128 × 128 element SSFLC matrix devices to demonstrate their usefulness as both polarization-based (XOR and XNOR) and intensity-based (OR using dark true logic) FLC logic gate devices. They also demonstrated the potential of these devices as Fredkin logic gates, input/output to continuous media optical associative memories, and as an optical interconnect mask for a discrete matrix-vector multiplier (optical crossbar), and have also proposed using high-contrast (125:1) SSFLC matrix devices as an adaptive Fourier filter for optical inspection systems.[163] Single-element, bistable SSFLC devices have been used as polarization rotation elements for a wide variety of optical devices. Masterson et al.[164] employed them as electrically controlled phase retarders for three-stage tunable Lyot filters. These devices, which consisted of four polarizers, seven SSFLC wave plates, and three birefringent elements, were capable of room-temperature switching between two transmission maxima (475 and 625 nm) at speeds of less than 20 µs using modest (±10 V) drive voltages. McAdams et al.[165] fabricated a 1–x–N optical routing switch (Figure 34) consisting of polarizing beam splitters paired with SSFLC polarization rotators, each pair comprising one port of the 1–x–N switch. In the initial state, all polarization rotators are aligned to pass the incident polarized light. Activation of the SSFLC device at the selected output port rotates the plane of polarization of the incident light and the output is extracted by the polarizing beam splitter. This configuration largely overcomes the cross-talk accumulation problem observed in previously reported device geometries.[166,167] Any unrotated component of the incident polarization remains in the switch, contributing to loss but not to cross-talk. Although the polarization rotators must have high extinction ratios between crossed polarizers, only modest extinction ratios are required between parallel polarizers. The experimental 1–x–4 optical switch reported had a signal-to-cross-talk ratio ranging from 21.6 to 37.1 dB, an insertion loss of 3.5 dB, and switched at 50 µs. Ferroelectric LC switchable half-wave plates have also been used by McRuer et al.[168] as active filter elements in a digital optical scanning device in conjunction with a passive nematic liquid crystal prism. The device concept is diagrammed in Figure 35. The ferroelectric LC wave plate is aligned so that a linear polarized output is produced that is either parallel or perpendicular to the polarization direction of the incident light. The nematic LC prism, a wedge-shaped cell filled with nematic liquid crystal aligned parallel to the substrates, deflects the light according to its polarization. Individual binary deflector units can be cascaded to produce one- and two-dimensional scanners. A 1–x–64 scanner employing six ferroelectric LC wave plates was fabricated that displayed 400 µs switching times at ±12 V and −5.3 dB of average loss.

Although ferroelectric LC's have been most frequently employed as active phase retardation devices, other electro-optic switching mechanisms and applications have also been explored. Total internal reflection switching devices have been investigated for applications including high-performance shutters and choppers, fiber-optic switches, optical interconnects, and optical waveguide switches. Meadows et al.[169] fabricated a TIR
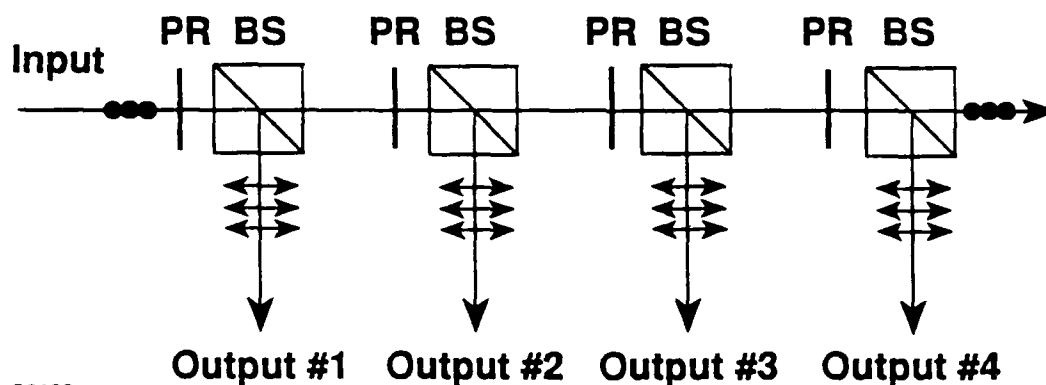
G3268

FIGURE 34 Architecture of the liquid crystal 1 × N optical switch. Polarized light enters the switch and travels through N ferroelectric LC polarization rotators (PS) and N polarizing beam splitters (BS) before leaving the device as output. [From McAdams, L. R. and Goodman, J. W., *Opt. Lett.*, 15, 1150, 1990. With permission.]
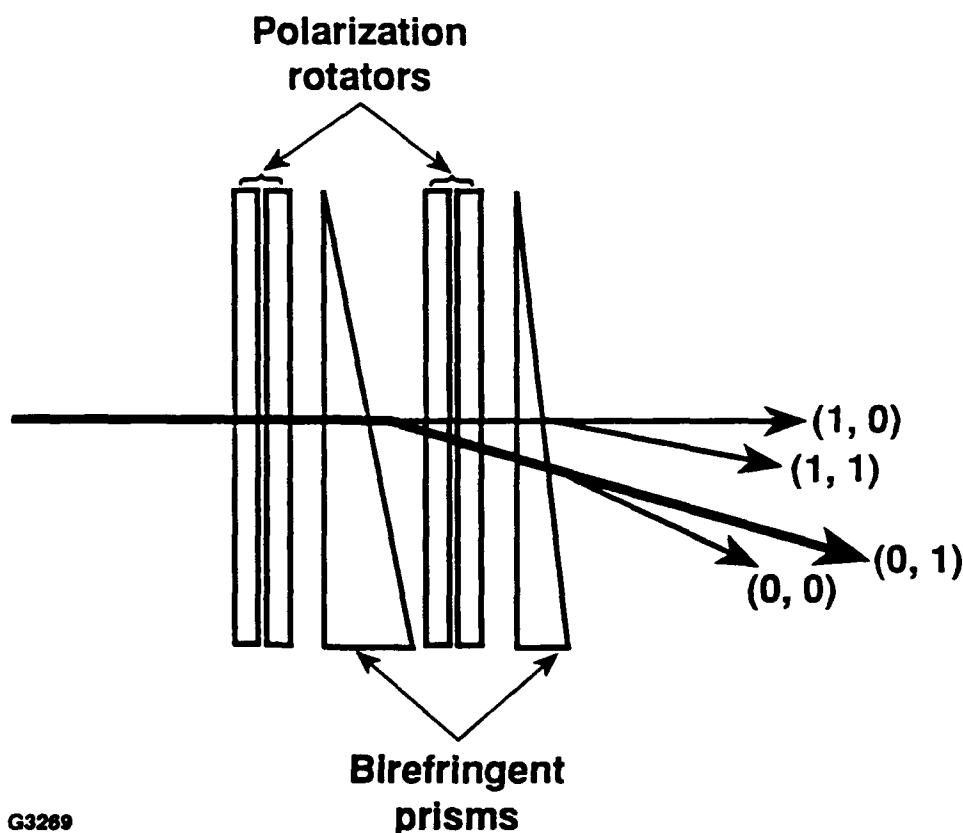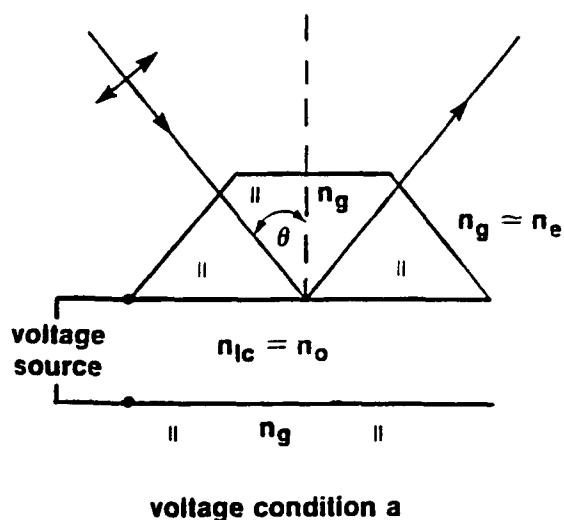

G3269

FIGURE 35 Diagram of the ferroelectric LC digital scanner. The incident beam can be output into four different locations depending on whether both, none, or either the first or second of the polarization rotators are activated. [From McRuer, R., McAdams, L. R., and Goodman, J. W., *Opt. Lett.*, 15, 1415, 1990. With permission.]

53

switch using high-tilt ferroelectric LC materials (tilt angle θ near 45°) based on a device concept previously introduced by Soref[170] in which nematic materials were used. The device, shown schematically in Figure 36, consists of a layer of aligned ferroelectric LC material contained between two glass prisms, the inner surfaces of which are coated with a transparent conductive film, (e.g., indium tin oxide) and an alignment layer. The prism material is chosen so that its refractive index (n_g) is approximately equal to the extraordinary index of the LC material (n_e). In the device "off" state, the LC optic axis is oriented so that incident polarized light experiences the ordinary LC refractive index (n_o); since $n_o < n_e = n_g$, the incident beam undergoes total internal reflection. Application of an electric field causes a 90° rotation of the LC optic axis; the polarized incident beam now experiences n_e, and is transmitted through the LC layer. Electro-optic switching between the two orthogonal optic axis positions is accomplished using the same dc-drive techniques employed for the previously described polarization rotation devices. Bistable operation is also possible if the proper surface anchoring conditions are achieved. Contrast ratios of 40,000:1 over the entire spectral range and 500,000:1 at 633 nm in selected areas of the device were reported, along with switching times of approximately 150 μs.

A variation of this TIR switching concept has also been successfully employed in the fabrication of a polymer/SSFLC optical waveguide switching device.[171,172] The device geometry, shown in Figure 37, consists of a layer of SSFLC material contained between two conductive substrates, one of which has been coated with polymer waveguide material of index n_p. The ferroelectric LC material functions as an active substrate material on a passive polymer waveguide, which eliminates the large on-state transmission losses due to Rayleigh scattering that occur in device geometries where the LC material is used as the waveguide medium.[173,174] Figure 38 shows the optic axis orientation in both the device on-state ($n_e < n_p$) and off-state ($n_e > n_p$). The smectic molecules are aligned so that the angle between the smectic layer normal and the incident light (30°) is slightly less than the device critical angle ($\theta_c = 30.5°$). Since only a small change in director orientation is required to exceed the critical angle and defeat the TIR effect, the electro-optic performance is not materially affected by the molecular tilt angle of the particular ferroelectric LC material employed. The device is therefore not limited to materials with large tilt angles, as was the case in the previously described TIR beam switch, but can function successfully with nearly any ferroelectric LC material. Unlike the SSFLC device, in which contrast is dependent on the tilt angle and is thus sensitive to temperature, the contrast ratio in the waveguide device is primarily a function of the transmittance in the polymer waveguide and the leakage of the scattered light in the LC material and is not materially affected by temperature variations. Contrast ratios of about 40:1 and response times in the microsecond regime were reported in a waveguide device using a 4-μm path length of a single-component LC material with high spontaneous polarization (3M2CPOOB); the driving waveform for these measurements was a ±35 V rectangular wave at 10 KHz. Substantial improvements in drive voltage requirements of the device are possible if thinner waveguide and LC layers are used.[173,174]

A unique device concept that has recently been proposed makes use of ferroelectric LC arrays as diffractive phase modulators for unpolarized light.[175] The device is best envisioned as a diffraction grating formed by a linear array of phase modulators, or wave

$\theta \simeq 70°$ for
$\Delta n_{lc} = 0.15$

n_g

$n_g \simeq n_e$

$n_{lc} = n_o$

voltage source

n_g

voltage condition a

(a) $n_{lc} = n_o < n_g \longrightarrow$ TIR

G1952

n_g

voltage source

$n_{lc} \simeq n_e \simeq n_g$

n_g

voltage condition b
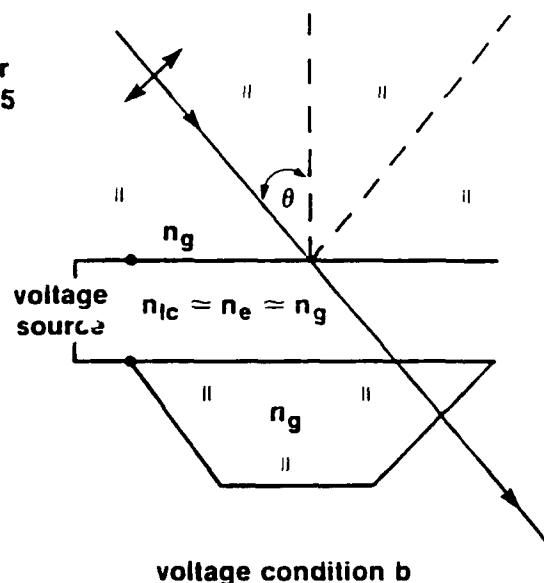
(b) $n_{lc} \simeq n_e \simeq n_g \longrightarrow$ transmission (frustrated TIR)

FIGURE 36   Schematic diagram of the total internal reflection switching device. (a) In the initial state, the LC molecules are oriented so that the incoming polarization experiences n_o and the incident beam undergoes total internal reflection. (b) Application of an electric field causes molecular reorientation and the incoming polarization now experiences n_e, which is approximately equal to the index of the glass prisms. The resulting index match allows the incident beam to be transmitted through the LC layer.

55
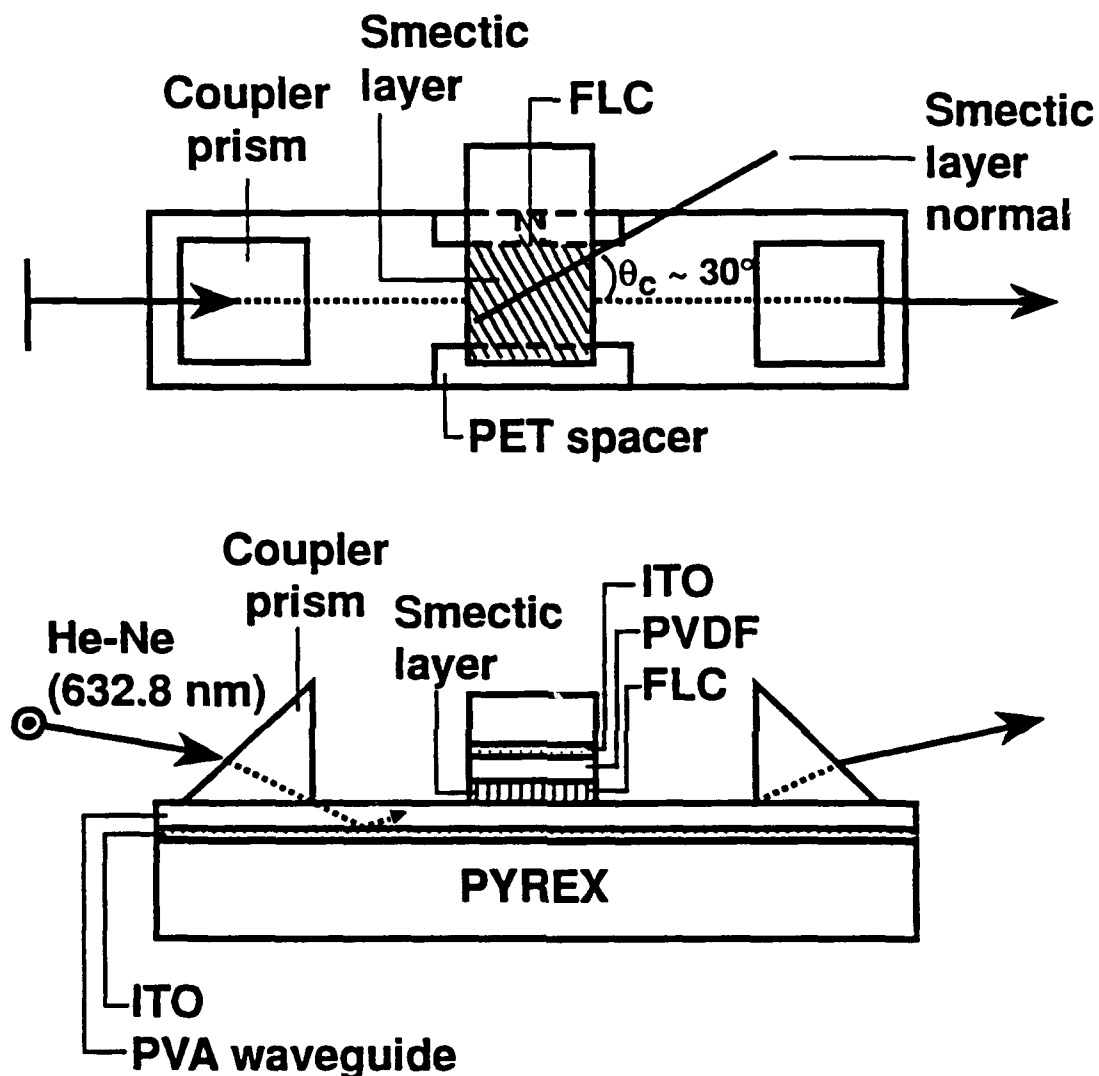
FIGURE 37 A waveguide switching device employing a ferroelectric LC material as an active substrate in conjunction with a passive PVA polymer waveguide. Scattering losses in this configuration are considerably reduced as compared to those in which the LC material is used as an active waveguiding medium. The critical angle (θ_c) is approximately 30°. [From Yoshino, K., Ozaki, M., Tagawa, A., Hatai, T., Asada, K., Sadohara, Y., Daido, K., and Ohmori, Y., *Mol. Cryst. Liq. Cryst.*, 202, 163–169, 1991. With permission.]
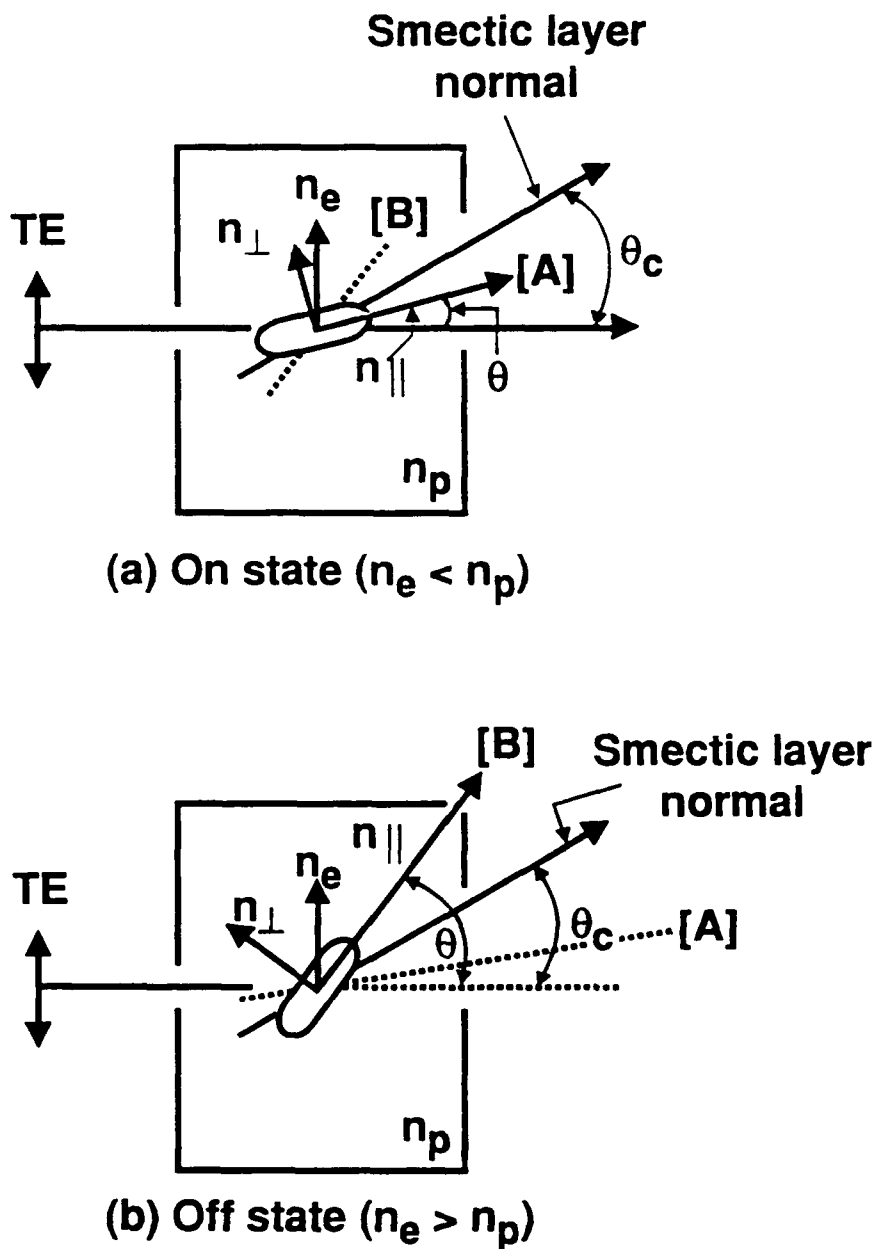
FIGURE 38 Optic axis orientation in the waveguide switching device of Yoshino *et al.*
(a) The device "on" state: the incident light is transmitted by TIR along the waveguide, since the optic axis is oriented so that n_e of the LC material is smaller than the index of the polymer waveguide n_p. (b) The device "off" state: here the optic axis orientation causes n_e to be greater than n_p, which defeats the TIR condition and allows the incident beam to pass from the polymer waveguide through the LC layer. [A] and [B] indicate the optic axis orientation in the device "on" and "off" states, respectively. [From Ozaki, M., Sadohara, Y., Hatai, T, and Yoshino, K, *Jpn. J. Appl. Phys. 2, Lett.*, 29, L843–L845, 1990. With permission.]

plates, that can be electrically switched between phase shift states of (0, π, 0, π, . . . 0, π) and (0,0, . . . 0,0) to alternately transmit or fully diffract the incident beam. This is accomplished by utilizing a series of strip electrodes to which a positive or negative drive voltage can be applied to switch the LC material between two optic axis orientations corresponding to phase delay states of 0 and π (Figure 39). Both low-tilt and high-tilt materials can be used, but each requires a slightly different device geometry. A tandem modulator in which light passes through two half-wave plates that switch in opposite directions is required for low-tilt materials in order to achieve the desired π phase shift, while a single-modulation device is sufficient when high-tilt materials are used. The tandem, low-tilt modulation device is inherently polarization-preserving; the high-tilt device is not inherently so, but can be made polarization preserving by placing it in series with a fixed orientation half-wave plate. A diagram of the optic axis orientation in the two device types is shown in Figure 40. Contrast ratios of 70:1 for the tandem, low-tilt device and 30:1 for the high-tilt device were obtained using an unpolarized He-Ne laser as the light source. Modulation efficiency of the device is somewhat wavelength-dependent, with a complete off-state occurring only at the wavelength for which the device retardance is exactly a half-wave. However, operation at wider incident spectral widths (up to ±20%) is possible if lower contrast ratios can be tolerated.[175]

Light scattering has also been explored as a potential modulation mechanism in ferroelectric LC's. Such devices make use of scatter reduction caused by electric field-induced unwinding of the helical structure in thick (25–100 μm) cells in which the helix axis is oriented parallel to the substrates (i.e., the "bookshelf" geometry). This configuration represents a radical departure from the SSFLC-based device concepts discussed up to this point in that (a) short-pitch ferroelectric LC materials are preferred, since they scatter more strongly than do their long-pitch counterparts that were developed for SSFLC applications; and (b) unlike the SSFLC device, in which the suppression of the helical structure by surface forces and thin cell spacings is vital to its operation, molecular alignment and cell thickness in these devices have relatively little impact on their performance. Two modes of operation, illustrated in Figures 41 and 42, are known for ferroelectric LC light-scattering devices. The simplest case (Figure 41) operates by field-induced helix unwinding as described above, alternating between a strongly scattering (field-off) state and a highly transparent (field-on) state. This device is easy to fabricate and displays high contrast but is hampered by a relatively slow relaxation time.[176] A more generally useful variant of this device form is the transient (light-)scattering mode (TSM) device of Yoshino and Ozaki,[177,178] shown in Figure 42. The initial application of an electric field produces the highly transparent, helix-unwound state shown in Figure 41. The electric field polarity is then rapidly reversed and the violent molecular motion, which occurs as the ferroelectric LC domains align with the new field direction, results in intense light scattering of light. The transmissive state is then immediately restored as the new spontaneous polarization direction is established. Transient (light-)scattering devices, fabricated using the classical Schiff-base ferroelectric LC material DOBAMBC, possessed contrast ratios ranging from 50:1 (25 μm cell at 40 V, 70°C) to 175:1 (100 μm cell at 75 V, 70°C) with response times in the microsecond regime.[178] Both contrast ratio and response time were seen to improve at increased drive voltages. Thicker cells showed

y_o

$5 \longrightarrow x_o$

y_i

S

S

S $\longrightarrow x_i$

S

S

V_a

V_b

Electrode detail

(a)

(b)
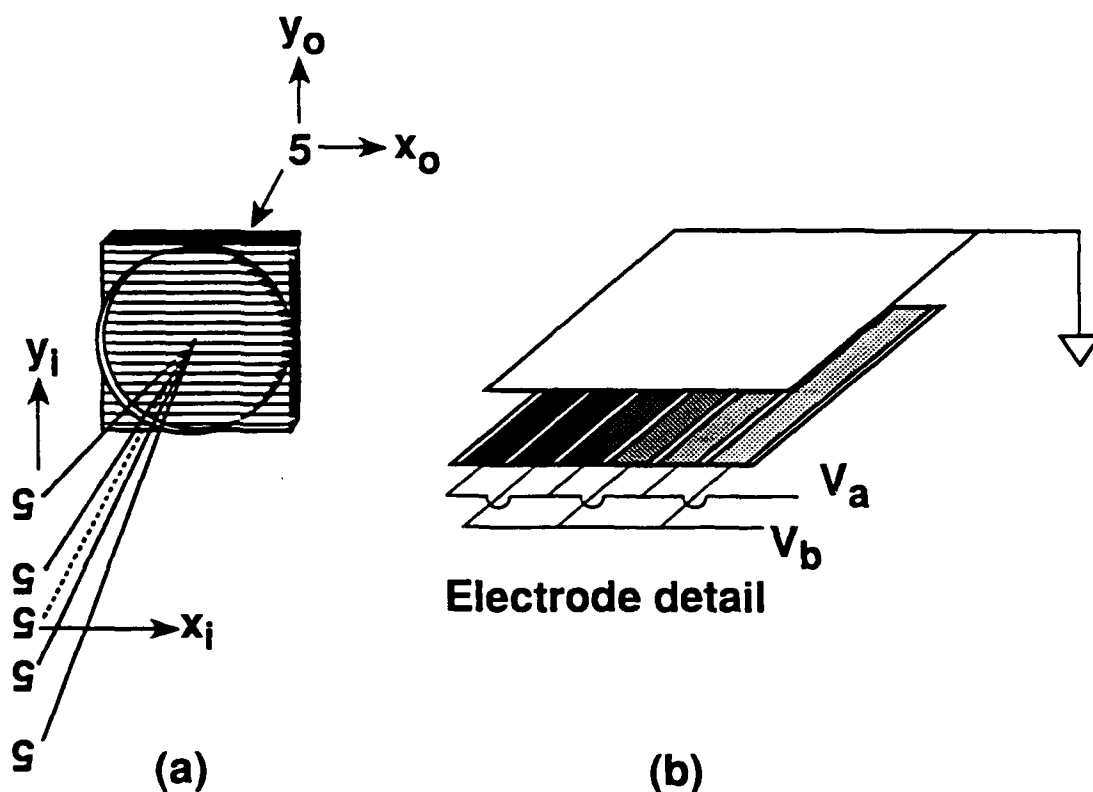
G3272

FIGURE 39 The diffractive SSFLC phase modulation array device. (a) A simplified schematic drawing showing the formation of diffracted images using a lens in combination with the ferroelectric LC array. (b) The electrode structure used in the array device. When $V_a = V_b$, all the segments are in the same state and no diffraction occurs; changing the applied voltage state to $V_a = -V_b$ causes light passing through adjacent strips to differ in phase by π, thus producing the diffraction effect. [From O'Callaghan, M. J. and Handschy, M. A., *Opt. Lett.*, 16, 771, 1991. With permission.]

59

higher contrast ratios, but responded much more slowly compared to thin cells at equivalent voltage levels. Although the scattering effect is transient in nature, it was shown that its duration could be extended to longer time intervals by applying a driving waveform consisting of a series of voltage pulses, whose temporal characteristics allow the individual scattering states to overlap.[177] These characteristics, combined with the fact that TSM devices require no polarizers and are capable of broad-band operation due to the low dependence of scattering on wavelength, have made them of interest for optical-switching applications in the near-and mid-infrared spectral regions. Devices employing DOBAMBC have been used to modulate optical radiation at selected wavelengths in the near infrared (1.2–2.5 μ),[179] and the usefulness of a TSM device as an electro-optic chopper for the mid-infrared region (8–12 μm) has recently been demonstrated.[180]

An electro-optic mode of operation in ferroelectric LC materials that has only very recently become of interest for device applications is the deformed helix ferroelectric (DHF) effect. The device geometry, which is shown in Figure 43, is similar in many ways to the TSM device described above, but uses a very weak electric field to partially unwind the helical structure and requires polarizers in order to function. Although the existence of the effect has been known for some time,[181–184] it had not been exploited for device applications until recently[185] because of a lack of ferroelectric materials with the required short helical pitch lengths (<1 μm) and high molecular tilt angles. The DHF effect has several interesting features that make it particularly attractive for optical-modulation applications: (a) high contrast (>100:1) at low electric field strengths (1 V peak-to peak/μm of cell thickness), (b) gray-scale operation that is linearly dependent on the applied field, and (c) fast response times (around 300 μs) that depend only on the unperturbed helix pitch, smectic C* twist elastic constant, and rotational viscosity of the ferroelectric LC material. Response times are independent of voltage amplitude, layer thickness, and spontaneous polarization value.[185] High-quality homogeneous alignment can be readily obtained, even for relatively thick cell spacings, using common orientation techniques such as buffed polymer alignment layers or oblique evaporation. Device fabrication is therefore greatly simplified.[185] The DHF effect has been employed by both Beresnev et al.[186] and Landreth et al.[187] in the construction of optically addressed spatial light modulators. Electro-optic color modulation in DHF devices employing ferroelectric LC materials with visible region selective reflection has also been described by both Jakli et al.[188] and Abdulhalim and Moddel.[189]

Orthogonal Ferroelectrics

If an electric field is applied parallel to the layer planes of an orthogonal smectic phase composed of chiral molecules, a change in birefringence of the medium occurs as the molecules within the layers undergo a coordinated tilt from the layer normal. This "electroclinic" effect, which was first observed by Garoff and Meyer[190] in the smectic A* phase of DOBAMBC near the smectic A*–C* transition temperature, results from a biasing of free rotation about the long molecular axis produced by alignment of transverse dipole moments with the applied electric field. Due to a reduction in symmetry (see the earlier discussion in this article), a macroscopic polarization appears along the electric field direction and a molecular tilt is induced perpendicular to the plane containing the layer

(a)

(b)

G3273
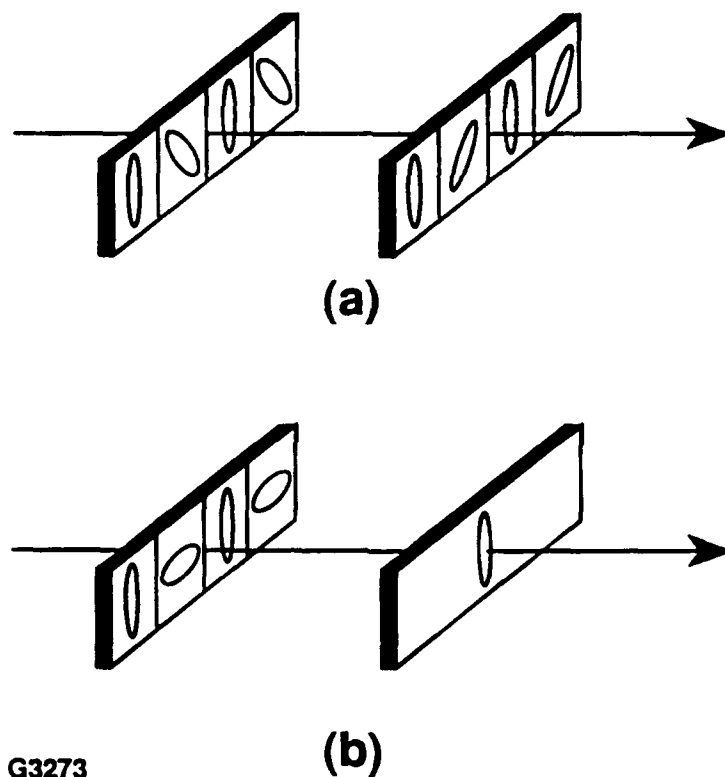
FIGURE 40   Optic axis orientations in diffractive SSFLC phase modulators. (a) The
tandem, low-tilt device geometry. The first device rotates the plane of
polarization by +45°, while the second device rotates the plane of
polarization by -45°, resulting in a 90° difference in orientation. (b) The
high tilt device geometry, shown here with an optional wave plate used to
preserve polarization. [From O'Callaghan, M. J. and Handschy, M. A.,
Opt. Lett., 16, 772, 1991. With permission.]

cell thickness (d)

incident
radiation
(I_0)

ITO
glass

pitch
(p)

I_0

V = O - high scattering

V > ± V_{th} - transparent
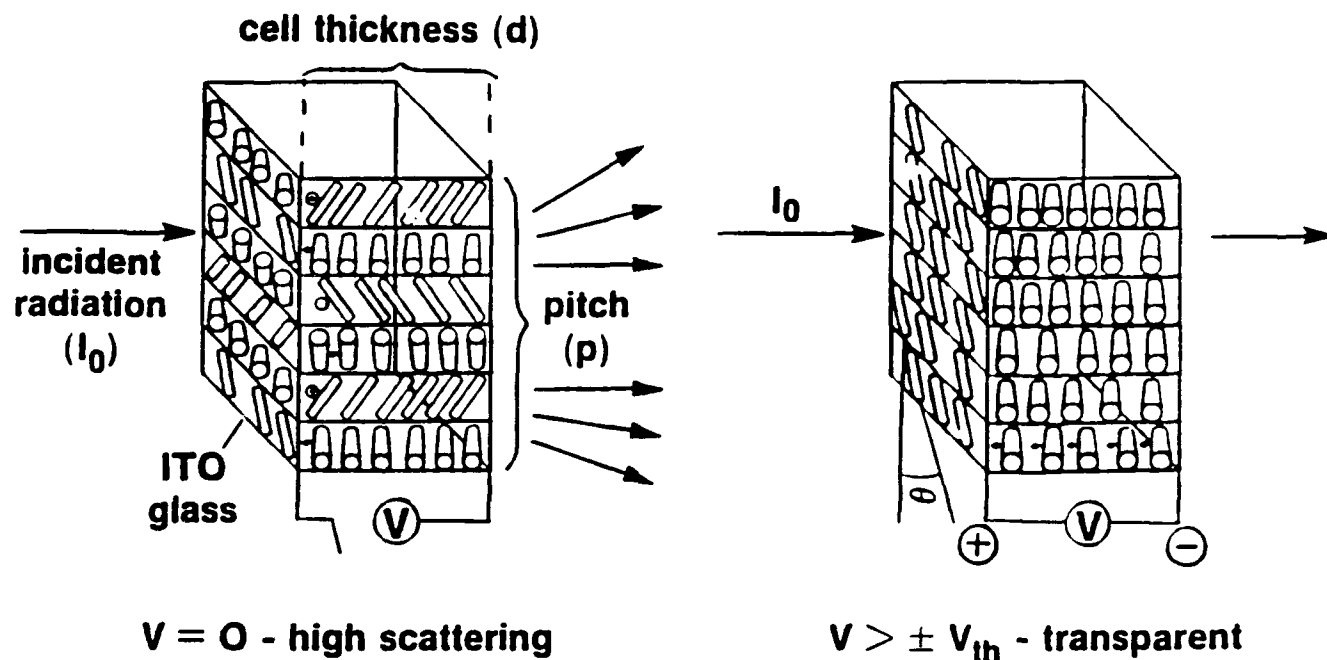
- incident light polarized or unpolarized
- slow response

G1993

FIGURE 41   Light modulation by field-induced helix unwinding in thick ferroelectric LC
cells. In the absence of an electric field, the helical structure produces a
strongly scattering texture; application of an electric field causes the
molecular dipoles to align with the applied field direction, which unwinds
the helix and produces a highly transparent state.

Cell thickness (d)

I_o

Incident radiation (I_o)

Pitch (p)

I_o

ITO glass $\oplus$ Ⓥ $\ominus$

ITO glass Ⓥ

$\ominus$ Ⓥ $\oplus$

V = –V	V = 0	V = +V
Transparent	Scattering	Transparent
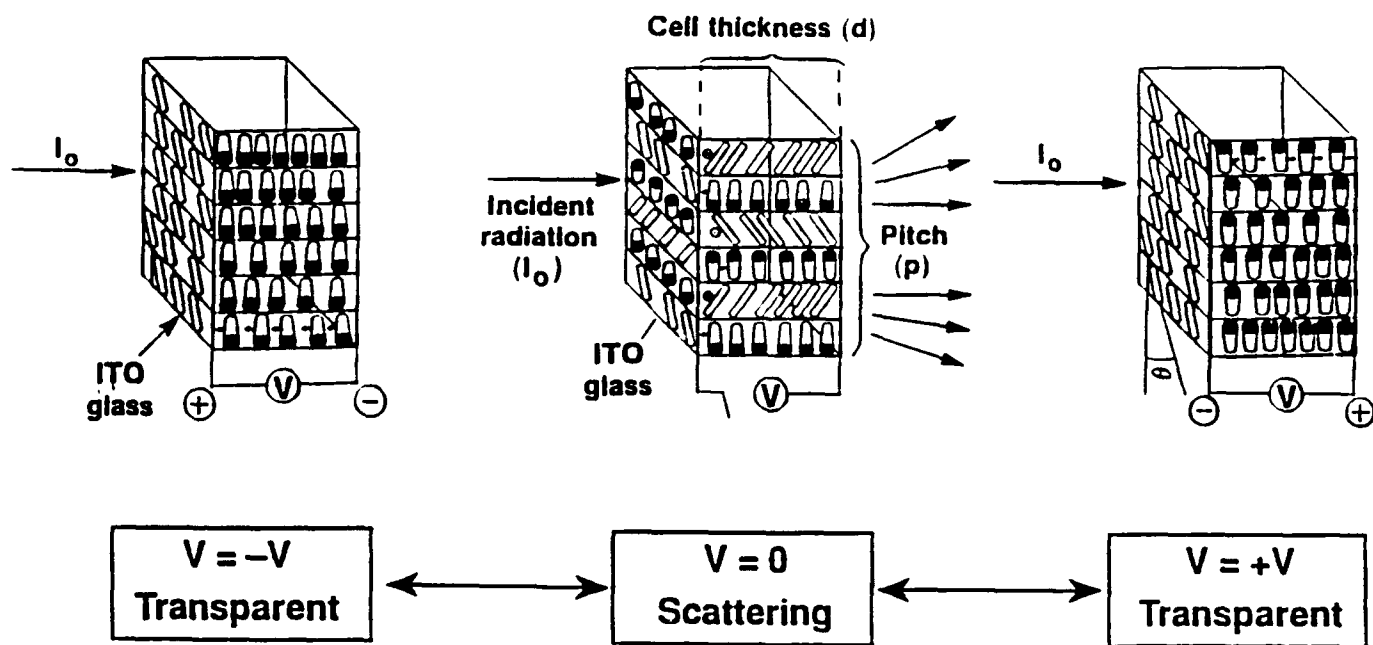
- **Reversal of dc field polarity through zero voltage state produces transient scattering effect**

G2777

FIGURE 42   The transient light scattering mode device. Initial application of a dc electric field unwinds the helix and renders the device highly transparent: rapid reversal of the electric field polarity causes the device to pass through an intermediate, transient scattering state into a second transparent state as the ferroelectric LC molecules attempt to align with the applied field.

63

Light beam a >> p_o

Polarizer P

β

LC

p_o

Helix axis

$L >> p_o$

Θ_o

y

x

z

Glass with electrodes

Analyzer A

$\pi/2-\beta$
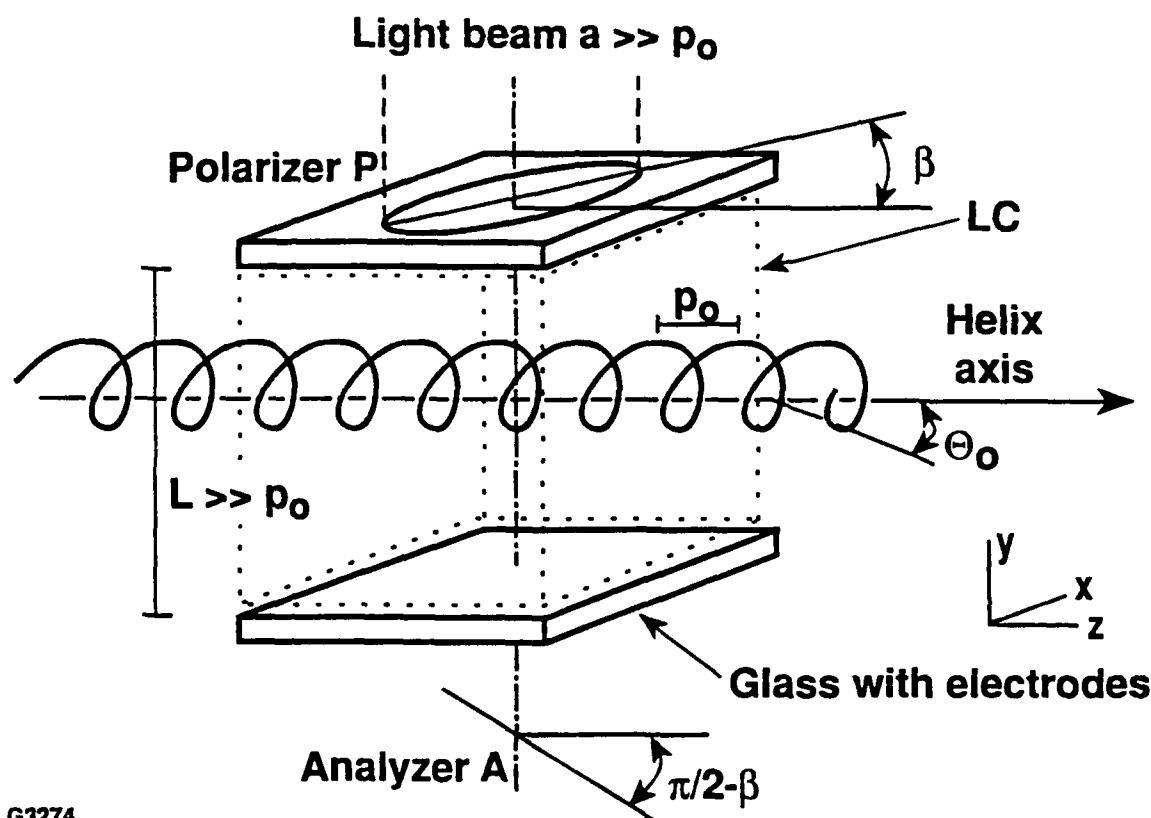
G3274

FIGURE 43   Schematic diagram of the deformed helix ferroelectric LC device, or DHF-LCD. The DHF cell is similar in construction to TSM scattering devices, but must be operated between crossed polarizers. The smectic C* helix, with pitch length p_0 and director tilt angle Θ_0, is oriented at an angle β to the first polarizer. The incident light striking the cell must satisfy the condition a >> p_0, where a is the aperture of the incident light. Application of a weak ac field (1–2 V/μm of cell path length) deforms the helix and produces a variation of the effective refractive index of the LC material. [From Beresnev, L. A., Chigrinov, V. G., Dergachev, D. I., Poshidaev, E. P., Fünfschilling, J., and Schadt, M., *Liq. Cryst.*, 5, 1171–1177, 1989. With permission.]

64

P

E

$\hat{n}(0)$

$\hat{n}(E)$

θ

$\hat{n}$ = director orientation
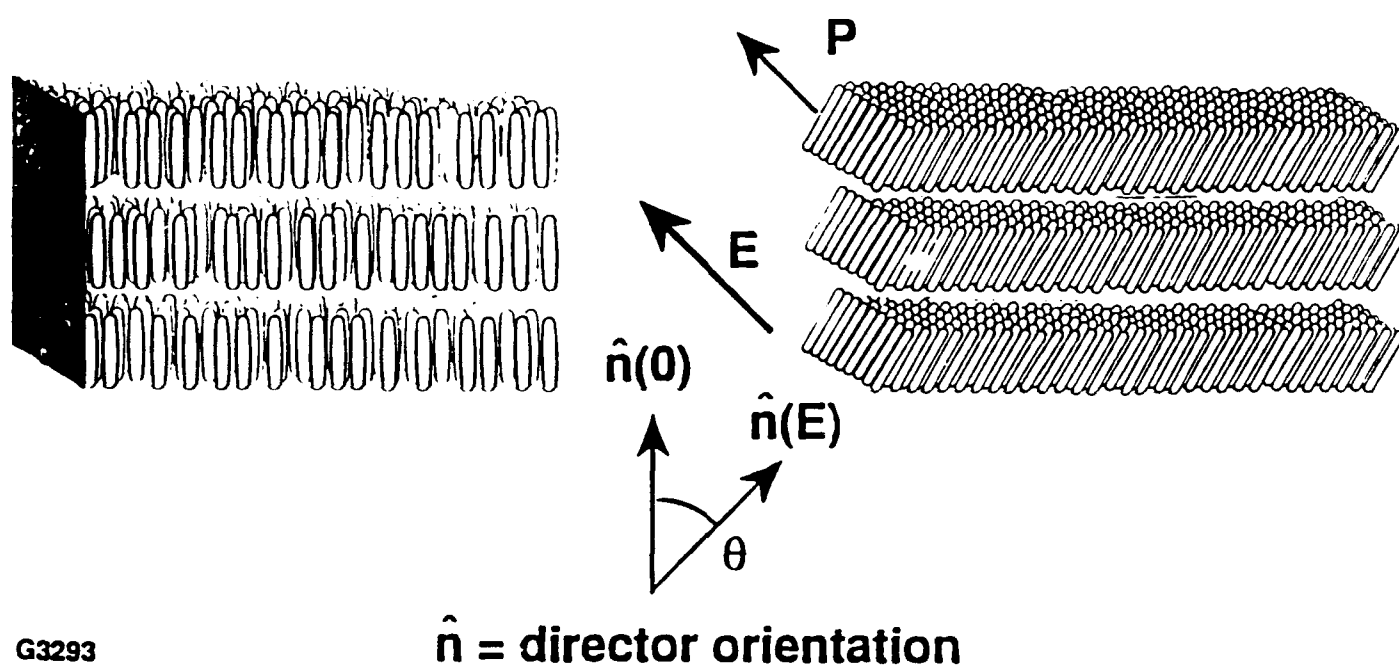
G3293

FIGURE 44   The electroclinic effect in orthogonal smectic liquid crystals. Application of an electric field (E) parallel to the layer planes biases the free rotation about the molecular axes, producing a spontaneous polarization (P) oriented along the electric field direction. A change in the molecular tilt angle (θ) perpendicular to both the electric field direction and the layer normal occurs as a linear function of applied field strength.

normal and the macroscopic polarization direction[25] (see Figure 44). The magnitude of this molecular tilt, and thus the induced birefringence, was found by Garoff and Meyer to be a *linear* function of the applied field strength—a highly unusual electro-optic effect in liquid crystal media. The temporal response characteristics were also remarkable, ranging from 13–17 μs near the S_A^*-S_C^* transition temperature.[190] Limitations in the applied electric field strength imposed by the experimental geometry used by Garoff and Meyer, in which the smectic layer planes were parallel to the glass substrates, resulted in a very weak induced birefringence that required phase-sensitive detection methods.[190]

Interest in orthogonal ferroelectric materials for device applications was considerably heightened when, nearly ten years later, Andersson et al.[191] showed that if the smectic A* material is oriented in the bookshelf geometry of the SSFLC device (smectic layer planes perpendicular to the substrates) and thin cells (1–3 μm) are used, the magnitude of the induced birefringence is considerably larger. Drive voltage levels are also substantially reduced, and the effect is accessible at CMOS-compatible voltage levels (e.g., 10–30 V). In accordance with the earlier findings of Garoff and Meyer, the magnitude of the induced birefringence was found to be linearly dependent on the applied field strength. The temporal response in the bookshelf geometry was also reported to be nearly two orders of magnitude faster than the corresponding SSFLC mode for a given ferroelectric LC material at the same applied field strength. This new device geometry was named the *soft-mode* device by Andersson et al.[192] after traditional spectroscopic nomenclature used to describe a change in tilt; however, both the terms "electroclinic" and "soft-mode" are used interchangeably in the current literature and refer to the same effect. The basic geometry of the soft-mode device is shown in Figure 45. In this configuration, the field-induced tilt of the optic axis of the orthogonal smectic material causes it to behave like a variable retardation plate.[192] Generation of high-quality homogeneous alignment in these devices is considerably less difficult than in corresponding SSFLC devices due to the absence of the helical structure, but is still more difficult to achieve than in other, less ordered phases (e.g., nematics). Although bistable operation is not possible in soft-mode devices, the field-linear nature of the electro-optic response allows it to function as either a light modulator with continuous gray-scale or as a tunable color filter, depending on the particular polarizer or retarder combination used.[192] The combination of gray-scale ability, fast response, and relative ease of alignment has made soft-mode devices particularly attractive for numerous optical device applications, including analog gray-scale and full-color displays and TV screens, spatial light modulators, color switches, and tunable wave plate or color filter devices.[192] Several examples of soft-mode device applications have recently been demonstrated. Optically addressed gray-scale spatial light modulators with response times of 40 μs at 29°C and 4 μs at 50°C have been constructed by Abdulhalim et al.;[193,194] Sharp et al.[195] have also used smectic A* soft-mode cells in a continuously tunable color filter with a 115 nm tuning bandwidth, 10 MHz response, and low drive voltage requirements (±30V).

At present, the single greatest limitation on performance in soft-mode devices is the relatively small field-induced tilt angles (2°–18°) that can be obtained at reasonable voltage levels in existing electroclinic materials. As a direct result of this limitation, considerable interest has been generated in the development and characterization of new orthogonal

Det —[**Osc**

I(ΔI)

Analyzer

$\hat{n}(0)$

θ $\hat{n}(E)$

V_{dc} ⊕
V_{ac} ⊕

E↓

Polarizer
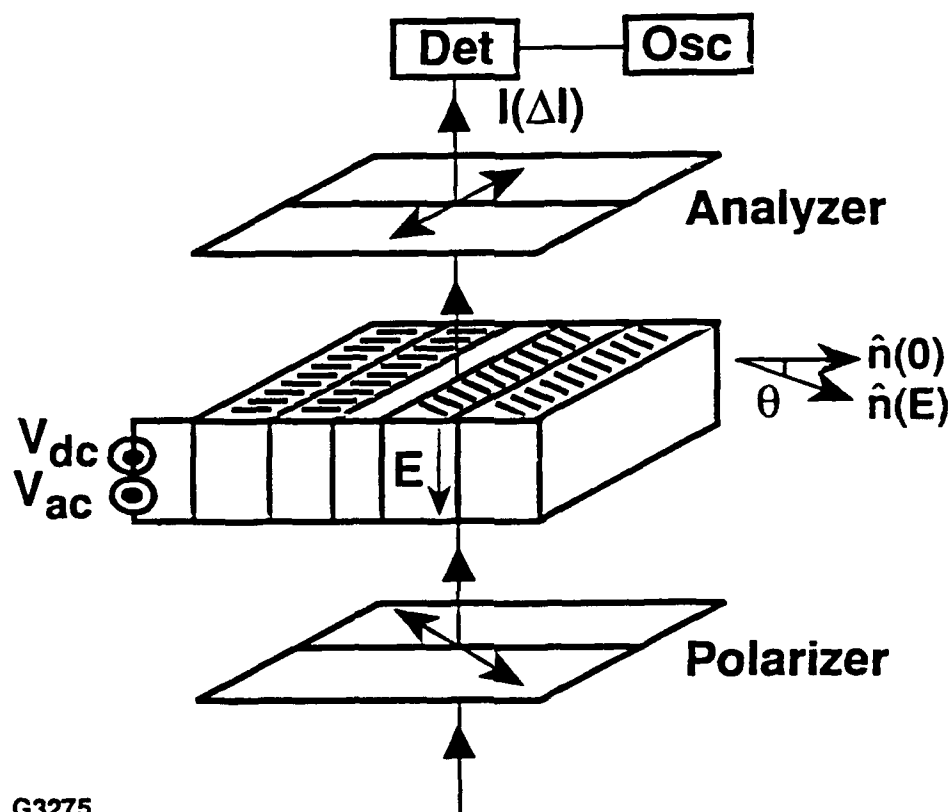
G3275

FIGURE 45   The basic geometry of the soft-mode device. The orthogonal smectic
material is oriented in the bookshelf geometry, with the layer planes normal
to the substrates. The field-induced change in tilt angle allows the device to
behave as a variable retardation plate when the device is operated between
crossed polarizers. [From Andersson, G., Dahl, I., Kuczynski, W.,
Lagerwall, S. T., Skarp, K., and Stebler, B., *Ferroelectrics*, 84, 285–315,
1988. With permission.]

smectic materials with large field-induced tilt angles that are capable of satisfying existing and future device requirements. In addition to new smectic A* materials with large spontaneous polarization,[196–198] other orthogonal smectic phases are also being investigated. Materials possessing the smectic B and E phases are particularly promising; Bahr and Heppke[199] have reported induced tilt/applied field ratios in the smectic B and E phases of 4-(4-methyl-2-chloropentanoyloxy)-4'-pentyloxybiphenyl that are nearly twice as large as those measured in its smectic A* phase.

Molecular Alignment Issues

The presence of both a layered, helical structure and a spontaneous polarization direction in smectic C* liquid crystals introduces an additional level of complexity in device fabrication as compared to nematic and cholesteric mesogens. In addition to the need for establishing a uniform director orientation, smectic systems have an additional requirement for the layer planes to be oriented parallel to some common direction (usually perpendicular to the substrate surfaces) so that switching states with high-optical uniformity will be obtained.[28] This is of particular importance in devices employing the SSFLC geometry, in which the presence of twisted or splayed layers results in multiple, asymmetrical switching states and poor contrast.[30] The anchoring strength of the LC molecules to the substrate walls is also an important factor. Strong surface anchoring tends to lock the director into one particular orientation, favoring one switchable state over another and compromising the bistability.[26] An alignment technique employing weak surface anchoring conditions that was initially used in SSFLC prototype device development was to use gentle shearing of the two substrate surfaces while the LC material was heated into the smectic A phase.[156] This method gives excellent results over small (1–2 cm^2) areas but is somewhat difficult to reproduce. Other techniques that rely on weak surface anchoring, such as cooling from the smectic A phase in the presence of a large magnetic field[200] and epitaxial growth of an aligned phase by using a thermal gradient,[201] have also been used with varying degrees of success. Rubbed polymer alignment coatings are currently the most widely used alignment technique for ferroelectric LC devices, since such coatings provide good alignment over large areas in both thick (helixed) cells and the SSFLC geometry.[28] Ferroelectric LC materials having the phase sequence on cooling of "isotropic-smectic A-smectic C*" can be used to fabricate devices with well-aligned layers and uniform switching, if a cell employing rubbed polymer alignment layers is filled in the smectic A phase and slowly cooled into the smectic C* phase.[28] Materials with the phase sequence "isotropic-cholesteric-smectic C*" can also be aligned by this method, but an applied dc field or low-frequency ac field is required during the cooling process to avoid switching-state degeneracy produced by tilt of the smectic layers away from the fixed director orientation.[202] Other methods and materials that have been reported to improve alignment quality or enhance bistability include the use of Langmuir-Blodgett orientation films,[203] metal-oxide thin films in combination with electric fields,[204] and charge-transfer complexes doped into polyimide alignment layers.[205,206] The effect of rubbing strength on bistability[207] and the relationship between physical properties of polymer alignment layers and SSFLC cell quality[208] have also recently been examined.

LC/Polymer Composite Devices

Although the monomeric liquid crystal devices reviewed up to this point differ considerably in the type of mesogen, alignment conditions, and cell construction employed to generate the desired electro-optic effect, they nevertheless can be viewed generically as consisting of a bulk LC fluid contained between a pair of rigid, conductive substrates coated with a molecular alignment layer and joined together by a sealing material. Liquid crystal/polymer composite devices represent a radical departure from this familiar configuration in that the LC material is distributed as *microdroplets* within the body of a polymer film. The process for fabrication of these composite devices consists of coating a conductive substrate with a water- or solvent-borne slurry of the liquid crystal material that has been dispersed in an appropriate polymer. A film is then formed upon evaporation of the solvent. Lamination of a second conductive substrate onto the exposed surface of the film forms the finished device. Because the active LC material is contained as submicron- to micron-sized droplets within a polymer film ranging in thickness from 5 to 30 μm, accurate control of the film thickness over large areas becomes less important, and devices as large as several square meters can be readily fabricated on rigid or flexible substrates using commercial roll-, bar-, or blade-coating techniques.[209] Separate alignment layers on the substrates are not required, since the average direction of orientation of liquid crystal molecules within each microdroplet is established by the surrounding polymer host material. For most polymeric materials, the LC molecules will align parallel to the curved polymer/LC interface; this induces a nonparallel alignment condition in the bulk of the droplet with accompanying disclinations that scatter incident light. In the absence of an applied electric field, the orientation of the individual droplets within the film is random and the resulting strong forward scattering gives the film a translucent, milky appearance. Application of an electric field across an LC/polymer composite film containing an LC material with positive dielectric anisotropy causes the molecules to align with the applied field (see Figure 46) and, if the LC refractive index perpendicular to the director approximately matches the refractive index of the polymer matrix, the device becomes highly transparent.[210] As with other LC devices based on electrically controlled light scattering, polarizers are not required for device operation. By adding either a dichroic[209,211] or an isotropic dye[212] to the LC material before dispersion into the polymer matrix, both transmissive and reflective devices that modulate light through a combination of scattering and absorption effects can also be produced.

Several different techniques have been developed for the fabrication of liquid crystal/polymer composite devices. Craighead *et al.*[213] have prepared electrically switchable films by filling the internal voids of several types of preformed porous polymer sheets with an LC material;[213] however, this technology has not yet proven to be commercially viable for device applications and will not be addressed here. Methods for the *in situ* formation of microdroplets of LC material within solid polymer films have been extensively investigated and can be divided into two classes: (1) the NCAP (nematic curvilinear aligned phase) class, in which the LC material has been suspended in the polymer matrix by standard *microencapsulation* or *emulsification* techniques as described by Fergason;[214] and (2) the polymer-dispersed liquid crystal (PDLC) class introduced by Doane *et al.*,[215] in which LC microdroplet formation is induced by *phase separation* of a

69
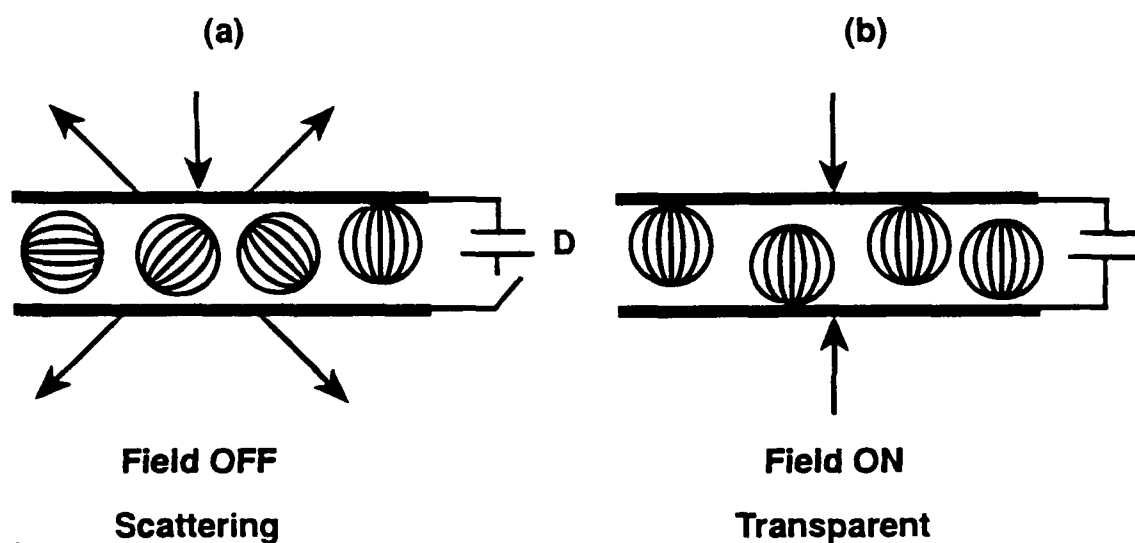
FIGURE 46   Schematic representation a LC/polymer composite electro-optic device. (a) Light-scattering disinclinations and a non-parallel bulk alignment condition are produced within the LC droplets inside the film, in the absence of an applied field. The film produces strong forward scattering of incident light. (b) An applied electric field aligns the molecules in the droplets in a common direction and the device becomes transparent. The LC material must possess both a positive dielectric anisotropy and a refractive index perpendicular to the director that approximately matches the refractive index of the polymer matrix.

70

low molar mass liquid crystal material from either oligomeric precursors or fully polymerized systems in solution.[215] Films belonging to these two classes are similar in appearance and operate by the same electro-optic mechanism but differ somewhat in their physical properties and performance characteristics.

Films of the NCAP type are most conveniently and frequently prepared by the emulsification (EM) process, in which an aqueous-based polymer solution (e.g., polyvinyl alcohol)[214] or a colloidal dispersion of a water-insoluble latex polymer[211] is used as both the capsule wall material and the film binder. The use of the latter type of polymer as the emulsification medium results in films with greatly improved moisture resistance over those prepared using water-soluble polymer systems. The microstructure of EM NCAP films can be represented as consisting of interconnected, oblate spheroid-shaped cells, filled with nematic LC material, whose major axis is oriented within the film plane. This shape is believed to be caused by anisotropic shrinkage of the film during the drying process.[211] Although EM NCAP films cannot be considered microencapsulated in the strictest sense, because of the presence of interconnecting channels within the polymer matrix, the resulting electro-optic effect is identical to that produced in systems that have been truly microencapsulated prior to suspension in a separate polymeric film-forming material.[209] Operating voltages for EM NCAP films range from 20 to 100 V and are dependent on many factors, including nematic droplet size and shape, LC elastic constants and dielectric anisotropy, polymer matrix dielectric constant, and film conductivity and thickness.[214] Advantages of the NCAP system are the large LC concentration levels possible (up to 65% of the total film mass),[209] which allow for large effects at small film thicknesses, and the low solubility of dichroic dyes in the polymers commonly used to form the films. The latter property is particularly important because display performance is substantially reduced as the dye becomes more soluble in the polymer. Under these conditions, it cannot align with the applied electric field.[214] Disadvantages include the limited ability to control the size distribution of the nematic microdroplets, which results in relatively high switching field requirements.[216]

Polymer-dispersed LC films can be prepared by using any of three different phase-separation techniques. In the *thermally induced phase separation* technique (TIPS), the LC material is dissolved into a molten thermoplastic polymer at elevated temperature; phase separation of the LC material from the polymer host occurs upon cooling to room temperature.[210] Thermoplastic polymers that are stable at the melt temperature, such as polymethyl methacrylate (PMMA) or polyvinylformal (PVF), are required for the TIPS process. The size distribution of the LC droplets is controlled by the rate of cooling from solution into the LC/polymer host immiscibility temperature region, as well as other materials factors (e.g., viscosity and chemical potential).[217] For thermoplastic polymers that decompose at or below the melt temperature or if solution coating techniques are required, the *solvent-induced phase separation* (SIPS) process is employed. Here the polymer and LC material are dissolved in a common solvent to form a homogeneous solution. Evaporation of the solvent ultimately results in phase separation of the LC material and solidification of the polymer film. The polymer matrix contains some dissolved LC material that acts as a plasticizer, lowering the polymer glass transition and enhancing its processability.[210] Although both TIPS and SIPS have been actively

71

investigated for device applications,[218,219] the process of *polymerization-induced phase separation* (PIPS) has received the greatest attention[220–229] due to the degree of control over both the nematic droplet size and the physical/optical properties of the polymer matrix. A low molar mass liquid crystal is mixed with a polymer precursor and the polymerization reaction is initiated. As the reaction proceeds, the solubility of the LC material in the mixture decreases until the LC material phase separates as droplets, which continue to grow until the polymer mixture gels and the droplet morphology is locked in. A number of different polymeric systems cured by condensation, free-radical, or photoinitiated reaction mechanisms have been investigated, including thermosetting[220,221,225–227,229] and UV-cured[222,224] epoxies, polyurethanes,[223] and UV-cured acrylates.[229,230] Droplet size and morphology in the PIPS technique is dependent on the polymerization rate, relative concentrations of the LC material and polymer, and other physical parameters such as viscosity, diffusion rate, and solubility of the LC material in the polymer host.[210] Films with a carefully controlled LC droplet size distribution can be prepared by adjusting the cure temperature (thermosetting systems) or light intensity (photoinitiated systems) to control the rate of polymerization.[216,228] Drive voltage requirements for PDLC films are governed by many of the same parameters that affect NCAP films and range between 1–4 V/μm of film thickness, depending on droplet size and shape and the particular polymer medium employed.[210,217,227,228]

Several novel device geometries and interesting new electro-optic modes of operation in LC/polymer composite devices have recently been reported. Pirs *et al.*[231] have described a color modulation device employing PDLC shutters in conjunction with three nonabsorbent dichroic mirrors successively mounted at a 45° angle to the incident light. This device is useful for applications such as color projection systems and in the examination and processing of color photographic prints, where high incident light intensity and low-light losses are important. Optical limiting devices employing hybrid optical bistability with linear feedback in PDLC films have also recently been reported by several investigators.[232,233] Dual-frequency addressing has also been recently employed to improve the contrast and multiplexability of PDLC films;[234,235] and, in conjunction with electric fields applied during the film-curing process, to generate "reverse mode" PDLC devices that switch from transparent to opaque with increasing drive voltage or frequency.[236,237] *Other novel device concepts and material systems include polymer-dispersed LC films containing a cholesteric LC material with negative dielectric anisotropy that switch from a weakly scattering "dark" state to a highly colored reflective state,[238–240] and anisotropic gels produced by photopolymerizing a liquid crystal mixture containing LC diacrylates that undergo light scattering on application of an electric field.[241]

NONLINEAR OPTICAL EFFECTS AND DEVICES

Currently no commercially available, general-purpose or application-specific nonlinear-optical LC devices exist. Nonlinear optical phenomena in organic monomeric and polymeric materials are, however, studied with considerable vigor. Liquid crystals are a subgroup of this general category of organic materials. The many efforts of preparing and analyzing organic compounds for the purpose of providing organic alternatives to inorganic materials in nonlinear optical applications have prompted the appearance of several

monographs and many review articles on the matter.[242-255] However, for the pulse-length and power regimes typical of applications in optical signal processing, a pivotal driving force in organic optical material development, liquid crystalline phases of organic molecules offer no distinct advantages over non-mesogenic compounds. Comparatively little effort is therefore spent on liquid crystal-specific developments for fast opto-optic switching applications. In the few reports on measurements of fast $\chi^{(3)}$ in mesogenic compounds ($\chi^{(3)}$ is the physical parameter governing opto-optic material response), the samples were either deliberately studied in their isotropic phase[256-260] or no significant difference in response was observed when $\chi^{(3)}$ in a mesophase was compared with $\chi^{(3)}$ in the isotropic phase.[121,256]

There are several physical mechanisms contributing to $\chi^{(3)}$: molecular polarizability of the molecular electron-charge distribution, molecular reorientation caused by torque exerted by the E-field of the light on the dipole moment of the molecule, electrostriction, and thermal effects. There is some recent evidence[261,262] that light-induced reorientation on a picosecond time scale cannot be ruled out, even for molecules as large as common mesogens. Yet, the prevalent interpretation of fast $\chi^{(3)}$ effects in liquid crystals still holds that the fast, liquid crystal $\chi^{(3)}$ response is dominated by the electronic polarizability. On this evidence, one would expect that, except for possible extraneous advantages such as chemical compatibility, stability or manufacturing ease, liquid crystals *per se* will not be major factors in future, high-speed, opto-optic device development.

The potential usefulness of mesogenic compounds is much better relative to moderate-speed $\chi^{(3)}$ effects as well as to parametric nonlinear optical effects governed by the second-order susceptibility $\chi^{(2)}$. The latter comprise the well known effects of frequency mixing, harmonic conversion and electro-optic switching. As the light field does not do any work on the medium in $\chi^{(2)}$ processes, the medium response-time limitations described above do not apply here. Second-order nonlinear optical effects are based on symmetry principles that rule out their occurrence in isotropic media or in media with molecular inversion symmetry. Many *inorganic*, noncentrosymmetric crystals exist that serve $\chi^{(2)}$ applications over the wavelength range from 12 μm down to 210 nm and up to very large clear-aperture sizes. Research into and development of *organic* materials for similar applications is spurred by the hope that compounds will be found with larger second-order polarizability than available in currently existing crystals. Integrated-optics and microphotonics applications ranging from optical data storage to diode-laser based high-resolution printers pose challenges that are to be met through the use of nonlinear optical polymers.

In polymers, the intrinsic $\chi^{(2)}$ symmetry restrictions are removed by methods such as electric dc-field contact or corona poling of the polymer matrix.[263-266] The low poling efficiencies and, more important, the relaxation of the forced polymer order with time open opportunities for those self-organizing media that combine application flexibility with structural stability. For these reasons, liquid crystals are both developed for $\chi^{(2)}$ applications and characterized by $\chi^{(2)}$ methods.

Second-Order Nonlinearity

Since they lack inversion symmetry, ferroelectric chiral smectic C phases are attractive candidate materials for second-order nonlinear optical devices. Blinov and his group[267] recognized this advantage in 1984. They demonstrated, by unwinding the smectic helix with the help of a dc field, that their choice of molecule, DOMAMBC, offers the proper molecular structure for both generating the second harmonic of an incident beam and for phase-matching the propagation of fundamental and second harmonic to generate the second harmonic with high efficiency. The latter is readily accomplished by tuning the refractive indices at the two respective wavelengths through adjusting the tilt angle of the molecules. Shtykov et al.[268] chose a different approach for the same purpose. They controlled the tilt angle by varying the LC temperature. The use of a dc field in the unwinding of the chiral helix makes this effect, by a strict definition, a $\chi^{(3)}$ phenomenon (often called EFISH for electric-field induced second-harmonic generation). However, surface stabilization techniques as described earlier have become available for helix unwinding of chiral smectics, so the dc field is no longer an essential requirement. Solely for convenience reasons, it is, however, still frequently used today.[269,270] As an alternative to the temperature-tuned phase matching pioneered by Shtykov et al.,[268] angular tuning of aligned samples akin to angular tuning of conventional, inorganic crystals can be employed.[271]

Frequency-Conversion Devices

Implementation of liquid crystals in actual frequency-conversion devices has been hampered mostly by the low conversion efficiencies of available LC materials (even under phase-matching conditions). The best reported conversion efficiencies, in terms of effective d coefficient, rank ferroelectric liquid crystals an order of magnitude below the *de facto* standard in the field, $LiNbO_3$.[272-274] Rational approaches to optimizing the molecular structure/nonlinear optical response relation in conventional organic crystals are yielding materials with d coefficients an order of magnitude larger than that of $LiNbO_3$. Applied to liquid crystals, similar rational design approaches to increasing the magnitude of d coefficients have been attempted by Fouquet, Lehn and Malthete[275] and are currently being methodically explored by the two Boulder groups under Walba and Clark.[276,277] In the same vein, improved frequency-conversion liquid crystal *polymers* are synthesized by LeBary et al.,[278] Kapitza et al.,[279] and Findlay et al.[280]

Material Characterization Methods Using Second-Order Nonlinearity

The guiding principles for developing materials for $\chi^{(2)}$-device applications can also be used for employing $\chi^{(2)}$ techniques in the characterization of liquid crystal materials. This has been done with particular success in situations where the electric dipole symmetry selection rules normally forbid $\chi^{(2)}$ effects, i.e., wherever the inversion symmetry of the medium is broken by a surface or by orientational deformations in the nematic bulk. The former situation is usually referred to as surface second-harmonic generation. For liquid crystals, this technique has been pioneered and extended, through a series of elegant experiments by Shen and his group,[280-283] to the study of liquid crystal anchoring and boundary behavior on substrates. The use of frequency-mixing $\chi^{(2)}$ measurements in

conjunction with angular resolution in the plane of surface anchoring provides heretofore unaccessible answers to LC alignment questions. IR vibrational spectra of anchored LC molecules offer unique insight into LC/surfactant interactions. Questions as to whether LC alkyl chains anchor either upright and straight or kinked were, until the arrival of the atomic force microscope, the lone domain of this nonlinear optical spectoscopy. This interface-sensitive technique, much like the bulk-sensitive third-harmonic-generation $\chi^{(3)}$ technique employed by Wong and Garito[284] earlier, provides information on the LC order parameter. The surface-specific order information permits this technique to be used as a quality-control tool for verifying substrate rub and alignment success.[285]

Testing symmetry-breaking structural disorder in bulk nematics is exemplified by the theoretical prediction and experimental verification by Sukhov and Timashev[286,287] of the appearance of second-harmonic signals originating from *nematic* bulk deformations that, in their particular setup, are generated by a separate, pulsed laser.

Slow Third-Order Nonlinearity

The most interesting contribution by liquid crystals to nonlinear optics lies in the area of slow $\chi^{(3)}$ nonlinearities. Here liquid crystals are unique for two reasons: a change in refractive index brought about by the laser-induced reorientation of molecules is, first, absent in solids, and second and more important, extraordinarily large. In the early literature[288,289] on this effect, it was referred to as the "giant nonlinearity." Reorientation of molecules with birefringence of $\Delta n = 0.15$–0.2 can, for a full $90°$ turn, produce a refractive-index change of the order of 10%, which is truly *extraordinary for an optically driven effect.*

The effect occurs in two versions depending on the initial state of the liquid crystal. Each of the two versions may be accompanied, again depending on the circumstances, by other slow, laser-induced effects, such as laser-heating and/or electrostriction. When the liquid crystal is in its isotropic phase or in a poorly ordered state, linearly polarized light exerts a torque on the anisotropically polarizable molecules. This torque will align those molecules into enhanced order within the irradiated volume. This is akin to the "nuclear" nonlinearity in fluid CS_2. This is, by definition, a saturable nonlinearity, but saturation fluences for any of the LC materials for which the effect has been observed are not yet known. Initial observations of the effect in isotropic MBBA by Prost and Lalanne[290] and by Wong and Shen[291] in the 1970's showed that the optically driven order in this material yields, for multi-nanosecond excitation, a third-order susceptibility twenty times larger than that of CS_2.

In an interesting variant of this effect, the laser-induced structure in the isotropic phase of MBBA becomes helical when circularly polarized light is used to drive the medium. Such a laser-induced structure had been proposed by Ye and Shen[292] and was observed experimentally by Yu *et al.*[293]

When the liquid crystal is in an aligned state, the optical-field-induced torque may cause a *collective* molecular reorientation. Such a response is known to produce the largest

nonlinear optical susceptibilities reported for any material, i.e., 10^9 times larger than that of CS_2.

The reorientational risetime is generally of the order of seconds if a drive intensity of the order of 10–100 W/cm^2 is used. Such intensities are readily generated by simple, inexpensive, cw lasers and, together with the promise of observing large effects, have prompted a host of experimental investigations. Results from these studies are compiled and critiqued in the reviews by Arakelyan,[294] Khoo,[295] Palffy-Muhoray,[296] Shen,[297] Zeldovich and Tabiryan,[286] and Tabiryan, Sukhov and Zeldovich.[298] From a laser device application viewpoint, several new developments have taken place with significant promise. These are briefly described next.

Nematic Associative-Memory Device

The experiments by Akhmanov *et al.*[299,300] open a rich field for studies of 2-D bistability, multistability and chaos physics, all facilitated by the slow LC third-order nonlinearity. The first application uses a liquid crystal element in the development of an associative memory useful in optical neural computing. Here MBBA is enclosed in a nonlinear Fabry-Perot element that is located within a passive ring resonator.[299] The slow third-order reorientational nonlinearity of the LC medium introduces space-time transverse instabilities in the beam that yield steady-state or rotating spatial intensity patterns with scale lengths of the order of the beam diameter. In a later, similar passive-resonator feedback system a faster-response nonlinear medium has also been used, i.e., a photorefractive crystal.[300] The major advantage of the liquid crystal approach over the competing technology is the more gradual cost increase with size scaling for liquid crystals. Growing large photorefractive crystals is much more expensive.

Chiral Laser-Beam and Resonator Control Devices

The other nonlinear-optical LC prototypes documented in the literature are intended for laser-beam or resonator control. Two of these make use of chiral-nematic LC properties and address pulse compression and cw laser-cavity stabilization, respectively. The final example involves wavefront correction by phase conjugation via degenerate four-wave mixing.

The pulse-compression scheme originated with theoretical work by the Yerevan group[301–303] and was subsequently tested using a temperature-tuned cholesteric mixture.[304] For a 30-ps, chirped input pulse with a 4–5 cm^{-1} bandwidth, a factor of two pulse compression was achieved in a 300-μm-thick LC cell. The underlying mechanism for this pulse shortening is different from the more often employed nonlinear effect of shortening by transient stimulated Brillouin scattering that can be initiated in many fluids, including liquid crystals.[305] In this novel approach, different spectral components of the chirped, finite-bandwidth input pulse are reordered in time with the cholesteric performing the function of a conventional parallel grating pair. As such, the approach allows simplification and space savings in short-pulse laser systems whose dispersive-delay-line compression stages often take up significant, expensive table space. Because of LC alignment flaws, the spectrally integrated energy efficiency of prototype devices did not

exceed 20%, a figure that falls short of efficiencies typical of state-of-the-art gratings. The nonlinearity in this case comprises two effects: (1) the CLC mixture adjustment such that its Bragg resonance bandwidth is much narrower than the input-pulse spectral bandwidth, and (2) self-phase modulation as a function of local intensity.[306] Effect (1) causes different spectral pulse components to experience different optical path lengths, enabling different pulse portions of the chirped pulse to overtake one another. Effect (2), at sufficiently high intensities, leads to further spatio-temporal pulse compression. More recently, in an extension of this work, the same group[307] has postulated the appearance of higher-order reflections from chiral-nematic structures, reflections that originate from an external-field-induced periodic modulation of the pure cholesteric structure. One of the physical consequences of such nonlinearly driven waves is the appearance of squeezed polarization states. However, these theoretical predictions still await experimental confirmation.

The second nonlinear LC prototype device using a chiral structure is the already mentioned flexible, LC laser-cavity end mirror.[105] This device has so far proven successful in a continuous-laser cavity, with the proof of concept still pending for pulsed applications. At low incident intensity, the mirror retains its initial optical power (curvature, which may be zero). However, even under that condition (I~100 mW/cm^2), the chiral axis orientation is adjusted by the torque of the incident laser field if the mirror is slowly tilted from its initial orientation. Continued on-axis lasing action with minimum output power loss in a 1064-nm laser cavity was observed for mirror misalignment up to 5° from normal incidence. This self-correcting property of the CLC mirror offers attractive solutions to operating lasers in vibrationally noisy environments.

At higher intensities, the mirror can be optically "empowered," i.e., it exhibits effective curvature through spatial phase control, depending on how the CLC selective reflection band is matched to the lasing wavelength. This effect is again the result of torque exerted by the light field on the polarizable molecules. The torque arises from the periodic mismatch between the circularly polarized light vector and the LC pitch and director in each plane, a mismatch directly proportional to the mistuning between the laser wavelength and the center of the selective reflection band. Depending on whether the laser wavelength is shifted to shorter or longer wavelengths relative to the reflection band center, the mirror attains effective concave or convex power.[106] In cavity use, this effect facilitates single-transverse-mode operation, and if a spectrally narrowing etalon is added to the cavity, "quiets" the laser sufficiently for single-longitudinal-mode operation to proceed without mode-hopping for time intervals exceeding 30 min. This occurs in a cavity with 1.2-W single-mode output power, mounted on a vibrationally un-isolated aluminum rail and pumped by a ~15% stabilized, cw flash lamp. The challenge now lies in demonstrating similar efficacy of chiral-nematic end mirrors in pulsed and/or additively mode-locked lasers.

Wave-Mixing Prototype Devices

Significant progress is being made in using the slow LC $\chi^{(3)}$ nonlinearity in four-wave-mixing arrangements aimed at image upconversion, phase conjugation, etc. In this arrangement, the phase grating that two intense "write" beams produce by overlapping in

77

the LC medium is usually probed by a third, weak wave ("read" beam) of identical or different color. The grating modifies the read beam. This modification of the read beam can be utilized to either make a liquid crystal laser control device or to learn about the grating formation dynamics and the material physics of the liquid crystal. The latter activities are described in many papers. Notable recent examples among them are Refs. 308–312.

Wave-mixing device concepts based on slow thermal or orientational nonlinearities have been discussed and demonstrated by several groups. Efforts directed by I C. Khoo since the late 1970's have resulted in: (1) an infrared to visible image conversion device driven by dn/dT due to absorption of a 20-ns, 1064-nm pulse in a low weight-% dye-doped nematic;[313] (2) a phase conjugator for 10.6 μm radiation that directly heats the liquid crystal[314] without the need for an additional absorber as in Ref. 313 (an earlier embodiment of a liquid crystal, 10.6-μm phase conjugator was developed by Richard et al.[315]); and (3) a total internal reflection power limiter with millisecond response time,[316] again based on a thermally induced nonlinearity driven by a dopant in the nematic.

Russian development activities in this area are spearheaded by Zeldovich and have also led to demonstration devices: forward-gain[317] and backward phase-conjugation devices[318,319] based on *orientational* nonlinearities in nematics and chiral nematics, both implementations of an earlier proposed approach[320,321] to wave mixing. The grating generated in the Zeldovich approach is a periodic *bulk* director modulation in a planar LC, driven by interference between two *orthogonally polarized* pump (write) beams. In the case of nematics, the write polarizations are linear; in the case of chiral nematics they are circularly polarized of opposite handedness. The polarization directions are aligned with the LC's n_e and n_o axes, causing a phase shift between E_o and E_e and corresponding interference along the beams' propagation direction that torques the director with a spatially periodic modulation. A read wave then diffracts off this director-undulation grating. Read-wave amplification (phase conjugation reflectivity) of up to 50% of the pump intensity has so far been achieved in a cw setup (50-mW pump power) using a 1-mm nematic cell. A 40% backward intensity conversion efficiency for a read wave generated from thermal noise is quoted for a 35-μm-thick, nematic cell with dielectric anisotropy $\Delta\epsilon = 0.3$–0.5, pumped by a 800-μs, free-running ruby laser.[318] The grating spacing generated by this method is very tight, permitting high spatial resolution phase conjugation. The grating build-up time, dominated by inertial and viscous hindrance is, however, still longer than would be useful for Q-switched or mode-locked lasers.

The limitation of the discussion of nonlinear optical LC devices to devices and prototypes of immediate use to laser practitioners consulting this book has excluded a body of literature from review. Papers reporting novel nonlinear response mechanisms, novel liquid crystal optical drive configurations, or model-system studies, all making use of lasers for characterization purposes, are many. For reference, some important papers of this nature are listed here by topic:

- Angular momentum transfer by elliptically polarized light to homeotropic nematics[322-324]

- Optical Freedericksz-transition studies on homeotropically aligned nematics, using cw lasers at various incidence angles,[325–329] or on smectics[330]

- Conformational optical nonlinearity (photochemical transformation) in certain, undoped nematic monomers[331–333] and side-chain LC polymers[334,335]

- Refractive-index change due to local heating[336–339]

Laser-Damage Considerations

Owing to the inherently small magnitudes of fast molecular nonlinear susceptibilities, high laser intensities are required to raise the nonlinear effects above detection threshold. The same high intensities often suffice to initiate secondary processes (i.e., heating by residual absorption, energy transfer into vibrational overtones, stimulated Brillouin scattering and laser damage), some of which may be fatal to the optical material.

Laser damage is usually distinguished by its perceived, physical origins as extrinsic or intrinsic damage. Extrinsic damage sources are most commonly introduced during preparation and handling and can include such comtaminants as trace impurities, polishing residues, dust on surfaces, etc. The improvements in optical survival strength in inorganic materials achieved over the last two decades are largely attributed to reductions in such extrinsic factors. The same is true, on more limited evidence, for liquid crystal, organic materials. In one documented instance, after clean-room-assembly procedures and material-filtration efforts were added to liquid crystal device manufacture, laser-damage events in liquid crystal circular polarizers previously caused by localized impurities (Figure 47) sharply diminished.[83]

Intrinsic laser damage results from limits in the "ideal-material" optical survival strength. Such limits are set by two-photon or higher-order nonlinear absorption processes, electrostriction, transverse stimulated Raman or Brillouin scattering, and other fundamental mechanisms. In organic materials, the higher polarizability of delocalized electrons acts as an effective mediator for both linear or nonlinear energy transfer from the laser into the organic structure and also for nonlinear refractive effects [real part of $\chi^{(3)}$]. There is compelling evidence that damage thresholds of liquid crystal monomers are sensitive to the degree of conjugation in the liquid crystal core. Irradiation by 1-ns, low-repetition-rate pulses of identically prepared biphenyl- and bicyclohexyl-core nematic samples yield higher damage thresholds for the saturated-core compounds.[83] Since residual absorption at the irradiating wavelength was, in this instance, three times larger for the saturated-core compound than for the aromatic compound, a reverse result would have been expected if linear absorption had been the damage dominating factor. The distinction in damage threshold between aromatic and saturated LC's becomes even more pronounced at shorter wavelengths, approaching an order-of-magnitude difference when benzene $\pi \rightarrow \pi^*$ electronic transitions become accessible via nonlinear (two-photon) absorption.[78] Table 8 lists single-shot and multiple-shot damage thresholds for various pure and mixed LC monomers that bear out this distinction. Aliphatic LC cores are identified as CCH, mixed cores as PCH, and fully aromatic cores as PPH. These thresholds rank aliphatic LC compounds among the most robust optical materials, well above most dielectric thin films used in laser systems for reflective and antireflective surface treatments. Note, however,

79

0.75×   8×   0.75×   8×

(a) Burst   **(b) Web**
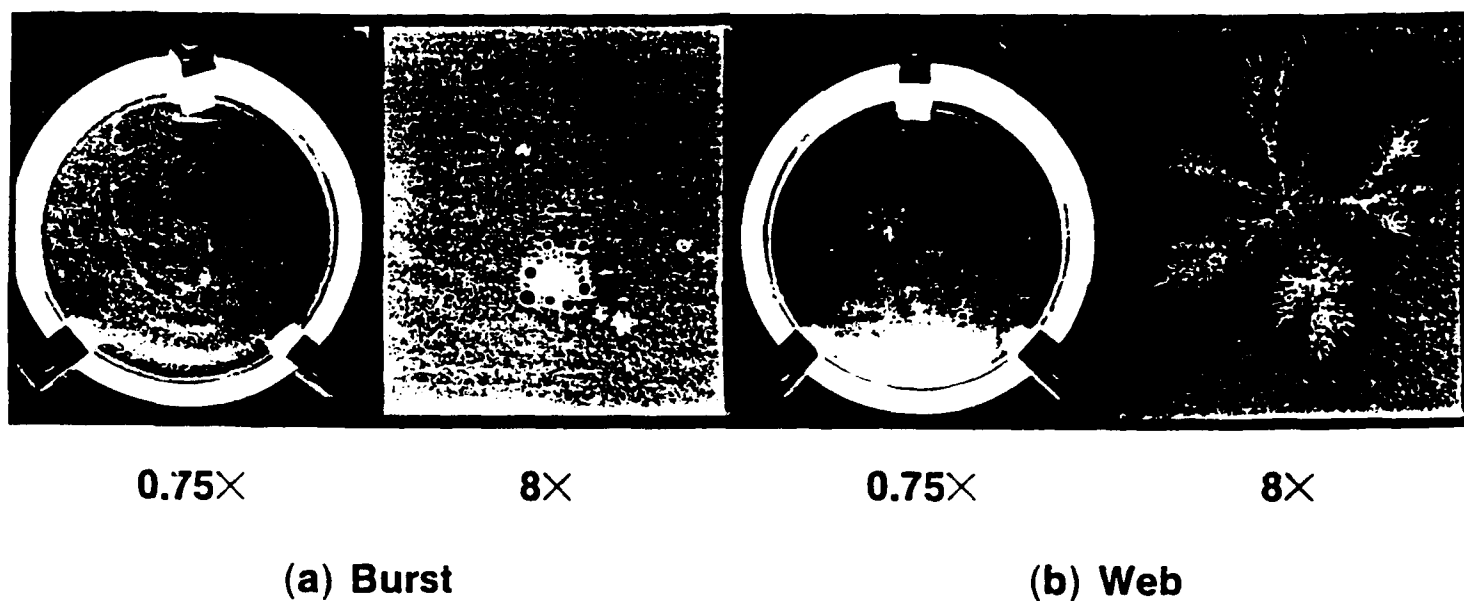
G2212

FIGURE 47   Two forms of laser-induced damage initiated by extrinsic impurities in LCP devices after multiple irradiations with a high peak power, 1053-nm laser source (2–3.8 J/cm^2, 1-ns pulse): (a) a burst that shows a high amount of scatter and often involves bubbles in the liquid crystal and chips in the glass surface at the center of the damage site; (b) a web that has lines of scatter radiating from a center; bubbles, if present, are usually at the ends of the arms.

TABLE 8

Single and multiple-irradiation laser-damage thresholds of monomeric liquid-crystal compounds with aromatic and cycloaliphatic cores.

Wavelength	Pulse-length, ns	Compound*	Core	Threshold, J/cm²		Measurement Temperature, °C (phase)	Comment
				1-on-1	N-on-1		
1053 nm	22	BDH 14616/14627†	fluor. CCH	—	22.4±0.7	20 (nematic)	Rep: 20 Hz
	11	BDH 14616/14627†	fluor. CCH	—	19.0±0.5	20 (nematic)	Rep: 20 Hz
	1	BDH 14616/14627†	fluor. CCH	12.6±1.5	—	20 (nematic)	
	1	ZLI-1185 pure	CCH	>16.6	14.6±0.5	90 (isotropic)	
	1	ZLI-2140 mix	PPH/PCH	6.8±1.2	6.7±1.0	20 (nematic)	
	1	ZLI-2359 mix	CCH	8.9±1.5	7.0±1.2	20 (nematic)	
	1	ZLI-2244 mix	CCH/PCH	10.5±1.7	—	20 (nematic)	
	1	ZLI-2256 pure	CCH ester	12.0±1.6	—	90 (isotropic)	
	1	ZLI-1646 mix	PCH/CCH	8.5±0.5	8.5±0.6	20 (nematic)	
	1	ZLI-3125 mix	CCH	16.6±1.0	7.8±0.1	20 (nematic)	
	1	ZLI-1114 pure	PCH	8.8±1.1	—	65 (isotropic)	
	1	BDH K-15 pure	PPH	9.6±2.4	4.4±1.3	20 (nematic)	
	1	HLR 5859 pure	PCH alkenyl	10.6±0.6	11.2±1.0	20 (nematic)	
351 nm	0.8	BDH 14616/14627†	CCH	10.5±2.5	5.9±0.9	20 (nematic)	
	0.8	ZLI-1185 pure	CCH	8.9±0.9	—	90 (isotropic)	
	0.8	ZLI-1167 mix	CCH	7.3±0.5	4.95±0.6	90 (isotropic)	
	0.8	ZLI-3125 mix	CCH	9.1±1.3	—	20 (nematic)	
	0.8	ZLI-1114 pure	PCH	<0.9	—	70 (isotropic)	

†50/50 wt. % blend

*BDH = Merck, Ltd. (Poole) (Formerly BDH Chemicals)
ZLI = E. Merck, Darmstadt
HLR = Roche Liquid Crystal Division, F. Hoffmann LaRoche & Co. Ch-4002 Basle, Switzerland

that under 20-Hz irradiation test conditions materials do not exhibit what is required in high-bit-rate applications. At proposed bit rates exceeding 10^9 bits per second, even very low molecular quantum dissociation yields become important. Assuming a nonresonant quantum yield of 10^{-12}, an irradiated LC device volume would decompose in about 20 minutes of continuous use if just one dissociation event occurs per pulse. Low-repetition-rate systems that permit recovery of the irradiated volume by diffusion of photolytic products are excellent application areas for select liquid crystal compounds.

ACKNOWLEDGMENTS

REFERENCES

1. **Blinov, L. M.,** *Electro-Optical and Magneto-Optical Properties of Liquid Crystals,* John Wiley and Sons, New York, 1983.

2. **Hilsum, C. and Raynes, E. P., Eds.,** *Physics, Chemistry and Applications of Thermotropic Liquid Crystals, Philos. Trans. R. Soc. Lond. A (GB),* 309, 69–239, 1983.

3. **Kapustina, O. A.,** *Acoustooptical Phenomena in Liquid Crystals,* Gordon and Breach, New York, 1984.

4. **Gray, G. W. and Goodby, J. W. G.,** *Smectic Liquid Crystals: Textures and Structures,* Leonard Hill, Philadelphia, PA, 1984.

5. **Gray, G. W., Ed.,** *Thermotropic Liquid Crystals,* Series (Critical Reports on Applied Chemistry, Vol. 22), John Wiley and Sons, New York, 1987.

6. **Ivashchenko, A. V. and Rumyantsev, V. G.,** *Dyes in Liquid Crystals,* Gordon and Breach, New York, 1987.

7. **Vertogen, G. and de Jeu, W. H.,** *Thermotropic Liquid Crystals, Fundamentals (Springer Ser. Chem. Phys.,* **Schäfer, F. P., Ed.,** Vol. 45), Springer-Verlag, Berlin, 1988.

8. **Kobayashi, S., Ed.,** *Papers in Honor of the One Hundredth Anniversary of Liquid Crystal Research: Molecular Crystals and Liquid Crystals (Mol. Cryst. Liq. Cryst. Special Topics:32,* Vol. 165), Gordon and Breach, New York, 1988.

9. **Doane, J. W. and Yaniv, Z., Eds.,** *Liquid Crystal Chemistry, Physics, and Applications,* SPIE Vol. 1080, SPIE, Bellingham, WA, 1989.

10. **McArdle, C. B., Ed.,** *Side Chain Liquid Crystal Polymers,* Chapman and Hall, New York, 1989.

11. **Bahadur, B., Ed.,** *Liquid Crystals: Applications and Uses,* Vols. 1, 2, 3, World Scientific, Singapore, 1990, 1991, 1992.

12. **Koswig, H.-D.,** *Selected Topics in Liquid Crystal Research,* Akademie-Verlag, Berlin, 1990.

13. **Lam, L. and Prost, J., Eds.,** *Solitons in Liquid Crystals* (Partially Ordered Systems Series), Springer-Verlag, New York, 1992.

14. **Tsykalo, A. L.,** *Thermophysical Properties of Liquid Crystals,* Gordon and Breach, New York, 1991.

15. **Collings, P. J.,** *Liquid Crystals: Nature's Delicate Phase of Matter,* Princeton University Press, Princeton, 1990.

16. **Goodby, J. W., Pikin, S. A., Osipov, M. A., Blinc, R., Yoshino, K., Zeks, B., Sakaurai, T., Clark, N. A., and Lagerwall, S. T.,** *Ferroelectric Liquid Crystals: Principles, Properties, and Applications* (Ferroelectricity and Related Phenomena Series), Vol. 7, Gordon and Breach, New York, 1991.

17. **Khoo, I.-C. and Simoni, F.,** *Physics of Liquid Crystalline Materials: Based on Lectures Delivered at the Summer School on the Physics of Liquid Crystals, Bra, Italy, Oct. 4–14, 1988,* Gordon and Breach, New York, 1991.

18. **Blinc, R. and Zeks, B.,** *Ferroelectric and Antiferroelectric Liquid Crystals and Their Electro-Optic Applications,* World Scientific, Singapore, 1992.

19. **Drzaic, P. S. and Efron, U., Eds.,** *Liquid-Crystal Devices and Materials,* SPIE Vol. 1455, SPIE, Bellingham, WA, 1991.

20. **Jacobs, S. D., Ed.,** *Selected Papers on Liquid Crystals for Optics,* SPIE Vol. MS46, SPIE, Bellingham, WA, 1992.

21. The International Liquid Crystal Society was formed in 1990. Its newsletter, *Liquid Crystals Today,* is published quarterly. Information may be obtained from the Secretary, D. A. Dunmer, Department of Chemistry, University of Sheffield, Sheffield 53,7Hf, UK.

22. The work of DeGennes in liquid crystals is well represented by the text *The Physics of Liquid Crystals,* Clarendon Press, Oxford, England, 1974.

23. **Meyer, R. B., Liébert, L., Strzelecki, L., and Keller, P.,** Ferroelectric liquid crystals, *J. Phys. Lett. (France),* 36, L-69–L-71, 1975.

24. **Heppke, G., Lötzsch, D., Demus, D., Diele, S., Jahn, K., and Zaschke, H.,** The S_M phase: Evidence for a new type of tilted smectic phase, *Mol. Cryst. Liq. Cryst.,* 208, 9–19, 1991.

25. **Blinov, L. M. and Beresnev, L. A.,** Ferroelectric liquid crystals, *Sov. Phys.-Usp. (USA),* 27, 492–514, 1984.

26. **Lagerwall, S. T. and Dahl, I.,** Ferroelectric liquid crystals, *Mol. Cryst. Liq. Cryst.,* 114, 151–187, 1984.

27. **Lagerwall, S. T., Otterholm, B., and Skarp, K.,** Material properties of ferroelectric liquid crystals and their relevance for applications and devices, *Mol. Cryst. Liq. Cryst.,* 152, 503–587, 1987.

28. **Skarp, K. and Handschy, M. A.,** Ferroelectric liquid crystals. Material properties and applications, *Mol. Cryst. Liq. Cryst.,* 165, 439–509, 1988.

29. **Lagerwall, S. T., Clark, N. A., Dijon, J., and Clerc, J. F.,** Ferroelectric liquid crystals: The development of devices, *Ferroelectrics,* 94, 3–62, 1989.

30. **Handschy, M. A. and Clark, N. A.,** Structures and responses of ferroelectric liquid crystals in the surface-stabilized geometry, *Ferroelectrics,* 59, 69–116, 1984.

31. **Patel, J. S. and Goodby, J. W.,** Ferroelectric liquid crystal devices, in *Nonlinear Optics and Applications,* Yeh, P., Ed., SPIE Vol. 613, SPIE, Bellingham, WA, 1986, 130–134.

32. **Goodby, J. W. and Leslie, T. M.,** Ferroelectric liquid crystals—Structure and design, *Mol. Cryst. Liq. Cryst.,* 110, 175–203, 1984.

33. **Patel, J. S.,** Room-temperature switching behavior of ferroelectric liquid crystals in thin cells, *Appl. Phys. Lett.,* 47, 1277–1279, 1985.

34. **Higuchi, R., Honma, M., Sakurai, T., and Mikami, N.,** Eur. Pat. Appl. #85302567 C09K-019/12, 1985.

35. **Walba, D. M.,** U.S. Pat. Appl. #4,556,727, Dec. 3, 1985.

36. **Bone, M. F., Bradshaw, M. J., Chan, L. K. M., Coates, D., Constant, J., Gemmell, P. A., Gray, G. W., Lacey, D., Toyne, K. J.,** Synthesis and physical evaluation of novel ferroelectric materials with high spontaneous polarization, *Mol. Cryst. Liq. Cryst.,* 164, 117–134, 1988.

37. Loseva, M. V., Ostrovskii, B. I., Rabinovich, A. Z., Sonin, A. S., Strukov, B. A., and Chernova, N. I., Ferroelectricity in ester-group liquid crystal, *JETP Lett.*, 28, 374–378, 1979.

38. Walba, D. M., Slater, S. C., Thurmes, W. N., Clark, N. A., Handschy, M. A., and Supon, F., Design and synthesis of a new ferroelectric liquid crystal family. Liquid crystals containing a nonracemic 2-alkoxy-1-propoxy unit, *J. Am. Chem. Soc.*, 108, 5210–5221, 1986.

39. Walba, D. M., Vohra, R. T., Clark, N. A., Handschy, M. A., Xue, J., Parmar, D. S., Lagerwall, S. T, and Skarp, K., Design and synthesis of new ferroelectric liquid crystals. 2. Liquid crystals containing a nonracemic 2,3-epoxy alcohol unit, *J. Am. Chem. Soc.*, 108, 7424–7425, 1986.

40. Sakurai, T., Mikami, N., Higuchi, R., Honma, M., Ozaki, M., and Yoshino, K., Synthesis of new ferroelectric liquid crystals and their novel ferroelectricity, *J. Chem. Soc., Chem. Commun.*, 12, 978–979, 1986.

41. Otterholm, B., Alstermark, C., Flatischler, K., Dahlgren, A., Lagerwall, S. T., and Skarp, K., Synthesis and electro-optical properties of some ferroelectric liquid crystals derived from lactic acid, *Mol. Cryst. Liq. Cryst.*, 146, 189–216, 1987.

42. Geelhaar, T., Ferroelectric mixtures and their physico-chemical properties, *Ferroelectrics*, 85, 717–737, 1988

43. Benguigui, L. G., Dielectric properties and dipole ordering in liquid crystals, *Ferroelectrics*, 58, 269–281, 1984.

44. Michelson, A., Benguigui, L., and Cabib, D., Phenomenological theory of the polarized helicoidal smectic C phase, *Phys. Rev. A*, 16, 394–401, 1977.

45. Osipov, M. A., Molecular-statistical theory of ferroelectricity in smectic C liquid crystals, *Ferroelectrics*, 58, 305–319, 1984.

46. Beresnev, L. A., Pozhidayev, E. P., and Blinov, L. M., On mechanisms of dipolar ordering in ferroelectric liquid crystals, *Ferroelectrics*, 59, 1–10, 1984.

47. Nakagawa, M., A molecular theory of chiral smectic C liquid crystals I, *Mol. Cryst. Liq. Cryst.*, 130, 349–390, 1985.

48. Meyer, R. B., Ferroelectric liquid crystals: A review, *Mol. Cryst. Liq. Cryst.*, 40, 33–48, 1977.

49. Beresnev, L. A. and Blinov, L. M., Pyroelectric properties of liquid crystals, *Ferroelectrics*, 33, 129–138, 1981.

50. Goodby, J. W., Chin, E., Leslie, T. M., Geary, J. M., and Patel, J. S., Helical twist sense and spontaneous polarization direction in ferroelectric smectic liquid crystals. 1., *J. Am. Chem. Soc.*, 108, 4729–4735, 1986.

51. Goodby, J. W. and Chin, E., Helical twist and spontaneous polarization direction in ferroelectric smectic liquid crystals. 2., *J. Am. Chem. Soc.*, 108, 4736–4742, 1986.

52. Walba, D. M., Ros, M. B., Clark, N. A., Shao, R., Robinson, M. G., Liu, J.-Y., Johnson, K. M., and Doroski, D., Design and synthesis of new ferroelectric liquid crystals. 14. An approach to the stereocontrolled synthesis of polar organic thin films for nonlinear optical applications, *J. Am. Chem. Soc.*, 113, 5471–5474, 1991.

53. **Coles, H. J., Gleeson, H. F., Scherowsky, G., and Schliwa, A.,** Ferroelectric polymer liquid crystals: II The dye guest host effect, *Mol. Cryst. Liq. Cryst. Lett.,* 7, 125–130, 1990.

54. **Dumon, M., Nguyen, H. T., Mauzac, M., Destrade, C., and Gasparoux, H.,** Ferroelectric liquid crystal siloxane homo and copolymers, *Liq. Cryst.,* 10, 475–493, 1991.

55. **Eich, M., Wendorff, J. H., Ringsdorf, H., and Schmidt, H. W.,** Nonlinear optical self diffraction in a mesogenic side chain polymer, *Makromol. Chem.,* 186, 2639–2647, 1985.

56. **Tsutsui, T. and Tanaka, R.,** Solid cholesteric films for optical applications, *Polym.: Polym. Commun. (UK),* 21, 1351–1352, 1980.

57. **Tsutsui, T. and Tanaka, R.,** Network polymers with cholesteric liquid crystalline order prepared from poly(γ-butyl L-glutamate)-butyl acrylate liquid crystalline system, *Polymer,* 22, 117–123, 1981.

58. **Freidzon, Y. S., Boiko, N. I., Shibaev, V. P., and Platé, N. A.,** Thermotropic liquid crystalline polymers—22* Optical properties and structure of some cholesteric copolymers, *Eur. Polym. J.,* 22, 13–16, 1986.

59. **Krishnamurthy, S. and Chen, S. H.,** Facilitating the formation of the Grandjean texture in thermotropic chiral nematic side-chain copolymers via modulation of backbone flexibility, *Macromolecules,* 24, 4472–4474, 1991.

60. **Bhadani, S. N. and Gray, D. G.,** Cellulose-based liquid crystalline polymers; Esters of (hydroxypropyl) cellulose, *Mol. Cryst. Liq. Cryst.,* 99, 29–38, 1983.

61. **Werbowyj, R. S. and Gray, D. G.,** Optical properties of (hydroxypropyl) cellulose liquid crystals. Cholesteric pitch and polymer concentration, *Macromolecules,* 17, 1512–1520, 1984.

62. **Koide, N.,** Synthesis, characterization and some aspects for application of polymer liquid crystals, *Mol. Cryst. Liq. Cryst.,* 139, 47–80, 1986.

63. **Finkelmann, H., Koldehoff, J., and Ringsdorf, H.,** Synthesis and characterization of liquid-crystalline polymers with cholesteric phase, *Angew. Chem. Int. Ed. Engl.,* 17, 935–937, 1978.

64. **Finkelmann, H. and Rehage, G.,** Investigations on liquid crystalline polysiloxanes. 2. Optical properties of cholesteric phases and influence of the flexible spacer on the mesogenic groups, *Makromol. Chem., Rapid Commun.,* 1, 733–740, 1980.

65. **Finkelmann, H. and Kock, H. J.,** Liquid crystal side chain polymers: Properties and aspects for applications, *Disp. Technol.,* 1, 81–94, 1985.

66. **Talroze, R. V., Kostromin, S. G., Shibaev, V. P., Plate, N. A., Kresse, H., Sauer, K., and Demus, D.,** Thermotropic liquid crystalline polymers. 5. Electrooptical phenomena in liquid crystalline polymers, *Makromol. Chem., Rapid Commun.,* 2, 305–309, 1981.

67. **Talroze, R. V., Sinitzyn, V. V., Shibaev, V. P., and Plate, N. A.,** Thermotropic liquid crystalline polymers. VII. New cooperative structure transition in liquid crystalline polymers induced by an electric field, *Polym. Bull.,* 6, 309–314, 1982.

68. **Ringsdorf, H. and Zentel, R.,** Liquid crystalline side chain polymers and their behavior in the electric field, *Makromol. Chem.,* 183, 1245–1256, 1982.

69. **Finkelmann, H., Naegele, D., and Ringsdorf, H.,** Orientation of nematic liquid crystalline polymers in the electric field, *Makromol. Chem.,* 180, 803–806, 1979.

70. **Finkelmann, H., Kiechle, U., and Rehage, G.,** Behavior of liquid crystalline side chain polymers in an electric field, *Mol. Cryst. Liq. Cryst.,* 94, 343–358, 1983.

71. **Scherowsky, G., Beer, A., and Coles, H. J.,** A coloured ferroelectric side chain polymer, *Liq. Cryst.,* 10, 809–819, 1991.

72. **Wu, S.-T.,** Infrared properties of nematic liquid crystals: An overview, *Opt. Eng.,* 26, 120–128, 1987.

73. **Wu, S.-T. and Lim, K.-C.,** Absorption and scattering measurements of nematic liquid crystals, *Appl. Opt.,* 26, 1722–1727, 1987.

74. **Wu, S.-T., Ramos, E., and Finkenzeller, U.,** Polarized UV spectroscopy of conjugated liquid crystals, *J. Appl. Phys.,* 68, 78–85, 1990.

75. **Wu, S.-T. and Wu, C.-S.,** A three-band model for liquid-crystal birefringence dispersion. *J. Appl. Phys.,* 66, 5297–5301, 1989.

76. **Wu, S.-T., Efron, U., and Hess, L. D.,** Birefringence measurements of liquid crystals, *Appl. Opt.,* 23, 3911–3915, 1984; also, Infrared birefringence of liquid crystals, *Appl. Phys. Lett.,* 44, 1033–1035, 1984.

77. **Lackner, A. M., Margerum, J. D., and Van Ast, C.,** Near ultraviolet photostability of liquid crystal mixtures, *Mol. Cryst. Liq. Cryst.,* 141, 289–310, 1986.

78. **Papernov, S., Marshall, K., Guardalben, M., Schmid, A., and Jacobs, S. D.,** 351 nm, 0.7 ns laser damage thresholds of monomeric liquid-crystalline systems, *Liq. Cryst.,* 9, 71–76, 1991.

79. **Gray, G. W. and McDonnell, D. G.,** The relationship between helical twist sense, absolute configuration and molecular structure for non-sterol cholesteric liquid crystals, *Mol. Cryst. Liq. Cryst. Lett.,* 34, 211–213, 1977.

80. **Tsai, M. L. and Chen, S. H.,** Helical sense in thermotropic liquid crystal copolymers in relation to the structure of a pendant chiral moiety, *Macromolecules,* 23, 1908–1911, 1990.

81. **Chen, S. H. and Tsai, M. L.,** New thermotropic chiral nematic copolymers using (1S,2S,3S,5R)–(+)– and (1R,2R,3R,5S)–(–)–Isopinocampheol as building blocks, *Macromolecules,* 23, 5055–5058, 1990.

82. **Krishnamurthy, S. and Chen, S. H.,** New thermotropic chiral nematic copolymers. 2. A study of helical sense and twisting power based on copolymers containing (S)–(–)–1–Phenylethanol and (R)–(–)–Methyl Mandelate, *Macromolecules,* 24, 3481–3484, 1991.

83. **Jacobs, S. D., Cerqua, K. A., Marshall, K. L., Schmid, A., Guardalben, M. J., and Skerrett, K. J.,** Liquid-crystal laser optics: Design, fabrication, and performance, *J. Opt. Soc. Am. B,* 5, 1962–1979, 1988.

84. **Lee, J.-C. and Jacobs, S. D.,** Design and construction of 1064-nm liquid-crystal laser cavity end mirrors, *J. Appl. Phys.,* 68, 6523–6525, 1990.

85. Lee, J.-C., Kelly, J. H., Smith, D. L., and Jacobs, S. D., Gain squaring in a Cr:Nd:GSGG active-mirror amplifier using a cholesteric liquid crystal mirror. *IEEE J. Quantum Electron.*, 24, 2238–2242, 1988.

86. Müller, W. U. and Stegemeyer, H., Birefringence of compensated cholesteric liquid crystals, *Ber. Bunsenges. Phys. Chem.*, 77, 20–23, 1973.

87. Lee, J.-C., Schmid, A., and Jacobs, S. D., Effects of anchoring under intense optical fields in a cholesteric liquid crystal, *Mol. Cryst. Liq. Cryst.*, 166, 253–265, 1989.

88. Takezoe, H., Ouchi, Y., Sugita, A., Hara, M., Fukuda, A., and Kuze, E., Experimental observation of the total reflection by a monodomain cholesteric liquid crystal, *Jpn. J. Appl. Phys.*, 21, L390–L392, 1982.

89. Takezoe, H., Hashimoto, K., Ouchi, Y., Hara, M., Fukuda, A., and Kuze, E., Experimental study on higher order reflection by monodomain cholesteric liquid crystals, *Mol. Cryst. Liq. Cryst.*, 101, 329–340, 1983.

90. Takezoe, H., Ouchi, Y., Hara, M., Fukuda, A., and Kuze, E., Experimental studies on reflection spectra in monodomain cholesteric liquid crystal cells: Total reflection, subsidiary oscillation and its beat or swell structure, *Jpn. J. Appl. Phys.*, 22, 1080–1091, 1983.

91. Berreman, D. W. and Scheffer, T. J., Reflection and transmission by single-domain cholesteric liquid crystal films: Theory and verification, *Mol. Cryst. Liq. Cryst.*, 11, 395–405, 1970.

92. Belyakov, V. A and Dmitrienko, V. D., Theory of the optical properties of cholesteric liquid crystals, *Sov. Phys. Solid State*, 15, 1811–1815, 1974.

93. Takezoe, H., Ouchi, Y., Hara, M., Fukuda, A., and Kuze, E., A tunable 90° rotator using a total reflection by a monodomain cholesteric liquid crystal cell, *Jpn. J. Appl. Phys. 2, Lett.*, 22, L185–L187, 1983.

94. Schadt, M. and Fünfschilling, J., New liquid crystal polarized color projection principle, *Jpn. J. Appl. Phys.*, 29, 1974–1984, 1990.

95. Shankar, N. K., Morris, J. A. Yakymyshyn, C. P., and Pollock, C. R., A 2 × 2 fiber optic switch using chiral liquid crystals, *IEEE Photonics Tech. Lett.*, 2, 147–149, 1990.

96. Soref, R. A., $N \times N$ and $1 \times N$ switching with chiral nematic liquid crystals, *Appl. Opt.*, 30, 183–184, 1991.

97. Cesarz, T., Klosowicz, S., Nowinowski-Kruszelnicki, E., and Zmija, J., Liquid crystal elements of laser optics. The optical isolator, *Mol. Cryst. Liq. Cryst.*, 193, 19–23, 1990.

98. Boehly, T. R., Craxton, R. S., Hutchison, R. J., Kelly, J. H., Kessler, T. J., Kumpan, S. A., Letzring, S. A., McCrory, R. L., Morse, S. F. B., Seka, W., Skupsky, S., Soures, J. M., and Verdon, C. P., The upgrade to the OMEGA laser system, SPIE Proceedings 1627, Paper #38, January 21, 1992.

99. Charlet, G. and Gray, D., Chiroptical filters from aqueous (hydroxypropyl) cellulose liquid crystals, *J. Appl. Polym. Sci.*, 37, 2517–2527, 1989.

100. Ishihara, S., Yokotani, F., Matsuo, Y., and Morimoto, K., Preparation and properties of optical notch filters of cholesteric liquid crystals, *Polymer*, 29, 2141–2145, 1988.

101. Tsai, M. L., Chen, S. H., and Jacobs, S. D., Optical notch filter using thermotropic liquid crystalline polymers, *Appl. Phys. Lett.*, 54, 2395–2397, 1989.

102. Häberle, N., Leigeber, H., Maurer, R., Miller, A., Stohrer, J., Buchecker, R., Fünfschilling, J., and Schadt, M., Right and left circular polarizing color filters made from crosslinkable cholesteric LC-silicones, in *Conference Record of the 1991 International Display Research Conference*, 57–59, San Diego, CA, 15–17 October, 1991.

103. Lee, J.-C., Jacobs, S. D., and Skerrett, K. J., Laser beam apodizer utilizing gradient-index optical effects in cholesteric liquid crystals, *Opt. Eng.*, 30, 330–336, 1991.

104. Danilov, V. V., Danilov, O. B., Sidorov, A. I., and Sosnov, E. N., Transversely excited atmospheric CO_2 laser with an intracavity liquid crystal stop, *Sov. J. Quantum Electron.*, 21, 1099–1101, 1991.

105. Lee, J.-C., Jacobs, S. D., and Gingold, R. J., Nd:YAG laser with cholesteric liquid crystal cavity mirrors, in *Advances in Nonlinear Polymers and Inorganic Crystals, Liquid Crystals, and Laser Media*, Musikant, S., Ed., SPIE Vol. 824, SPIE, Bellingham, WA, 1987, 7–17.

106. Lee, J.-C., Jacobs, S. D., and Schmid, A., Retro-self-focusing and pinholing effect in a cholesteric liquid crystal, *Mol. Cryst. Liq. Cryst.*, 150b, 617–629, 1987.

107. Lee, J.-C., Jacobs, S. D., Gunderman, T., Schmid, A., Kessler, T. J., and Skeldon, M. D., TEM_{00}-mode and single-longitudinal-mode laser operation with a cholesteric liquid-crystal laser end mirror, *Opt. Lett.*, 15, 959–961, 1990.

108. Pinsl, J., Bräuchle, Chr., and Kreuzer, F. H., Liquid crystalline polysiloxanes for optical write-once storage, *J. Mol. Electron.*, 3, 9–13, 1987.

109. Winter, C. S., Rush, J. D., and Smith, D. G., Liquid crystal materials' refractive index matched to silica, *Liq. Cryst.*, 2, 561–564, 1987.

110. Sage, I. and Chaplin, D., Low RI liquid crystals for integrated optics, *Electron. Lett.*, 23, 1192–1193, 1987.

111. Ioannidis, Z. K., Giles, I. P., and Bowry, C., Liquid crystal all-fibre optical polariser, *Electron. Lett.*, 24, 1453–1455, 1988.

112. Ioannidis, Z. K., Giles, I. P., and Bowry, C., All-fiber optic intensity modulators using liquid crystals, *Appl. Opt.*, 30, 328–333, 1991.

113. Lin, H., Palffy-Muhoray, P., and Lee, M. A., Liquid crystalline cores for optical fibers, *Mol. Cryst. Liq. Cryst.*, 204, 189–200, 1991.

114. Green, M. and Madden, S. J., Low loss nematic liquid crystal cored fiber waveguides, *Appl. Opt.*, 28, 5202–5203, 1989.

115. Merck Ltd. product literature, available from EM Industries, Inc., Advanced Chemicals Division, 5 Skyline Dr., Hawthorne, NY 10532.

116. Jacobs, S. D. Liquid crystals as large aperture waveplates and circular polarizers, in *Polarizers and Applications*, Trapani, G. B., Ed., SPIE Vol. 307, SPIE, Bellingham, WA, 1981, 98–105.

117. Sherman, R., Grob, J., and Whitlock, W., Dry surface cleaning using CO_2 snow, *J. Vac. Sci. Technol. B*, 9, 1970–1977, 1991.

118. **Hayden, J., Kessler, T. J., and Jacobs, S. D.,** Automated spatially scanning ellipsometer for retardation measurements of transparent materials, to be published in *Applied Optics.*

119. **Wu, S.-T. and Efron, U.,** Optical properties of thin nematic liquid crystal cells, *Appl. Phys. Lett.,* 48, 624–626, 1986.

120. **Gunderman, T. E., Lee, J.-C., Kessler, T. J., Jacobs, S. D., Smith, D. J., and Skupsky, S.,** Liquid crystal distributed polarization rotator for improved uniformity of focused laser light, in *Conference on Lasers & Electro-Optics 1990 Technical Digest Series,* Vol. 7, 354–356, Anaheim, CA, May 1990; and LLE Review, 45, 1–12, 1990.

121. **Schmid, A., Papernov, S., Li, Z-W., Marshall, K., Gunderman, T., Lee, J.-C., Guardalben, M., and Jacobs, S. D.,** Liquid-crystal materials for high peak-power laser applications, *Mol. Cryst. Liq. Cryst.,* 207, 33–42, 1991.

122. **Longhurst, R. S.,** *Geometrical and Physical Optics,* 2nd ed., John Wiley & Sons, NY, 1967, 501.

123. **Gilman, S. E., Baur, T. G., Gallagher, D. J., and Shankar, N. K.,** Properties of tunable nematic liquid crystal retarders, in *Polarization Considerations for Optical Systems II,* **Chipman, R. A., Ed.,** SPIE Vol. 1166, SPIE, Bellingham, WA, 1989, 461–471.

124. **Sharp, R. C., Resler, D. P., Hobbs, D. S., and Dorschner, T. A.,** Electrically tunable liquid-crystal wave plate in the infrared, *Opt. Lett.,* 15, 87–89, 1990.

125. **Staromlynska, J.,** Electro-optic broadband tunable filters using liquid crystals, *J. Mod. Opt.,* 37, 639–652, 1990.

126. **Miller, P. J.,** Tunable narrowband birefringent filters for astronomical imaging, in *Instrumentation in Astronomy VII,* **Crawford, D. L., Ed.,** SPIE Vol. 1235, SPIE, Bellingham, WA, 1990, 466–473.

127. **Andrews, J. R,** Low voltage wavelength tuning of an external cavity diode laser using a nematic liquid crystal-containing birefringent filter, *IEEE Photon. Tech. Lett.,* 2, 334–336, 1990.

128. **Patel, J. S., Saifi, M. A., Berreman, D. W., Lin, C., Andreadakis, N., and Lee, S. D.,** Electrically tunable optical filter for infrared wavelength using liquid crystals in a Fabry-Perot étalon, *Appl. Phys. Lett.,* 57, 1718–1720, 1990.

129. **Patel, J. S. and Lee, S.-D.,** Electrically tunable and polarization insensitive Fabry-Perot étalon with a liquid-crystal film, *Appl. Phys. Lett.,* 58, 2491–2493, 1991.

130. **Patel, J. S. and Maeda, M. W.,** Tunable polarization diversity liquid-crystal wavelength filter, *IEEE Photon. Tech. Lett.,* 3, 739–740, 1991.

131. **Patel, J. S.,** Polarization insensitive tunable liquid-crystal etalon filter, *Appl. Phys. Lett.,* 59, 1314–1316, 1991.

132. **Hirabayashi, K., Tsuda, H., and Kurokawa, T.,** Narrow-band tunable wavelength-selective filters of Fabry-Perot interferometers with a liquid crystal intracavity, *IEEE Photon. Tech. Lett.,* 3, 213–215, 1991.

133. **Tsuda, H., Hirabayashi, K., Tohmori, Y., and Kurokawa, T.,** Tunable light source using a liquid-crystal Fabry-Perot interferometer, *IEEE Photon. Tech. Lett.*, 3, 504–506, 1991.

134. **Hirabayashi, K., Tsuda, H., and Kurokawa, T.,** New structure of tunable wavelength-selective filters with a liquid crystal for FDM systems, *IEEE Photon. Tech. Lett.*, 3, 741–743, 1991.

135. **Hirabayashi, K., Ohiso, Y., and Kurokawa, T.,** Polarization-independent tunable wavelength-selective filter using a liquid crystal, *IEEE Trans. Photon. Tech. Lett.*, 3, 1091–1093, 1991.

136. **McAdams, L. R., McRuer, R. N., and Goodman, J. W.,** Oblique-incidence liquid-crystal-tunable étalon, *Opt. Lett.*, 16, 864–866, 1991.

137. **Sato, S.,** Liquid-crystal lens-cells with variable focal length, *Jpn. J. Appl. Phys.*, 18, 1679–1684, 1979.

138. **Sato, S., Sugiyama, A., and Sato, R.,** Variable-focus liquid-crystal Fresnel lens, *Jpn. J. Appl. Phys.*, 24, L626–L628, 1985.

139. **Sato, S., Nose, T., Yamaguchi, R., and Yanase, S.,** Relationship between lens properties and director orientation in a liquid crystal lens, *Liq. Cryst.*, 5, 1435–1442, 1989.

140. **Kowel, S. T., Kornreich, P., and Nouhi, A.,** Adaptive spherical lens, *Appl. Opt.*, 23, 2774–2777, 1984.

141. **Kowel, S. T., Cleverly, D. S., and Kornreich, P. G.,** Focusing by electrical modulation of refraction in a liquid crystal cell, *Appl. Opt.*, 23, 278–289, 1984.

142. **Brinkley, P. F., Kowel, S. T., and Chu, C.,** Liquid crystal adaptive lens: Beam translation and field meshing, *Appl. Opt.*, 27, 4578–4586, 1988.

143. **Nose, T. and Sato, S.,** A liquid crystal microlens obtained with a non-uniform electric field, *Liq. Cryst.*, 5, 1425–1433, 1989.

144. **Nose, T., Masuda, S., and Sato, S.,** Optical properties of a hybrid-aligned liquid crystal microlens, *Mol. Cryst. Liq. Cryst.*, 199, 27–35, 1991.

145. **Patel, J. S. and Rastani, K.,** Electrically controlled polarization-independent liquid-crystal Fresnel lens arrays, *Opt. Lett.*, 16, 532–534, 1991.

146. **Fergason, J. L.,** Performance of a matrix display using surface mode, in *Conference Record of 1980 Biennial Display Research Conference*, 177–179, Cherry Hill, NJ, 21–23 October, 1980.

147. **Fergason, J. L.,** Use of strong surface alignment in nematic liquid crystals for high speed light modulation, in *Liquid Crystals and Spatial Light Modulator Materials*, **Penn, W. A.,** Ed., SPIE Vol. 684, SPIE, Bellingham, WA, 1986, 81–86.

148. **Fergason, J. L. and Berman, A. L.,** A push/pull surface-mode liquid-crystal shutter: Technology and applications, *Liq. Cryst.*, 5, 1397–1404, 1989.

149. **Bos, P. J. and Koehler/Beran, K. R.,** The pi-cell: A fast liquid-crystal optical-switching device, *Mol. Cryst. Liq. Cryst.*, 113, 329–339, 1984.

150. **Wu, S.-T. and Wu, C.-S.,** Small angle relaxation of highly deformed nematic liquid crystals, *Appl. Phys. Lett.*, 53, 1794–1796, 1988.

151. **Wu, S.-T. and Wu, C.-S.,** High-speed liquid-crystal modulators using transient nematic effect, *J. Appl. Phys.*, 65, 527–532, 1989.

152. **Wu, S.-T., Finkenzeller, U., and Reiffenrath, V.,** Physical properties of diphenyldiacetylenic liquid crystals, *J. Appl. Phys.,* 65, 4372–4376, 1989.

153. **Schadt, M., Buchecker, R., Villiger, A., Leenhouts, F., and Fromm, J.,** The cooperative effects of heterocycles, NCS-polar groups, and double bonds on the material properties of new nematic liquid crystals, *IEEE Trans. Electron. Devices,* ED-33, 1187–1194, 1986.

154. **Wu, S.-T.,** Nematic liquid crystal modulator with response time less than 100 μs at room temperature, *Appl. Phys. Lett.,* 57, 986–988, 1990.

155. **Wu, S.-T. and Wu, C.-S.,** High speed nematic liquid crystal modulators, *Mol. Cryst. Liq. Cryst.,* 207, 1–15, 1991.

156. **Clark, N. A. and Lagerwall, S. T.,** Submicrosecond bistable electro-optic switching in liquid crystals, *Appl. Phys. Lett.,* 36, 899–901, 1980.

157. **Clark, N. A. and Lagerwall, S. T.,** Surface-stabilized ferroelectric liquid crystal electro-optics: New multistate structures and devices, *Ferroelectrics,* 59, 25–67, 1984.

158. **Armitage, D., Thackara, J. I., Clark, N. A., and Handschy, M. A.,** Ferroelectric liquid crystal spatial light modulator, *Mol. Cryst. Liq. Cryst.,* 144, 309–316, 1987.

159. **Takahashi, N. S., Asada, H., Miyahara, M., Kurita, S., and Kuriyama, H.,** High-speed light valve using an amorphous silicon photosensor and ferroelectric liquid crystals, *Appl. Phys. Lett.,* 51, 1233–1235, 1987.

160. **Moddel, G., Johnson, K. M., Li, W., Rice, R. A., Pagano-Stauffer, L. A., and Handschy, M. A.,** High-speed binary optically addressed spatial light modulator, *Appl. Phys. Lett.,* 55, 537–539, 1989.

161. **Waters, C. M., Green, B. J., Surguy, P. W. H., Gibbons, D. J., and Smith, J. H.,** Viewing angle dependence and optimisation of the SSFLCD for full colour LCD TV, *Mol. Cryst. Liq. Cryst.,* 152, 631–650, 1987.

162. **Johnson, K. M., Handschy, M. A., and Pagano-Stauffer, L. A.,** Optical computing and image processing with ferroelectric liquid crystals, *Opt. Eng.,* 26, 385–391, 1987.

163. **Johnson, K. M, Cormack, R., Cathey, W. T., and Dolder, F.,** An electro-optical system for inspection of glass bottles using adaptive spatial filtering, in *Optical and Digital Pattern Recognition,* Liu, H.-K. and Schenker, P. S., Eds., SPIE Vol. 754, SPIE, Bellingham, WA, 1987, 130–136.

164. **Masterson, H. J., Sharp, G. D., and Johnson, K. M.,** Ferroelectric liquid-crystal tunable filter, *Opt. Lett.,* 14, 1249–1251, 1989.

165. **McAdams, L. R. and Goodman, J. W.,** Liquid crystal 1 × N optical switch, *Opt. Lett.,* 15, 1150–1152, 1990.

166. **McAdams, L. R., McRuer, R. N., and Goodman, J. W.,** Liquid crystal optical routing switch, *Appl. Opt.,* 29, 1304–1307, 1990.

167. **Johnson, K. M., Surette, M. R., and Shamir, J.,** Optical interconnection network using polarization-based ferroelectric liquid crystal gates, *Appl. Opt.,* 27, 1727–1733, 1988.

168. **McRuer, R., McAdams, L. R., and Goodman, J. W.,** Ferroelectric liquid-crystal digital scanner, *Opt. Lett.,* 15, 1415–1417, 1990.

169. **Meadows, M. R., Handschy, M. A., and Clark, N. A.,** Electro-optic switching using total internal reflection by a ferroelectric liquid crystal, *Appl. Phys. Lett.*, 54, 1394–1396, 1989.

170. **Soref, R. A. and McMahon, D. H.,** Total switching of unpolarized fiber light with a four-port electro-optic liquid crystal device," *Opt. Lett.*, 5, 147–149, 1980.

171. **Ozaki, M., Sadohara, Y., Hatai, T, and Yoshino, K,** Fast optical switching in polymer waveguide using ferroelectric liquid crystal, *Jpn. J. Appl. Phys. 2, Lett.*, 29, L843–L845, 1990.

172. **Yoshino, K., Ozaki, M., Tagawa, A., Hatai, T., Asada, K., Sadohara, Y., Daido, K., and Ohmori, Y.,** Electro-optic switching in polymer waveguide using surface stabilized ferroelectric liquid crystal, *Mol. Cryst. Liq. Cryst.*, 202, 163–169, 1991.

173. **Channin, D. J.,** Optical waveguide modulation using nematic liquid crystal, *Appl. Phys. Lett.*, 22, 365–366, 1973.

174. **Sheridan, J. P. and Giallorenzi, T. G.,** Electro-optically induced deflection in liquid-crystal waveguides. *J. Appl. Phys.*, 45, 5160–5163, 1974.

175. **O'Callaghan, M. J. and Handschy, M. A.,** Diffractive ferroelectric liquid-crystal shutters for unpolarized light, *Opt. Lett.*, 16, 770–772, 1991.

176. **Yoshino, K., Balakrishnan, K. G., Uemoto, T., Iwasaki, Y., and Inuishi, Y.,** Electro-optical effect in ferroelectric smectic liquid crystals, *Jpn. J. Appl. Phys.*, 17, 597–598, 1978.

177. **Yoshino, K. and Ozaki, M.,** New electro-optic effect of microsecond response utilizing transient light scattering in ferroelectric liquid crystals, *Jpn. J. Appl. Phys. 2, Lett.*, 23, L385–L387, 1984.

178. **Ozaki, M. and Yoshino, K.,** Characteristics of high speed electro-optic device utilizing ferroelectric liquid crystal and effect of space charge, *Technology Reports of the Osaka University*, 35, 53–60, 1985.

179. **Yoshino, K., Ozaki, M., and Kishio, S.,** Characteristics of electro-optic effect of ferroelectric liquid crystals in infrared range, *Jpn. J. Appl. Phys.*, 24, Supplement 24-3, 45–48, 1985.

180. **Marshall, K. L.,** An IR chopper for the 8–12 μm region employing the TLSM effect in ferroelectric liquid crystals, presented at the CECOM Center for Night Vision and Electro-Optics Optoelectronics Workshop #25: Liquid Crystal Materials and Devices for Optoelectronic Applications, Ft. Belvoir, VA, 5 December 1990.

181. **Yoshino, K., Balakrishnan, K. G., Uemoto, T., Iwasaki, Y., and Inuishi, Y.,** Electro-optical effect in ferroelectric smectic liquid crystal, *Jpn. J. Appl. Phys.*, 17, 597–598, 1978.

182. **Ostrovskii, B. I. and Chigrinov, V. G.,** Linear electrooptic effect in chiral smectic C liquid crystals, *Kristallografiya*, 25, 560–567, 1980.

183. **Ostrovskii, B. I., Rabinovich, A. Z., and Chigrinov, V. G.,** Behaviour of ferroelectric smectic liquid crystals in electric field, in *Advances in Liquid Crystal Research and Applications*, **Bata, L., Ed.**, Pergamon Press, Oxford–Akadémiai Kiadó, Budapest, 1980, 469–482.

184. Chigrinov, V. G., Baikalov, V. A., Pozhidaev, E. P., Blinov, L. M., Beresnev, L. A., and Allagulov, A. I., Flexoelectric polarization of a ferroelectric smectic liquid crystal, *Sov. Phys. JETP*, 61, 1193–1198, 1985.

185. Beresnev, L. A., Chigrinov, V. G., Dergachev, D. I., Poshidaev, E. P., Fünfschilling, J., and Schadt, M., Deformed helix ferroelectric liquid crystal display: A new electrooptic mode in ferroelectric chiral smectic C liquid crystals, *Liq. Cryst.*, 5, 1171–1177, 1989.

186. Beresnev, L. A., Blinov, L. M., and Dergachev, D. I., Electro-optical response of a thin layer of a ferroelectric liquid crystal with a small pitch and high spontaneous polarization, *Ferroelectrics*, 85, 173–186, 1988.

187. Landreth, B., Mao, C.-C., and Moddel, G., Operating characteristics of optically addressed spatial light modulators incorporating distorted helix ferroelectric liquid crystals, *Jpn. J. Appl. Phys.*, 30, 1400–1404, 1991.

188. Jákli, A., Bata, L., and Beresnev, L. A., Switching behaviour of a thermochromic ferroelectric liquid crystal with high spontaneous polarization, *Mol. Cryst. Liq. Cryst.*, 177, 43–57, 1989.

189. Abdulhalim, I. and Moddel, G., Electrically and optically controlled light modulation and color switching using helix distortion of ferroelectric liquid crystals, *Mol. Cryst. Liq. Cryst.*, 200, 79–101, 1991.

190. Garoff, S. and Meyer, R. B., Electroclinic effect at the *A-C* phase change in a chiral smectic liquid crystal, *Phys. Rev. A*, 19, 338–347, 1979.

191. Andersson, G., Dahl, I., Keller, P., Kuczynski, W., Lagerwall, S. T., Skarp, K., and Stebler, B., Submicrosecond electro-optic switching in the liquid-crystal smectic *A* phase: The soft-mode ferroelectric effect, *Appl. Phys. Lett.*, 51, 640–642, 1987.

192. Andersson, G., Dahl, I., Kuczynski, W., Lagerwall, S. T., Skarp, K., and Stebler, B., The soft-mode ferroelectric effect, *Ferroelectrics*, 84, 285–315, 1988.

193. Abdulhalim, I., Moddel, G., and Johnson, K. M., High-speed analog spatial light modulator using a hydrogenated amorphous silicon photosensor and an electroclinic liquid crystal, *Appl. Phys. Lett.*, 55, 1603–1605, 1989.

194. Abdulhalim, I., Moddel, G., Johnson, K. M., and Walker, C. M., Optically addressed electroclinic liquid crystal spatial light modulator with an *a*-Si:H photodiode, *J. Non-Cryst. Solids*, 115, 162–164, 1989.

195. Sharp, G. D., Johnson, K. M., and Doroski, D., Continuously tunable smectic *A** liquid-crystal color filter, *Opt. Lett.*, 15, 523–525, 1990.

196. Nishiyama, S., Ouchi, Y., Takezoe, H., and Fukuda, A., Giant electroclinic effect in chiral smectic A phase of ferroelectric liquid crystals, *Jpn. J. Appl. Phys. 2, Lett.*, 26, L1787–L1789, 1987.

197. Qiu, R., Ho, J. T., and Hark, S. K., Electroclinic effect above the smectic-*A*—smectic-*C** transition, *Phys. Rev. A*, 38, 1653–1655, 1988.

198. Etxebarria, J., Remón, A., Tello, M. J., and Serrano, J. L., Electroclinic effect near a smectic A–chiral smectic I transition, *Liq. Cryst.*, 4, 543–548, 1989.

199. Bahr, Ch. and Heppke, G., Electroclinic effect in smectic-*B* and -*E* phases of chiral molecules, *Phys. Rev. A*, 37, 3179–3181, 1988.

200. **Kondo, K., Sato, Y., Miyasato, K., Takazoe, H., Fukuda, A., Kuze, E., Flatischler, K., and Skarp, K.,** Magnetic field effects on preparing thin homogeneous ferroelectric smectic cells for electro-optical microsecond switches, *Jpn. J. Appl. Phys. 2, Lett.*, 22, L13–L15, 1983.

201. **Kondo, K., Takezoe, H., Fukuda, A., and Kuze, E.,** A practical method of preparing thin homogeneous ferroelectric smectic cells for electro-optical microsecond switches: Alignment control of liquid crystal molecules by utilizing spacer edges, *Jpn. J. Appl. Phys. 2, Lett.*, 22, L85–L87, 1983.

202. **Patel, J. S. and Goodby, J. W.,** Alignment of liquid crystals which exhibit cholesteric to smectic C^* phase transitions, *J. Appl. Phys.*, 59, 2355–2360, 1986.

203. **Ikeno, H., Oh-Saki, A., Nitta, M., Ozaki, N., Yokoyama, Y., Nakaya, K., Kobayashi, S.,** Electrooptic bistability of a ferroelectric liquid crystal device prepared using polyimide Langmuir-Blodgett orientation films, *Jpn. J. Appl. Phys. 2, Lett.*, 27, L-475–L-476, 1988.

204. **Kuwahara, M., Kawata, Y., Onnagawa, H., and Miyashita, K.,** A method for molecular alignment of ferroelectric smectic liquid crystal: Combination of metal oxide thin film and electric field, *Jpn. J. Appl. Phys.*, 27, 1365–1372, 1988.

205. **Nakaya, K., Zhang, B. Y., Yoshida, M., Isa, I., Shindoh, S., and Kobayashi, S.,** Electrooptic bistability of a ferroelectric liquid crystal device prepared using charge-transfer complex-doped polyimide-orientation films, *Jpn. J. Appl. Phys. 2, Lett.*, 28, L116–L118, 1989.

206. **Zhang, B. Y., Yoshida, M., Maeda, H., Kimura, M., Sekine, H., and Kobayashi, S.,** Electro-optic characteristics of charge-transfer-complex doped ferroelectric liquid crystal device: Realization of very high contrast ratio and perfect bistability, *Mol. Cryst. Liq. Cryst.*, 202, 149–162, 1991.

207. **Kuniyasu, S., Fukuro, H., Maeda, S., Nakaya, K., Nitta, M., Ozaki, N., and Kobayashi, S.,** The strength of rubbing worked on polyimide films for aligning nematic and chiral smectic liquid crystals: Controlling pretilt angles and some electrooptic performances of LCDs, *Jpn. J. Appl. Phys.*, 27, 827–829, 1988.

208. **Myrvold, B. O.,** The relationship between the physical properties of the alignment layer and the quality of SSFLC cells, *Mol. Cryst. Liq. Cryst.*, 202, 123–147, 1991.

209. **Drzaic, P. S.,** Polymer dispersed nematic liquid crystal for large area displays and light valves, *J. Appl. Phys*, 60, 2142–2148, 1986.

210. **Doane, J. W., Golemme, A., West, J. L., Whitehead, J. B., Jr., and Wu, B.-G.,** Polymer dispersed liquid crystals for display application, *Mol. Cryst. Liq. Cryst.*, 165, 511–532, 1988.

211. **Drzaic, P. S.,** Nematic droplet/polymer films for high-contrast coloured reflective displays, *Disp. Technol. Appl.*, 12, 2–15, 1991.

212. **West, J. L., Tamura-Lis, W., and Ondris, R.,** Polymer dispersed liquid crystals incorporating isotropic dyes, in *Liquid Crystal Chemistry, Physics, and Applications,* **Doane, J. W. and Yaniv, Z., Eds.,** SPIE Vol. 1080, SPIE, Bellingham, WA, 1989, 48–52.

213. **Craighead, H. G., Cheng, J., and Hackwood, S.,** New display based on electrically induced index matching in an inhomogeneous medium. *Appl. Phys. Lett.*, 40, 22–24, 1982.

214. **Fergason, J. L.,** Polymer encapsulated nematic liquid crystals for display and light control applications, *1985 Society for Information Displays International Symposium. Digest of Technical Papers*, 68–70, 1985.

215. **Doane, J. W., Vaz, N. A., Wu, B.-G., Zumer, S.,** Field controlled light scattering from nematic microdroplets, *Appl. Phys. Lett.*, 48, 269–271, 1986.

216. **Kelly, J. H.,** Overview of polymer dispersed liquid crystals, presented at the ALCOM Symposium on Novel Liquid Crystal Materials and Optical/Electro-Optical Effects, Akron, OH, 6–7 November 1991.

217. **Wu, B.-G., West, J. L., and Doane, J. W.,** Angular discrimination of light transmission through polymer-dispersed liquid-crystal films, *J. Appl. Phys.*, 62, 3925–3931, 1987.

218. **Nomura, H., Suzuki, S., and Atarashi, Y.,** Electrooptical properties of polymer films containing nematic liquid crystal microdroplets, *Jpn. J. Appl. Phys.*, 29, 522–528, 1990.

219. **Rout, D. K. and Jain, S. C.,** Refractive index and microscopic studies of polymer dispersed liquid crystal films containing low concentration of liquid crystals, *Jpn. J. Appl. Phys. 2, Lett.*, 30, L1412–L1414, 1991.

220. **Vaz, N. A. and Montgomery, G. P., Jr.,** Refractive indices of polymer-dispersed liquid crystal film materials: Epoxy based systems, *J. Appl. Phys.*, 62, 3161–3172, 1987.

221. **Smith, G. W. and Vaz, N. A.,** The relationship between formation kinetics and microdroplet size of epoxy-based polymer dispersed liquid crystals, *Liq. Cryst.*, 3, 543–571, 1988.

222. **Margerum, J. D., Lackner, A. M., Ramos, E., Lim, K.-C., and Smith, W. H., Jr.,** Effects of off-state alignment in polymer dispersed liquid crystals, *Liq. Cryst.*, 5, 1477–1487, 1989.

223. **Smith, G. W.,** Study of formation, phase behavior, and microdroplet size of a polyurethane-based polymer-dispersed liquid crystal, *Mol. Cryst. Liq. Cryst.*, 180B, 201–222, 1990.

224. **Vaz, N. A., Smith, G. W., and Montgomery, G. P., Jr.,** Polymer-dispersed liquid crystal films formed by electron beam cure, *Mol. Cryst. Liq. Cryst.*, 197, 83–101, 1991.

225. **Montgomery, G. P., Jr., West, J. L., and Tamura-Lis, W.,** Light scattering from polymer-dispersed liquid crystal films: Droplet size effects, *J. Appl. Phys.*, 69, 1605–1612, 1991.

226. **Montgomery, G. P., Jr.,** Angle-dependent scattering of polarized light by polymer-dispersed liquid-crystal films, *J. Opt. Soc. Am. B*, 5, 774–784, 1988.

227. **Montgomery, G. P., Jr. and Vaz, N. A.,** Contrast ratios of polymer-dispersed liquid crystal films. *Appl. Opt.*, 26, 738–743, 1987.

228. **Wu, B.-G., Erdmann, J. H., and Doane, J. W.,** Response times and voltages for PDLC light shutters, *Liq. Cryst.*, 5, 1453–1465, 1989.

229. **Chidichimo, G., Arabia, G., Golemme, A., and Doane, J. W.,** Electrooptic properties of polymer dispersed liquid crystals, *Liq. Cryst.*, 5, 1443–1452, 1989.

230. **Yamagishi, F. G., Miller, L. J., and van Ast, C. I.,** Morphological control in polymer-dispersed liquid crystal film matrices, in *Liquid Crystal Chemistry, Physics, and Applications,* Yaniv, Z. and Doane, J. W., Eds., SPIE Vol. 1080, SPIE, Bellingham, WA, 1989, 24–31.

231. **Gotoh, T. and Murai, H.,** Preparation and characteristics of new reverse mode film of polymer dispersed liquid crystal type, *Appl. Phys. Lett.,* 60, 392–394, 1992.

232. **Pirš, J., Olenik, M., Marin, B., Žumer, S., and Doane, J. W.,** Color modulator based on polymer dispersed liquid-crystal shutters, *J. Appl. Phys.,* 68, 3826–3831, 1990.

233. **Kim, J. Y. and Palffy-Muhoray, P.,** Optical power limiting and bistability in polymer-dispersed liquid-crystal films with linear feedback, *J. Appl. Phys.,* 66, 362–365, 1989.

234. **Tagawa, A., Ozaki, M., Munezawa, T., Nomura, Y., and Yoshino, K.,** Dynamic characteristics of optical bistability and limiting in polymer dispersed liquid crystal, *Jpn. J. Appl. Phys.,* 30, 301–306, 1991.

235. **Vaz, N. A. and Montgomery, G. P., Jr.,** Dual frequency addressing of polymer-dispersed liquid-crystal films, *J. Appl. Phys.,* 65, 5043–5050, 1989.

236. **Montgomery, G. P., Jr. and Vaz, N. A.,** Improving multiplexability of polymer-dispersed liquid crystal films by dual frequency addressing, *Mol. Cryst. Liq. Cryst.,* 185, 67–74, 1990.

237. **Nolan, P. and Coates, D.,** Reverse mode polymer dispersed liquid crystal display incorporating a dual frequency addressable liquid crystal mixture, *Mol. Cryst. Liq. Cryst. Lett.,* 8, 75–83, 1991.

238. **Crooker, P. P. and Yang, D. K.,** Polymer-dispersed chiral liquid crystal color display, *Appl. Phys. Lett.,* 57, 2529–2531, 1990.

239. **Yang, D. K. and Crooker, P. P.,** Field-induced textures of polymer-dispersed chiral liquid crystal microdroplets, *Liq. Cryst.,* 9, 245–251, 1991.

240. **Kitzerow, H.-S. and Crooker, P. P.,** Polymer-dispersed cholesteric liquiↄ crystals—challenge for research and application, *Ferroelectrics,* 122, 183–196, 1991.

241. **Hikmet, R. A. M.,** Electrically induced light scattering from anisotropic gels, *J. Appl. Phys.,* 68, 4406–4412, 1990.

242. **Chemla, D. S. and Zyss, J., Eds.,** *Nonlinear Optical Properties of Organic Molecules and Crystals,* Academic Press, Orlando, 1987.

243. **Kuhn, H. and Robillard, J., Eds.,** *Nonlinear Optical Materials,* CRC Press, Boca Raton, FL, 1992.

244. **Prasad, P. N. and Williams, D. J.,** *Introduction to Nonlinear Optical Effects in Molecules and Polymers,* John Wiley and Sons, New York, 1991.

245. **Marder, S. R., Sohn, J. E., and Stucky, G. D., Eds.,** *Materials for Nonlinear Optics: Chemical Perspectives,* ACS Symposium Series; 455, American Chemical Society, Washington, DC, 1991.

246. **Hann, R. A. and Bloor, D., Eds.,** *Organic Materials for Non-linear Optics: The Proceedings of a Conference Organised by the Applied Solid State Chemistry Group of the Dalton Division of the Royal Society of Chemistry, Oxford, 29th–30th June 1988*, Royal Society of Chemistry, London, 1989.

247. **Flytzanis, C. and Oudar, J. L., Eds.,** *Nonlinear Optics: Materials and Devices: Proceedings of the International School of Materials Science and Technology, Erice, Sicily, July 1–14, 1985*, Springer-Verlag, Berlin, 1986.

248. **Prasad, P. N. and Ulrich, D. R., Eds.,** *Nonlinear Optical and Electroactive Polymers*, Plenum Press, New York, 1988.

249. **Wendorff, J. H. and Eich, M.,** Nonlinear optical phenomena in liquid crystalline side chain polymers, *Mol. Cryst. Liq. Cryst.*, 169, 133–166, 1989.

250. **Willand, C. S. and Williams, D. J.,** Nonlinear optical properties of polymeric materials, *Ber. Bunsenges. Phys. Chem.*, 91, 1304–1310, 1987.

251. **Ulrich, D. R.,** Polymers for nonlinear optical applications, *Mol. Cryst. Liq. Cryst.*, 189, 3–38, 1990.

252. **Dalton, L. R., Yu, L., Sapochak, L., and Chen, M.,** Development of materials with enhanced optical nonlinearity: Theory and practice, *Mol. Cryst. Liq. Cryst.*, 189, 49–56, 1990.

253. **Basu, S.,** A review of nonlinear optical organic materials, *Ind. & Eng. Chem., Prod. Res. & Dev.*, 23, 183–186, 1984.

254. **Stegeman, G. I., Seaton, C. T., and Zanoni, R.,** Organic films in non-linear integrated optics structures, *Thin Solid Films*, 152, 231–263, 1987.

255. **Zyss, J.,** Nonlinear organic materials for integrated optics: A review, *J. Mol. Electron.*, 1, 25–45, 1985.

256. **Bunkin, A. F., Ivanov, S. G., Koroteev, N. I., Rezov, A. V., and Sybeva, M. L.,** Measurement of nonlinear optical susceptibilities of the liquid crystal MBBA in isotropic and nematic phases, using coherent active spectroscopy, *Moscow Univ. Phys. Bull.*, 32, 27–34, 1977.

257. **Aslanyan, L. S., Badalyan, N. N., Petrosyan, A. A., Khurshudyan, M. A., and Chilingaryan, Yu. S.,** Determination of cubic optical susceptibilities of liquid crystals by coherent four-photon spectroscopy, *Opt. Spectrosc. (USSR)*, 53, 54–58, 1982.

258. **Madden, P. A., Saunders, F. C., and Scott, A. M.,** Measurement of the nonlinear susceptibility of liquid crystal materials in the isotropic phase, *Opt. Acta*, 33, 405–417, 1986.

259. **Soileau, M. J., Van Stryland, W., Guha, S., Sharp, E. J., Wood, J. L, and Fohlmann, J. L.,** Nonlinear optical properties of liquid crystals in the isotropic phase, *Mol. Cryst. Liq. Cryst.*, 143, 139–143, 1987.

260. **Palffy-Muhoray, P., Yuan, H. J., Li, L., Lee, M. A., DeSalvo, J. R., Wei, T. H., Sheik-Bahae, M., Hagan, D. J., and Van Stryland, E. W.,** Measurements of the third order optical nonlinearities of nematic liquid crystals, *Mol. Cryst. Liq. Cryst.*, 207, 291–305, 1991.

261. **Rothschild, W. G., Perrot, M., and De Zen, J.-M.,** Picosecond dynamics and molecular aggregation from vibrational dephasing in the fluid phases of some 4-n-alkyl-4'-cyanobiphenyl liquid crystals, *J. Chem. Phys.*, 95, 2072–2079, 1991.

262. Deeg, F. W., Greenfield, S. R., Stankus, J. J., Newell, V. J., and Fayer, M. D., Nonhydrodynamic molecular motions in a complex liquid: Temperature dependent dynamics in pentylcyanobiphenyl, *J. Chem. Phys.*, 93, 3503–3514, 1990.

263. Singer, K. D., Kuzyk, M. G., Holland, W. R., Sohn, J. E., Lalama, S. J., Comizzoli, R. B., Katz, H. E., and Schilling, M. L., Electro-optic phase modulation and optical second-harmonic generation in corona-poled polymer films, *Appl. Phys. Lett.*, 53, 1800–1802, 1988.

264. Eich, M., Sen, A., Looser, H., Bjorklund, G. C., Swalen, J. D., Twieg, R., and Yoon, D. Y., Corona poling and real-time second-harmonic generation study of a novel covalently functionalized amorphous nonlinear optical polymer, *J. Appl. Phys.*, 66, 2559–2567, 1989.

265. Page, R. H., Jurich, M. C., Reck, B., Sen, A., Twieg, R. J., Swalen, J. D., Bjorklund, G. C., and Willson, C. G., Electrochromic and optical waveguide studies of corona-poled electro-optic polymer films, *J. Opt. Soc. Am. B*, 7, 1239–1250, 1990.

266. Girton, D. G., Kwiatkowski, S. L., Lipscomb, G. F., and Lytel, R. S., 20 GHz electro-optic polymer Mach-Zehnder modulator, *Appl. Phys. Lett.*, 58, 1730–1732, 1991.

267. Barnik, M. I., Blinov, L. M., and Shtykov, N. M., Phase-synchronous optical second-harmonic generation in a ferroelectric liquid crystal, *Sov. Phys. JETP*, 59, 980–981, 1984.

268. Shtykov, N. M., Barnik, M. I., Beresnev, L. A., and Blinov, L. M., A study of a ferroelectric liquid crystal using second optical harmonic generation, *Mol. Cryst. Liq. Cryst.*, 124, 379–390, 1985.

269. Liu, J.-Y., Robinson, M. G., Johnson, K. M., Walba, D. M., Ros, M. B., Clark, N. A., Shao, R., and Doroski, D., The measurement of second-harmonic generation in novel ferroelectric liquid crystal materials, *J. Appl. Phys.*, 70, 3426–3430, 1991.

270. Liu, J. Y., Robinson, M. G., Johnson, K. M., and Doroski, D., Second-harmonic generation in ferroelectric liquid crystals, *Opt. Lett.*, 15, 267–269, 1990.

271. Taguchi, A., Ouchi, Y., Takezoe, H., and Fukuda, A., Angle phase matching in second harmonic generation from a ferroelectric liquid crystal, *Jpn. J. Appl. Phys.*, 28, L997–L999, 1989.

272. Frazier, C. C., Cockerham, M. P., Chauchard, E. A., and Lee, C. H., Second-harmonic generation in aromatic organic compounds, *J. Opt. Soc. Am. B*, 4, 1899–1903, 1987.

273. Marder, S. R., Perry, J. W., and Schaeffer, W. P., Synthesis of organic salts with large second-order optical nonlinearities, *Science*, 245, 626–628, 1989.

274. Velsko, S. P., Davis, L., Wang, F., Monaco, S., and Eimerl, D., Organic nonlinear crystals and high power frequency conversion, in *Advances in Nonlinear Polymers and Inorganic Crystals, Liquid Crystals, and Laser Media*, SPIE Vol. 824, SPIE, Bellingham, WA, 1987, 178–181.

275. **Fouquey, C., Lehn, J. M., and Malthete, J.,** Liquid crystals for nonlinear optics: Mesophases formed by push-pull stilbenes and diacetylenes. *J. Chem. Soc., Chem. Commun.,* 19, 1424–1426, 1987.

276. **Walba, D. M., Clark, N. A., Razavi, H. A., and Parmar, D. S.,** A novel application of the guest-host paradigm: Design of organic optoelectronic materials, in *Proceedings of the Fifth International Symposium on Inclusion Phenomena and Molecular Recognition,* **Atwood, J. L., Ed.,** Plenum Press, New York, 1990.

277. **Walba, D. M., Ros, M. B., Sierra, T., Rego, J. A., Clark, N. A., Shao, R., Wand, M. D., Vohra, R. T., Arnett, K. E., and Velsco, S. P.,** Design and synthesis of ferroelectric liquid crystals. 15. FLC materials for nonlinear optics applications, *Ferroelectrics,* 121, 247–257, 1991; and references therein.

278. **Le Barny, P., Ravaux, G., Dubois, J. C., Parneix, J. P., Njeumo, R., Legrand, C., and Levelut, A. M.,** Some new side-chain liquid crystalline polymers for nonlinear optics, in *Molecular and Polymeric Optoelectronic Materials: Fundamentals and Applications,* SPIE Vol. 682, SPIE, Bellingham, WA, 1986, 56–64.

279. **Kapitza, H., Zentel, R., Twieg, R., Nguyen, C., Vallerien, S. U., Kremer, F., and Willson, C. G.,** Ferroelectric liquid crystalline polysiloxanes with high spontaneous polarization and possible applications in nonlinear optics, *Adv. Mater.,* 2, 539–543, 1990.

280. **Findlay, R. B., Lemmon, T. J., and Windle, A. H.,** A comparative study of side chain liquid crystalline polymers and their monomers designed for nonlinear optical applications, *J. Mater. Res.,* 6, 604–609, 1991.

281. **Shen, Y. R.,** Surface second harmonic generation: A new technique for surface studies, *Annu. Rev. Mater. Sci.,* 16, 69–86, 1986.

282. **Mullin, C. S., Guyot-Sionnest, P., and Shen, Y. R.,** Properties of liquid-crystal monolayers on silane surfaces, *Phys. Rev. A,* 39, 3745–3747, 1989.

283. **Shen, Y. R., Chen, W., Feller, M. B., Huang, J. Y., and Superfine, R.,** Probing the mechanisms for surface-induced alignment of liquid crystals, *Mol. Cryst. Liq. Cryst.,* 207, 77–85, 1991.

284. **Wong, K. Y. and Garito, A. F.,** Third-harmonic-generation study of orientational order in nematic liquid crystals, *Phys. Rev. A,* 34, 5051–5058, 1986.

285. **Chen, W., Ouchi, Y., Moses, T., Shen, Y. R., and Yang, K. H.,** Surface electroclinic effect on the layer structure of a ferroelectric liquid-crystal, *Phys. Rev. Lett.,* 68, 1547–1550, 1992.

286. **Sukhov, A. V.,** Spatially inhomogeneous quadratic susceptibility of nematics with light-induced orientational gratings, *Sov. Phys. JETP,* 71, 512–518, 1990.

287. **Sukhov, A. V. and Timashev, R. V.,** Optically induced deviation from central symmetry; lattices of quadratic nonlinear susceptibility in a nematic liquid crystal, *JETP Lett.,* 51, 413–418, 1990.

288. **Zel'dovich, B. Ya., Philipetskii, N. F., Sukhov, A. V., and Tabiryan, N. V.,** Giant optical nonlinearity in the mesophase of a nematic liquid crystal (NCL), *JETP Lett.,* 31, 263–267, 1980.

289. **Zel'dovich, B. Ya. and Tabiryan, N. V.**, Orientational optical nonlinearity of liquid crystals, *Sov. Phys. Usp.*, 28, 1059–1083, 1985.

290. **Prost J. and Lalanne, J. R.**, Laser-induced optical Kerr effect and the dynamics of orientational order in the isotropic phase of a nematogen, *Phys. Rev. A*, 8, 2090–2093, 1973.

291. **Wong, G. K. L. and Shen, Y. R.**, Study of pretransitional behavior of laser-field-induced molecular alignment in isotropic nematic substances, *Phys. Rev. A*, 10, 1277–1284, 1974.

292. **Ye, P., and Shen, Y. R.**, Four-wave mixing and optical-field-induced helical structure in liquid crystalline materials, *Appl. Phys.*, 25, 49–56, 1981.

293. **Yu, Z., Lu, H., Ye, P., and Fu, P.**, Laser-induced helical structure in the isotropic phase of nematic liquid crystal, *Appl. Phys. B*, 44, 51–56, 1987.

294. **Arakelyan, S. M.**, Optical bistability, multistability, and instabilities in liquid crystals, *Sov. Phys. Usp.*, 30, 1041–1064, 1987.

295. **Khoo, I. C.**, Nonlinear optics of liquid crystals, in *Progress in Optics*, Vol. XXVI, **Wolf, E., Ed.**, North-Holland, Amsterdam, 1988, 107–161.

296. **Palffy-Muhoray, P.**, The nonlinear optical response of liquid crystals, in *Liquid Crystals: Applications and Uses*, **Bahadur, B., Ed.**, Vol. 1, World Scientific, Singapore, 1990.

297. **Shen, Y. R.**, Nonlinear optics and liquid crystals, in *Laser Spectroscopy and Nonlinear Optics of Solids*, **Radhakrishna, S. and Tan, B. C., Eds.**, Springer-Verlag, Berlin, 1990.

298. **Tabiryan, N. V., Sukhov, A. V., and Zel'dovich, B. Ya.**, The orientational optical nonlinearity of liquid crystals, *Mol. Cryst. Liq. Cryst.*, 136, 1–139, 1986.

299. **Akhmanov, S. A., Vorontsov, M. A., and Ivanov, V. Yu.**, Large-scale transverse nonlinear interactions in laser beams; new types of nonlinear waves; onset of "optical turbulence", *JETP Lett.*, 47, 707–711, 1988.

300. **Akhmanov, S. A.**, private communication, 1989.

301. **Arakelyan, S. M., Gevorkyan, L. P., and Chilingaryan, Yu. S.**, Compression of electromagnetic radiation pulses in media with strong spatial dispersion, *Opt. Spectrosc. (USSR)*, 65, 58–61, 1988.

302. **Arakelyan, S. M., Gevorkyan, L. P., and Makarov, V. A.**, Compression of frequency-modulated pulses by dynamic scattering in the Laue geometry, *Sov. J. Quantum Electron.*, 19, 1188–1189, 1989.

303. **Gevorkyan, L. P., Makarov, V. A., and Cherepetskaya, E. B.**, Compression of laser pulses during dynamic scattering in a nonlinear cholesteric liquid crystal, *Sov. J. Quantum Electron.*, 19, 1604–1605, 1989.

304. **Alaverdian, R. B., Arakelian, S. M., Gevorkian, L. P., Makarov, B. A., Papazian, T. A., and Chilingarian, Yu. S.**, Large-aperture compression of picosecond laser pulses and bandwidth-limited radiation arising in a spatially periodic medium: Theory and experiment, *Phys. Lett. A*, 151, 317–324, 1990.

305. **Ghosh Roy, D. N., Rao, D. V. G. L. N., and Bronk, H.**, Optical pulse compression in a cholesteric liquid crystal, *Appl. Phys. Lett.*, 39, 474–475, 1981.

306. **Winful, H. G.,** Nonlinear reflection in cholesteric liquid crystals: Mirrorless optical bistability, *Phys. Rev. Lett.,* 49, 1179–1182, 1982.

307. **Alodzhants, A. P., Arakelyan, S. M., and Chilingaryan, Yu. S.,** Squeezed polarization states and photon antibunching in nonlinear selective reflection of light from a cholesteric liquid crystal, *Sov. J. Quantum Electron.,* 21, 570–575, 1991.

308. **Au, L. B., Solymar, L., Dettmann, C., Eichler, H. J., MacDonald, R., and Schwartz, J.,** Theoretical and experimental investigations of the reorientation of liquid crystal molecules induced by laser beams, *Physica A,* 174, 94–118, 1991.

309. **Lalanne, J. R., Buchert, J., Destrade, C., Nguyen, H. T., and Marcerou, J. P.,** Slowing down of molecular rotation at the Smectic-$A \rightarrow$ Smectic-C^* transition in liquid crystals, *Phys. Rev. Lett.,* 62, 3046–3049, 1989.

310. **Drevensek, I. and Copic, M.,** Properties of nematics studied by four wave mixing, *Mol. Cryst. Liq. Cryst.,* 207, 241–250, 1991.

311. **Simoni, F., Cipparrone, G., Duca, D., and Khoo, I. C.,** Threshold degenerate wave mixing in dye-doped polymer-dispersed liquid crystals, *Opt. Lett.,* 16, 360–362, 1991.

312. **Neubecker, R., Balzer, W., and Tschudi, T.,** Characterization of nematic liquid crystals for nonlinear optical applications, *Appl. Phys. B,* 51, 258–262, 1990.

313. **Khoo, I. C. and Normandin, R.,** Infrared to visible image conversion capability of a nematic liquid crystal film, *Appl. Phys. Lett.,* 47, 350–352, 1985.

314. **Khoo, I. C., Yan, P. Y., Finn, G. M., Liu, T. H., and Michael, R. R.,** Low-power (10.6-μm) laser-beam amplification by thermal-grating-mediated degenerate four-wave mixing in a nematic liquid-crystal film, *J. Opt. Soc. Am. B,* 5, 202–206, 1988.

315. **Richard, L., Maurin, J., and Huignard, J. P.,** Phase conjugation with gain at CO_2 laser line $\lambda = 10.6$ μm from thermally induced gratings in nematic liquid crystals, *Opt. Commun.,* 57, 365–370, 1986.

316. **Khoo, I. C., Michael, R. R., Mansfield, R. J., Lindquist, R. G., Zhou, P., Cipparrone, G., and Simoni, F.,** Experimental studies of the dynamics and parametric dependences of switching from total internal reflection to transmission and limiting effects, *J. Opt. Soc. Am. B,* 8, 1464–1470, 1991.

317. **Gusev, I. V., Zel'dovich, B. Ya., Krivoshchekov, V. A., and Sadovskiĭ, V. N.,** Steady-state stimulated scattering by a grating nonlinearity in a planar nematic liquid crystal, *JETP Lett.,* 55, 178–183, 1992.

318. **Galstyan, T. V., Sukhov, A. V., and Timashev, R. V.,** Energy exchange between optical waves counterpropagating in a cholesteric liquid crystal, *Sov. Phys. JETP,* 68, 1001–1005, 1989.

319. **Galstyan, T. V. and Sukhov, A. V.,** Observation of induced orientational backscattering of light in cholesterics, *Opt. Spectrosc. (USSR),* 66, 771–773, 1989.

320. **Zel'dovich, B. Ya., Merzlikin, S. K., Pilipetskiĭ, N. F., and Sukhov, A. V.,** Observation of stimulated forward orientational light scattering in a planar nematic liquid crystal, *JETP Lett.,* 41, 514–517, 1985.

321. Galstyan, T. V., Zel'dovich, B. Ya., Nemkova, E. A., and Sukhov, A. V., Nonstationary optical excitation of bulk short-period orientation lattices in a nematic, *Sov. Phys. JETP*, 66, 991–997, 1987.

322. Santamato, E., Daino, B., Romagnoli, M., Settembre, M., and Shen, Y. R., Collective rotation of molecules driven by the angular momentum of light in a nematic film, *Phys. Rev. Lett.*, 57, 2423–2426, 1986.

323. Santamato, E., Romagnoli, M., Settembre, M., Daino, B., and Shen, Y. R., Self-induced stimulated light scattering, *Phys. Rev. Lett.*, 61, 113–116, 1988.

324. Santamato, E., Abbate, G., Maddalena, P., Marrucci, L., and Shen, Y. R., Laser-induced nonlinear dynamics in a nematic liquid-crystal film, *Phys. Rev. Lett.*, 64, 1377–1380, 1990.

325. Zolot'ko, A. S., Kitaeva, V. F., Kroo, N., Sobolev, N. N., and Chillag, L., The effect of an optical field on the nematic phase of the liquid crystal OCBP, *JETP Lett.*, 32, 158–162, 1980.

326. Durbin, S. D., Arakelian, S. M., and Shen, Y. R., Optical-field-induced birefringence and Freedericksz transition in a nematic liquid crystal, *Phys. Rev. Lett.*, 47, 1411–1414, 1981.

327. Zel'dovich, B. Ya., Nersisyan, S. R., and Tabiryan, N. V., Threshold interaction of extraordinary light waves with nematics, *Sov. Phys. JETP*, 61, 712–718, 1985.

328. Santamato, E., Abbate, G., Calaselice, R., Maddalena, P., and Sasso, A., All-optical-field-induced first-order Freedericksz transitions and hysteresis in a nematic film, *Phys. Rev. A*, 37, 1375–1377, 1988.

329. Marquis, F., Meystre, P., Wright, E. M., and Kaplan, A. E., Dynamics of the optical Freedericksz transition, *Phys. Rev. A*, 36, 875–887, 1987.

330. Ong, H. L. and Young, C. Y., Optically induced molecular reorientation in a smectic-C liquid crystal, *Phys. Rev. A*, 29, 297–307, 1984.

331. Khyzhniak, A., Odoulov, S., Reznikov, Yu., and Soskin, M., Dynamic hologram recording and phase conjugation of low power laser radiation in nematic liquid crystals, in *Proceedings of the International Conference on Lasers '82*, Powell, R. C., Ed., STS Press, McLean, VA, 1982, 40–47.

332. Pinkevich, I. P., Reznikov, Yu. A., Reshetnyak, V. Yu., Klishnyak, A. I., and Yaroshchuk, O. V., Conformational optical nonlinearity of the isotropic phase of a nematic liquid crystal, *Sov. Phys. JETP*, 69, 537–541, 1989.

333. Vinogradov, V., Khizhnyak, A., Kutulya, L., Reznikov, Yu., and Reshetnyak, V., Photoinduced change of cholesteric LC-pitch, *Mol. Cryst. Liq. Cryst.*, 192, 273–278, 1990.

334. Anderle, K., Birenheide, R., Werner, M. J. A., and Wendorff, J. H., Molecular addressing? Studies on light-induced reorientation in liquid-crystalline side chain polymers, *Liq. Cryst.*, 9, 691–699, 1991.

335. Wiesner, U., Reynolds, N., Boeffel, C., and Spiess, H. W., Photoinduced reorientation in liquid-crystalline polymers below the glass transition temperature studied by time-dependent infrared spectroscopy, *Makromol. Chem., Rapid Commun.*, 12, 457–464, 1991.

336. **Zel'dovich, B. Ya. and Tabiryan, N. V.**, Induced light scattering in the mesophase of a nematic liquid crystal (NLC), *JETP Lett.*, 30, 478–482, 1979.

337. **Zel'dovich, R. Ya. and Tabiryan, N. V.**, Stimulated scattering of light in the mesophase of a smectic liquid crystal, *Sov. J. Quantum Electron.*, 10, 440–442, 1980.

338. **Alaverdyan, R. B., Arakelyan, S. M., and Chilingaryan, Yu. S.**, Optical bistability in a nonlinear system with distributed feedback (experiment), *JETP Lett.*, 42, 451–455, 1985.

339. **Boixader, F., Massaneda, J., Orriols, G., and Pi, F.**, Optical bistability in thermochromic liquid crystals, *Opt. Commun.*, 84, 214–222, 1991.